

SMALL MOLECULE REGULATOR of ENTPD5, an ER ENZYME
in the PTEN/AKT PATHWAY

APPROVED BY SUPERVISORY COMMITTEE

Xiaodong Wang, Ph.D.

Zhijian James Chen, Ph.D.

Melanie Cobb, Ph.D.

Benjamin Tu, Ph.D.

Dedication

To my parents who gave me endless love and inspiration

SMALL MOLECULE REGULATOR of ENTPD5, an ER ENZYME
in the PTEN/AKT PATHWAY

by

SONG HUANG

DISSERTATION

Presented to the Faculty of the Graduate School of Biomedical Sciences
The University of Texas Southwestern Medical Center at Dallas
In Partial Fulfillment of the Requirements
For the Degree of

DOCTOR OF PHILOSOPHY

The University of Texas Southwestern Medical Center at Dallas
Dallas, TX
December, 2010

Copyright

By

SONG HUANG 2010

All Rights Reserved

Acknowledgements

I believe this is the most important part of my thesis where I can express my gratitude to all the people that made this work possible. First and foremost, I owe my deepest gratitude to my supervisor, Dr. Xiaodong Wang, for offering me an opportunity to work in his laboratory and for his patience, encouragements, continual guidance, and inspiring discussion on all aspects concerning this thesis. Above all, he taught me a mentality, “Never give up before all the possibilities have been exhausted”, which I will benefit from for the rest of my life.

It is a pleasure for me to work as a team with Dr. Min Fang, a senior postdoctoral fellow and Zhirong Shen, another graduate student in our laboratory. Min has a pair of golden hands and a heart of gold. In the laboratory he is a perfectionist that every single one of his experiments was carried out immaculately, down to the slightest details. But aside from work, he is an easygoing friend and good family man. This thesis would not have been possible unless Dr. Fang observed the extraordinary nucleotide hydrolysis activity in PTEN knockout MEF cell lysate and went on to purify ENTPD5. Zhirong worked out the transcriptional regulation of ENTPD5 and created a mouse xenograft model to test its in vivo function. I would also like to thank Dr. Liping Zhao, an exchange scholar from National Institute of Biological Sciences (NIBS), Beijing, for her expertise in histochemistry and tumor biology, which lead to the key data

about ENTPD5 expression in multiple primary human tumors. All together, these works paved the way for in vitro reconstitution of ENTPD5 catalytic cycle, and justified the effort to search for ENTPD5 inhibitors as potential therapeutic agent in cancer treatment.

I am heartily thankful to my wonderful dissertation committee by Dr. James Chen, Dr. Melanie Cobb and Dr. Benjamin Tu, for the constructive suggestions and warm encouragements they gave me in the committee meetings along the way. I am also indebted to many of my colleagues, both current and former members of the laboratory, including Dr. Lai Wang, Dr. Zhigao Wang, Dr. Wenhua Gao, Dr. Hui Jiang and Fenghe Du for their intellectual and technical support. I am especially grateful to Dr. Lai Wang, for giving me the initial recruit training, which later developed into my core skill set underlining this thesis. It is also my pleasure to thank Dr. Qing Zhong, Dr. Rui Hong, Dr. Gelin Wang, Dr. Hyun-eui Kim, Dr. Asligul Yalcin-Chin, Dr. Sean Petersen, Dr. Sudan He, Libin Shang and Gregory Kunkel, Liping Zhao for their discussion, support and friendship.

I would like to show my gratitude to the HTS laboratory staff, without whom the ENTPD5 inhibitor screen would be impossible. Dr. Michael Roth and Dr. Bruce Posner provided me with invaluable suggestions on assay design guidelines. Dr. Shuguang Wei, Dr. David Padron-Perez, Mridula Vishwanath, and

Christina Von Reyn helped me running the HTS screen robot, while Chunhui Bu helped process the screen raw data. I would also like to thank Dr. John MacMillan, for providing his unique marine natural compound library, and for helping purify the active components, which leads to the discovery of a new class of sea sponge metabolites as ENTPD5 inhibitors.

Lastly, I offer my regards and sincere gratitude to all of my friends who supported me in any respect during the completion of the project, even though their names may not have been explicitly mentioned here.

SMALL MOLECULE REGULATOR of ENTPD5, an ER ENZYME
in the PTEN/AKT PATHWAY

SONG HUANG, Ph.D.

The University of Texas Southwestern Medical Center at Dallas, 2010

Supervising Professor: XIAODONG WANG, Ph.D.

PI3K signaling plays a crucial role in effecting alterations in a broad range of cellular functions in response to diverse extracellular stimuli (insulin, growth factors, integrins and GPCRs etc.). A key downstream effector of PI3K is the serine-threonine kinase Akt, which in response to PI3K activation, phosphorylates and regulates the activity of a large number of cellular protein targets. Through these targets, Akt modulates a variety of cellular functions, including glucose metabolism, protein synthesis, cell proliferation and survival. Tumor suppressor gene PTEN encodes a lipid phosphatase that antagonizes PI3K function and

consequently inhibits downstream signaling through Akt. Dysregulation of this pathway has been found in a variety of human cancer, mainly by loss of function of PTEN, or amplification and activating mutations of PI3K and/or Akt.

We were interested in the anti-apoptotic mechanism of PI3K/Akt signaling. We observed a defect in apoptosome formation in PTEN-null (PTEN $-/-$) MEF cell lysate. This defect is due to rapid depletion of ATP by a strong ATP hydrolysis activity in PTEN-null MEF lysate, which is absent in PTEN heterozygous (PTEN $+/-$) lysate. Following this activity, we purified three enzymes, namely ENTPD5, CMPK1 and AK1, that together forms a coupled enzymatic cycle, hydrolyzing ATP to AMP.

In the cell, ENTPD5 is an ER localized UDPase that hydrolyzes UDP, the by-product of glycosyl-transferase, into UMP. Only in its monophosphate form can Uridine nucleotide exits ER through an antiporter by exchanging a molecule of UDP-sugar from cytosol. Up-regulation of ENTPD5 in PTEN $-/-$ MEF cells accelerates glycosylation substrate replenishment, therefore promotes N-glycosylation and increases ER protein folding capacity to accommodate the increase of protein synthesis resulted from active PI3K/Akt signaling. Knockdown of ENTPD5 in PTEN-null cells suppresses global N-glycosylation, resulting in ER stress and degradation of several growth factor receptors. As a

consequence, the growth of PTEN-null cells is inhibited both in vitro and in mouse xenograft tumor models.

Given the essential role of ENTPD5 in PI3K/Akt pathway, we performed biochemical high-throughput screen for ENTPD5 inhibitors. The newly identified inhibitors recapitulate the phenotype of ENTPD5 knockdown in vitro. Interestingly, PTEN $-/-$ MEF cells are more susceptible to these inhibitors than PTEN $+/-$ MEF cells, in terms of the intensity of induced ER stress and cell death. Inhibition of ENTPD5 produces synthetic lethality with PTEN loss or PI3K/Akt hyperactivation, therefore provides a potential therapy for the cancers harboring these lesions.

TABLE OF CONTENTS

CHAPTER 1 : BACKGROUND INTRODUCTION	1
1.1 PI3K/PTEN/AKT PATHWAY OVERVIEW	1
1.1.1 <i>PI3K</i>	2
1.1.2 <i>PTEN</i>	5
1.1.3 <i>PKB/Akt</i>	6
1.2 AKT DOWNSTREAM EFFECTS	9
1.2.1 <i>Inhibition of Apoptosis</i>	9
1.2.2 <i>Enhanced Protein Synthesis</i>	11
1.3 N-GLYCOSYLATION AND QC OF PROTEIN FOLDING IN THE ER	12
1.4 UNFOLDED PROTEIN RESPONSE.....	14
1.5 THE SCOPE OF CURRENT STUDY	19
FIGURE FROM CHAPTER 1.....	21
CHAPTER 2 : IDENTIFICATION AND CHARACTERIZATION OF ENTPD5.....	27
2.1 HIGH ATP HYDROLYSIS ACTIVITY IN PTEN-NULL LYSATE	27
2.2 ENTPD5 IS UNDERLYING THE ELEVATED ATPASE ACTIVITY.....	28
2.3 ENTPD5, CMPK1, AND AK1 CONSTITUTE AN ATP TO AMP HYDROLYSIS CYCLE.....	30
2.4 ENTPD5 IS AN ER ENZYME.....	32
2.5 KNOCKDOWN OF ENTPD5 CAUSES ER STRESS AND GROWTH INHIBITION	33
FIGURES FROM CHAPTER 2.....	36
CHAPTER 3 : SCREEN FOR ENTPD5 INHIBITORS	51
3.1 INTRODUCTION.....	51
3.2 HTS ASSAY DEVELOPMENT AND OPTIMIZATION	52

3.3 COUNTER SCREEN DESIGN	56
3.4 IDENTIFICATION OF CONFIRMATION OF ENTPD5 INHIBITORS	58
3.5 STRUCTURAL CLASSIFICATION OF VERIFIED COMPOUNDS	60
3.6 BIOACTIVITY DIRECTED PURIFICATION OF NATURAL COMPOUNDS	61
3.7 CELLULAR EFFECTS OF IN VITRO CONFIRMED COMPOUND INHIBITORS	63
FIGURES FROM CHAPTER 3	67
CHAPTER 4 : CONCLUSIONS AND DISCUSSIONS.....	93
4.1 ENTPDASE FAMILY	93
4.2 ENTPD5 IS AN INDISPENSIBLE COMPONENT OF PI3K/AKT PATHWAY.....	95
4.3 ENTPD5 CONTRIBUTES TO WARBURG EFFECT.....	97
4.4 ENTPD5 IS A POTENTIAL ANTI-CANCER TARGET	99
MATERIALS AND METHODS.....	102
BIBLIOGRAPHY	118

PRIOR PUBLICATION

Min Fang, Zhirong Shen, Song Huang, Liping Zhao, She Chen, Tak W. Mak, Xiaodong Wang. The ER UDPase ENTPD5 Promotes Protein N-Glycosylation, the Warburg Effect, and Proliferation in the PTEN Pathway. *Cell*, Volume 143, Issue 5, 711-724, 11 November 2010.

LIST OF FIGURES

Figure 1-1 Overview of PI3K/PTEN/AKT Signaling Pathway.....	21
Figure 1-2 Reported Anti-apoptotic Mechanisms of Akt.	23
Figure 1-3 Distribution of mammalian proteins by subcellular origin	24
Figure 1-4 N-Glycosylation and Protein Folding in ER.....	25
Figure 2-1 In Vitro Casp3 Activation Defect in PTEN-null Lysate	36
Figure 2-2 Casp3 Activation Defect is Due to Lack of ATP.....	37
Figure 2-3 Rapid Depletion of ATP in PTEN-null Lysate	38
Figure 2-4 Tracing ATP Hydrolysis Products by TLC	39
Figure 2-5 ENTPD5 Purification Scheme.....	40
Figure 2-6 Confirmation of ENTPD5.....	41
Figure 2-7 ENTPD5 Substrate Specificity	42
Figure 2-8 Purification of CMPK1.....	43
Figure 2-9 Confirmation of AK1 as the third factor.....	44
Figure 2-10 In Vitro Reconstitution of ATP Hydrolysis Cycle.....	45
Figure 2-11 ENTPD5 is an ER Localized Enzyme	46
Figure 2-12 Working Model for ENTPD5	47
Figure 2-13 ENTPD5 Knockdown Induces ER Stress.....	48
Figure 2-14 Rescue Experiment for ENTPD5 Knockdown	49
Figure 2-15 Knockdown of ENTPD5 Causes Growth Arrest	50
Figure 3-1 Primary Screen Assay Design.....	67
Figure 3-2 Coupled Reaction of Recombinant ENTPD5 and UMPKeco.....	68
Figure 3-3 Titration of Substrate UMP	69
Figure 3-4 Test of Assay Sensitivity and Linearity	70

Figure 3-5 ENTPD5 is the Rate-Limiting Enzyme	71
Figure 3-6 Primary Screen Assay Protocol	72
Figure 3-7 Counter Screen Design	73
Figure 3-8 Secondary & Tertiary Assays	74
Figure 3-9 HTS Screen Flow Chart.....	75
Figure 3-10 Representative True ENTPD5 Inhibitor Profile.....	76
Figure 3-11 Representative False Positive ENTPD5 Inhibitor Profile	77
Figure 3-12 Representative Non-specific ENTPD5 Inhibitor Profile.....	78
Figure 3-13 Structural clustering of Confirmed Synthetic Inhibitors.....	79
Figure 3-14 Class II Core Structure Resembles ENTPD5 Substrate.....	80
Figure 3-15 Natural Compounds Purification Scheme.....	81
Figure 3-16 Activity of Crude Extracts from <i>S. aurea</i>	82
Figure 3-17 Response of BA07-092-Hex Silicone Gel Column Fractions.....	83
Figure 3-18 Aureol (BA07-092-A10) Dose Response	84
Figure 3-19 Dose Response of BA07-092-A9 HPLC Fractions.....	84
Figure 3-20 Sesquiterpene Hydroquinones Natural Compound Inhibitors	85
Figure 3-21 Knockdown ENTPD5 Induces BiP Increase and EGFR Decrease	86
Figure 3-22 Synthetic ENTPD5 Inhibitors Induce ER Stress in PTEN-null Cells	87
Figure 3-23 Dose Response of Synthetic Inhibitors.....	88
Figure 3-24 ER Stress Intensity Correlates with <i>in vitro</i> Potency of Natural Inhibitors	89
Figure 3-25 PTEN ^{-/-} MEF is More Susceptible to Synthetic Compound Inhibitor than PTEN ^{+/-} MEF.....	90
Figure 3-26 Natural Compound Inhibitors Induces Stronger ER Stress in PTEN ^{-/-} MEF.....	91
Figure 3-27 Effects of Inhibitors on Human Prostate Cancer Cell Line.....	92

LIST OF TABLES

Table 1-1 PI3K Family Members..... 4

Table 4-1 Activated Sugar Donors in Mammalian Cell 94

List of Definitions

4E-BP	eukaryotic translation initiation factor 4E Binding Protein
AKT	v-akt murine thymoma viral oncogene homolog
ATP	Adenosine-5'-TriPhosphate
CNX	Calnexin
CRT	calreticulin
dATP	2'-deoxyAdenosine 5'-TriPhosphate
ER	Endoplasmic Reticulum
ERAD	ER Associated Degradation
FBS	Fetal Bovine Serum
HTS	High-Throughput Screen
IAP	Inhibitors of Apoptosis Proteins
MEF	Mouse Embryonic Fibroblast
MS	Mass Spectrometry
NMR	Nuclear Magnetic Resonance spectrometry
ORF	Open Reading Frame
PBS	Phosphate Buffered Saline
PI3K	Phosphatidyl Inositol 3-Kinase
PTEN	Phosphatase and Tensin homolog deleted on chromosome Ten
RAS	RAt Sarcoma
RNAi	RNA interference
RT-PCR	Reverse Transcription Polymerase Chain Reaction
SDS	Sodium Dodecyl Sulfate
shRNA	short hairpin RNA
mTOR	mammalian Target Of Rapamycin
OST	Oligosaccharide Transferase
p70 S6K	ribosomal protein S6 Kinase
PI3K	Phosphatidylinositol 3-kinases

RTK	Receptor Tyrosine Kinases
Ub	Ubiquitin
UDP-Glc	UDP-glucose
UGGT	UDP-glucose glycoprotein glucosyl-transferase

Chapter 1 : Background Introduction

1.1 PI3K/PTEN/AKT Pathway Overview

Phosphoinositide 3-kinase (PI3K) is a large family of lipid kinases. PI3K signaling plays a pivotal role in translating the detection of extracellular cues into alterations in cellular physiology (Engelman et al., 2006). In the quiescent cell this pathway is inactive. Upon binding of growth factors to receptor tyrosine kinases (RTK) in the membrane, PI3K was recruited to and activated by RTK on the inner face of plasma membrane, where it phosphorylates its lipid substrate, which then mediates the activation of the serine-threonine kinases Akt, a key downstream effector of PI3K. Akt in turn phosphorylates and regulates the activity of a wide spectrum of targets, including kinases, transcription factors and other regulatory molecules, to promote glucose metabolism, cell proliferation and survival. Tumor suppressor gene PTEN encodes a dual-specificity phosphatase, which counteract the PI3K/Akt signaling axis (Figure 1-1). This pathway is highly conserved among different species including worms, fruit flies and mammals.

Deregulation of this pathway, typically manifested by constitutive activation, is common in human cancers, and is associated with resistance to several chemotherapeutic agents.

1.1.1 PI3K

PI3Ks are a large family of lipid kinases containing eight members, which can be categorized into three Classes based on substrate preference (see Table 1-1) (Fruman et al., 1998; Vanhaesebroeck and Waterfield, 1999). All mammalian cells express representatives of all three groups.

Class I PI3K have four members and can be further subclassified into Ia and Ib, based on their activation mechanism. Class Ia PI3Ks are heterodimers, consisting of two subunits: the catalytic p110 subunit, including p110 α , p110 β and p110 δ , plus the regulatory p85 subunit. The p85 subunit contains two SH2 (Src homology) domains that interact with phosphotyrosines on activated RTKs.

The Class Ia PI3K signaling is initiated by growth factors and hormones that bind receptor tyrosine kinases (RTKs), such as epidermal growth factor receptor (EGFR), vascular endothelial growth factor receptor (VEGFR), and platelet-derived growth factor receptor (PDGFR) (Schlessinger, 2000). This leads to dimerization and auto-phosphorylation on tyrosine residues of the intracellular parts of the receptors. This results in recruitment of the PI3K p110/p85 heterodimer to the plasma membrane, where the p110 catalytic subunit recognize and phosphorylate its preferred substrate phosphoinositol-4,5-diphosphate (PtdIns-4,5-P₂, or PIP₂) on the D3 position of the inositol ring to afford phosphoinositol-3,4,5-triphosphates (PtdIns-3,4,5-P₃, or PIP₃) (Whitman et al.,

1988). PIP3 is undetectable in the plasma membrane of resting cells. Accumulation of this special lipid recruits several pleckstrin homology (PH) domains containing serine/threonine kinases, such as Akt and PDK1 (phosphoinositide-dependent kinase 1) to the plasma membrane (Alessi et al., 1997; Franke et al., 1997). When brought into close vicinity at the membrane, PDK1 phosphorylates and activates Akt. In addition to RTKs, activated (GTP-bound) RAS can activate class Ia kinases by direct interaction with the catalytic subunit (Downward, 1998). Mice lacking the catalytic subunit of class Ia dies at embryonic day 9.5 due to lack of proliferation (Bi et al., 1999).

Class Ib PI3K, also known as p110 γ , is expressed primarily in leukocytes. It is activated by $\beta\gamma$ subunits of heterotrimeric GTP-binding protein-coupled receptors. Homozygous deletion of catalytic subunit of class Ib PI3K showed impaired thymocyte development and increases in neutrophil, monocyte, and eosinophil populations (Vanhaesebroeck et al., 2005).

Class II PI3K contains 3 members: PI3KC2 α , β and γ , characterised by a carboxyl-terminal phospholipid-binding domain. While no regulatory subunit has been identified, class II enzymes are predominantly membrane bound and activated by membrane receptors including RTKs and integrins.

The Class III PI3K consists of a single catalytic subunit VPS34 (homologue of the yeast vacuolar protein sorting-associated protein 34, also

known as PIK3C3. VPS34 only produces PtdIns3P which is an important regulator of membrane trafficking. It has been shown to function as a nutrient regulated lipid kinase that mediates through mTOR. It also seems to play an important regulatory role in autophagy, a cellular response to nutrient starvation.

Table 1-1 PI3K Family Members

Class	Catalytic Subunit	Regulatory Subunit	Activation Mechanism	Products
Ia	p110 α	P85	RTK, RAS	PtdIns-3,4,5-P ₃
	P110 β			PtdIns-3,4-P ₂
	P110 δ			PtdIns-3-P
Ib	p110 γ	p101	Heterotrimeric G proteins	PtdIns-3,4,5-P ₃ PtdIns-3,4-P ₂ PtdIns-3-P
II	PI3KC2 α		RTK, integrins	PtdIns-3,4,-P ₂
	PI3KC2 β			PtdIns-3-P
	PI3KC2 γ			
III	VSP34p			PtdIns-3-P

A causal link between activation of PI3K and the process of cellular transformation was established by the discovery in the mid 1980's that the oncogenic activity of Middle T antigen of Polyoma virus was dependent on its ability to induce PI3K activity (Whitman et al., 1985). The role of PI3K in human tumorigenesis is further consolidated by the biochemistry study of tumor

suppressor PTEN, that PTEN prevents tumor formation by catalyzing the reverse reaction of PI3K (Myers et al., 1998).

1.1.2 PTEN

PTEN was first identified as a candidate tumor suppressor gene in 1997 after its positional cloning from a region of chromosome 10q24 known to exhibit loss in a wide spectrum of tumor types (Li and Sun, 1997; Li et al., 1997; Steck et al., 1997). Since then PTEN mutations has been detected in a variety of human cancers, including glioblastomas, endometrial, breast, thyroid, prostate cancer and melanoma. Germline mutations in the PTEN gene are associated with a rare autosomal dominant, hereditary cancer predisposition syndrome called Cowden's disease (CD) (Nelen et al., 1997). This syndrome is characterized by the development of hamartomas that is lesions characterized by hyperplastic, disorganized and benign tumors. Homozygous disruption of PTEN in mice leads to embryonic lethality. Although PTEN^{+/-} are viable, they are cancer prone and develop a range of neoplasms, resembling Cowden's disease patients (Di Cristofano et al., 1998; Podsypanina et al., 1999; Stambolic et al., 2000; Suzuki et al., 1998). Human genetic studies, together with the studies in animal models, strongly support a critical role of PTEN in tumor suppression.

Studies on the biochemistry of PTEN have provided a great deal of insight into the mechanism of its involvement in tumor suppression. The PTEN protein

possesses both protein phosphatase and lipid phosphatase activity (Cantley and Neel, 1999; Maehama et al., 2001; Vazquez and Sellers, 2000). The lipid phosphatase activity of PTEN can dephosphorylate the D3 position of PtdIns-3,4-P₂ and PtdIns-3,4,5-P₃, the lipid products of the PI3K lipid kinase activity (Myers et al., 1998). In PTEN-null cells, PtdIns-3,4,5-P₃ increases by two folds (Stambolic et al., 1998).

Protein phosphatase activity of PTEN is more related to its involvement in regulation of cytoskeleton and cell motility. PTEN can dephosphorylate tyrosine-, serine-, and threonine-phosphorylated peptides in vitro (Myers and Tonks, 1997). When overexpressed in cells, PTEN can dephosphorylate focal adhesion kinase (FAK) (Tamura et al., 1999) and the adaptor protein Shc (Gu et al., 1999), resulting in a decrease in cell spreading and motility (Tamura et al., 1998). However, the protein phosphatase activity seems dispensable for the tumor suppression function of PTEN, as certain tumor- and germline-derived PTEN mutants exhibit intact protein phosphatase activity (Furnari et al., 1998; Myers et al., 1998; Ramaswamy et al., 1999). These findings suggest that PTEN's role as a tumor suppressor is mediated primarily through its lipid phosphatase activity.

1.1.3 PKB/Akt

The serine-threonine kinase PKB (Protein Kinase B)/Akt is a major target of PI3K, mediating most of its downstream effects. There are three closely related

enzymatic isoforms of AKT, namely PKB α /Akt1, PKB β /Akt2 and PKB γ /Akt3, encoded by three distinct genes. They share a high degree of structural similarity and sequence homology, and are believed to share the same activation mechanism (Okano et al., 2000). Akt1 and 2 are ubiquitously expressed, while expression of Akt3 is restricted to brain and testis (Konishi et al., 1995). It appears that each Akt isoform may play unique as well as common roles in cells. Both Akt1 and Akt2 knockout mice are viable, but with phenotypic differences. Akt1 knock-out mice are growth-retarded (Cho et al., 2001b), Akt2 knock-out mice develop diabetes-like symptoms because of the impaired insulin response (Cho et al., 2001a), and Akt3 knock-out mice show reduced brain size (Easton et al., 2005).

Akt contains an N-terminal pleckstrin homology (PH) domain, a central catalytic kinase domain and a C-terminal regulatory region. The PH domains can bind specifically to PIP3 with high affinity.

Activation of Akt is a multi-step process involving both membrane binding and phosphorylation. PI3K activation results in accumulation of PIP3, which recruits serine/threonine kinase phosphatidylinositol-dependent kinase 1 (PDK1) and Akt to the plasma membrane by binding to their pleckstrin homology domains (Alessi et al., 1997; Franke et al., 1997). PDK1 then phosphorylate Akt on Thr308, which lies within the kinase domain activation loop. This is thought to be the major activating phosphorylation event. A second phosphorylation site in

the C-terminus (Ser473 in Akt1) is required for full or maximal activity. The identity of the serine 473 kinase is recently revealed to be mTOR complex 2 by Sabatini's Laboratory (Sarbasov et al., 2005). mTOR Complex 2 (mTORC2) is composed of mTOR, rapamycin-insensitive companion of mTOR (Rictor), GβL, and mammalian stress-activated protein kinase interacting protein 1 (mSIN1), and it appears to respond to growth factors and nutrient levels (Frias et al., 2006; Sarbasov et al., 2005). In contrast to mTORC1, however, mTORC2 is not sensitive to Rapamycin (Sarbasov et al., 2005), neither does it directly phosphorylate mTORC1 targets, such as p70S6K.

The effects of Akt activation in the cell are numerous and diverse, but all contribute to anti-apoptosis, or pro-cell proliferation. Akt exerts its effects in the cell by phosphorylating a variety of downstream substrates. These targets include GSK3, IRS-1 (insulin receptor substrate-1), PDE-3B (phosphodiesterase-3B), BAD, human caspase 9, Forkhead and NF-κB transcription factors, mTOR, eNOS, Raf protein kinase, BRCA1, and p21^{Cip1} /WAF1 (Ahtiok et al., 1999; Datta et al., 1999; Galetic et al., 1999; Montagnani et al., 2001; Zhou et al., 2001; Zimmermann and Moelling, 1999).

1.2 Akt Downstream Effects

1.2.1 Inhibition of Apoptosis

The influence of Akt on apoptosis is multifaceted. One common theme of Akt-mediated substrate inhibition is through the regulation of subcellular localization by interaction with 14-3-3 proteins (i.e. BAD, FOXO transcription factors). 14-3-3 proteins are cytoplasmic proteins that bind specifically to phosphoproteins and sequester them from their sites of action (Yaffe et al., 1997). In particular the Akt consensus phosphorylation site is also a consensus 14-3-3 binding site.

BAD is a pro-apoptotic BH3 only protein. BAD can diminish the anti-apoptotic effect of Bcl-2 or Bcl_{XL} on the mitochondria by forming complex with them through BH3 domain interaction, and introduce apoptosis. When phosphorylated by Akt, BAD associates with 14-3-3 proteins in the cytoplasm, thus its pro-apoptotic function on mitochondria is inhibited.

The FoxO (Forkhead box O) class of transcription factors consists of four members: FoxO1, 3a, 4 and 6. They belong to the winged helix/forkhead transcription factors family characterized by a 100-amino acid, monomeric DNA binding domain (DBD) (Kops and Burgering, 1999). FoxO family members have been implicated in regulation of cell death, cell proliferation and cell metabolism. They induce apoptosis both through the upregulation of FasL (Brunet et al., 1999)

and Bcl-2 interacting mediator (Bim1) (Dijkers et al., 2000). These transcription factors are directly phosphorylated and negatively regulated by Akt. 14-3-3 binds phosphorylated FoxOs in the nucleus, and target them to the nuclear export machinery (Brunet et al., 2002). In the cytosol, binding of 14-3-3 serves as a cytoplasmic retention signal, which keeps FoxOs from reentering nucleus. In cancer cell lines lacking functional PTEN, FoxOs are constitutively phosphorylated by Akt and are hence constitutively cytoplasmic and unable to activate transcription.

Human Caspase-9, a member of the cysteine-aspartic protease family associated with the initiation of apoptosis, is thought to be phosphorylated and inhibited by Akt (Cardone et al., 1998). However, the Akt phosphorylation site is not conserved in the Caspase 9 proteins from other mammals making its *in vivo* importance unclear.

In addition to the inhibition of pro-apoptotic factors, Akt can also activate the transcription of anti-apoptotic genes, such as inhibitors of apoptosis (IAP) cIAP1 and 2, through the activation of the transcription factor NF κ B (Kane et al., 1999; Khwaja, 1999; Ozes et al., 1999; Romashkova and Makarov, 1999).

1.2.2 Enhanced Protein Synthesis

Akt is also involved in activation of the nutrient-dependent serine/threonine kinase, mTOR (mammalian Target of Rapamycin). The protein kinase mTOR, is a master regulator of cellular metabolism in all eukaryotes (Wullschleger et al., 2006). The holoenzyme consists of two largely independent multiprotein complexes, mTORC1 and mTORC2. mTORC1 contains the polypeptides raptor (regulatory associated protein of TOR) and Lst8, and controls cell growth by phosphorylating substrates that regulate transcriptional, translational and post-translational processes in response to PI3K/Akt signaling. Activated Akt phosphorylates tumor suppressor TSC2 at S939 and T1462, preventing it from forming complex with TSC1, and directs TSC2 for ubiquitin dependent proteasome degradation (Inoki et al., 2002; Manning et al., 2002; Potter et al., 2002). TSC1/2 complex functions as GTPase Activating Protein toward the rheb GTPase, which in its GTP bound form binds and activates mTORC1. In this way, phosphorylation of TSC2 results in release of their inhibition activity towards mTOR.

Activated mTOR enhances protein synthesis by phosphorylating its downstream targets, p70S6 kinases, which in turn, phosphorylate the ribosomal protein S6 leading to increase translation. In addition to S6K, activation of mTOR

also results in phosphorylation and inactivation of eIF4EBP (Eukaryotic Initiation Factor-4E Binding Protein), an inhibitor of the translation initiation factor eIF4E.

1.3 N-Glycosylation and QC of Protein Folding in the ER

It is estimated that about one third of the proteins encoded by eukaryotic genome has ER-targeting signals (Figure 1-3). The ER is the site for assembly of polypeptide chains destined either for secretion or routing into various subcellular compartments. Protein folding is not an event in isolation, but occurs co-translationally either with the synthesis of the protein by the ribosome or the translocation of the protein through the Sec61 channel into the endoplasmic reticulum (ER).

N-Glycosylation is one of the most common co- and post-translational modifications of eukaryotic proteins that occurs in the lumen of the ER. Recent studies have shown that the N-linked glycan chains on glycoproteins play important roles in facilitating to correct folding of proteins as well as in degrading proteins that fail to fold properly.

The dolichol-linked tetradecasaccharides, $\text{Glc}_3\text{Man}_9\text{GlcNAc}_2$ is synthesized on the cytosolic face of ER membrane before being flipped into the lumen of ER. During the translocation of proteins into the ER, an enzyme

complex called OST (oligosaccharyltransferase) transfers oligosaccharide moieties from the dolichol-linked donor substrates to asparagine residues located within the consensus sequence -Asn-Xaa-Ser/Thr- (Xaa: any amino acids except Pro) to form N-linked glycans on nascent polypeptide chains.

Glycan processing begins in the ER immediately after the transfer reaction: glucosidase I (GI) hydrolyses the outermost glucose, followed by glucosidase II (GII) that sequentially removes the remaining two glucose residues. Glycoprotein glucosylation is present in most eukaryotic cells, catalyzed by ER localized UDP-Glc:glycoprotein glucosyltransferase (UGGT), which was firstly purified from rat liver (Trombetta and Parodi, 1992). The most striking property of UGGT is that it recognizes improperly folded proteins with high mannose glycan as preferred substrate. It uses UDP-Glc as glucose donor and transfer the sugar moiety onto the glycan of its bound glycoprotein (Sousa et al., 1992). UGGT activity requires relatively high calcium concentrations.

Calnexin (CNX) and Calreticulin (CRT) are homologous lectin chaperones in the ER. They recognize and bind monoglucosylated glycans with high specificity and assist their folding (Ware et al., 1995). The interplay of glucosidase II, UGGT and CNX/CRT chaperones form a quality control mechanism (Hammond et al., 1994) (Figure 1-4).

The trimming of the two outermost glucose residues by GI and GII triggers the binding of monoglucosylated glycoproteins to CNX and/or CRT, an action that takes place either co- or post-translationally depending on the particular substrate. This complex is disrupted upon GII removal of the innermost glucose. At this stage, properly folded proteins may proceed to their final destinations. In contrast, deglucosylated misfolded species, folding intermediates or unassembled oligomers will be recognized by UGGT and the resulting reaction products will reassociate with the lectins (CNX/CRT). The complexes thus formed will then be retained in the ER. Deglucosylation–reglucosylation cycles driven by the opposite activities of GII and UGGT continues until the glycoprotein acquires its native fold or, alternatively, until ER-mannosidase I removes a mannose to form a Man₈ glycan that signals the glycoprotein for degradation by the ER associated degradation (ERAD) pathway. QC not only prevents the premature exit of immature glycoproteins, but also enhances the folding efficiency by inhibiting protein aggregation and allowing the the correct disulfide formation aided by ERp57, the protein disulfide isomerase (PDI).

1.4 Unfolded Protein Response

The ER is a major protein-folding compartment in a eukaryotic cell and is second only to the cytosol. It is the entrance site for proteins destined to reside in

the secretory pathway or the extracellular environment. Early steps in the maturation of secretory proteins take place in ER, e.g., the folding of the nascent polypeptide chains and posttranslational modifications important for proper folding and function of the protein. The ER relies on an efficient system of protein chaperones that prevent the accumulation of unfolded or aggregated proteins and correct misfolded proteins (Horwich, 2002). If the influx of nascent, unfolded polypeptides exceeds the capacity of the ER folding machinery, the normal physiological state of the ER is perturbed. The accumulation of improperly folded proteins in the ER leads to adaptive responses, collectively known as the unfolded protein response (UPR) (Horwich, 2002).

In order to make the folding capacity of the ER meet the folding challenge, cell needs to decrease the folding demand, while increase the folding capacity of the ER. On one hand, the transcription and translation of genes, encoding secretory proteins are downregulated (Harding et al., 1999), and the clearance of slowly folding or misfolded proteins through ER-associated degradation (ERAD) is increased (Travers et al., 2000). On the other hand, to increase the folding capacity of the ER, the synthesis of ER resident molecular chaperones and foldases is increased (Kozutsumi et al., 1988), and the ER increases in size (Dorner et al., 1989) to dilute the increased unfolded protein load. In this way, cell alleviates the ER stress, and restores the proper ER function.

The complex network of physiological responses to ER stress is orchestrated by only a few ER transmembrane signaling molecules: IRE1, PERK, and ATF6 (Teng et al., 1997). These pathways mediate UPR signal transduction by regulating the production of basic leucine zipper–containing (bZIP-containing) transcription factors that transcribe different subsets of UPR-responsive genes. In multi-cellular organisms, if these adaptive responses are not sufficient to relieve ER stress, the cell dies through apoptosis or necrosis.

The coordinated mechanism of UPR signaling initiation involves GRP78/BiP, the ER chaperone that regulates of the activation of the three proximal ER stress transducers: IRE1, PERK and ATF6. BiP serves as a negative regulator of IRE1, PERK and ATF6 activation by binding to their luminal domains in the resting state. Upon ER stress, improperly folded proteins sequester BiP from interacting with IRE1, PERK, and ATF6 to elicit their dimerization and activation. This BiP-regulated activation provides a direct mechanism to sense the folding capacity of the ER.

PERK is an ER transmembrane protein kinase that phosphorylates a subunit of translation initiation factor 2 (eIF2a) in response to ER stress. Phosphorylation of eIF2a reduces the formation of translation initiation complexes, which leads to reduced recognition of AUG initiation codons and therefore general translational attenuation (Scheuner et al., 2001). The PERK

pathway promotes cell survival not only by limiting the protein-folding load on the ER, but also by inducing transcription of UPR-activated genes. The translation of selective mRNAs that have a lower requirement for eIF2 and the translation initiation complex is enhanced, such as the mRNA encoding the activating transcription factor ATF4 (Harding et al., 2000).

ATF6 is an ER transmembrane-activating transcription factor. Upon ER stress, ATF6a and ATF6b transit to the Golgi compartment where they are cleaved by S1P and S2P proteases to yield a cytosolic fragment (Yoshida et al., 1998). The free ATF6 fragment migrates to the nucleus to activate transcription (Haze et al., 1999).

IRE1 is a type 1 transmembrane Ser/Thr protein kinase that also has a site-specific endoribonuclease (RNase) activity in the cytoplasmic domain. ER stress leads to its dimerization and *trans*-autophosphorylation that activates its RNase activity. The substrate of IRE1a and IRE1b in mammals, XBP1 mRNA, encodes a basic leucine-zipper-containing transcription factor (Mori et al., 2000). Splicing of XBP1 RNA is initiated by the RNase activity of IRE1 to generate mature XBP1 mRNA (Patil and Walter, 2001). Whereas the ATF6 and PERK pathways are not conserved in lower eukaryotes, the IRE1 signaling pathway is conserved in all known eukaryotic cells (Hollien and Weissman, 2006).

The signalling from downstream effectors of IRE1, PERK and ATF6 merges in the nucleus to activate transcription of UPR target genes. The mammalian ER stress element (ERSE) is present in the promoter regions of many, but not all, UPR target genes. Both XBP1 and ATF6 bind to ERSE, along with ATF4, to activate transcriptional induction of target genes. ATF6 also induces XBP1 transcription, providing a positive feedback for the UPR. In particular, upregulation of molecular chaperones and foldases increases the folding capacity of the ER, providing a protective effect for cell survival. In addition, activated Ire1p in yeast induces transcription of genes, such as INO1, that mediate phospholipid biosynthesis to increase the ER volume (Chang et al., 2004).

The UPR also induces transcription of genes encoding proteins that mediate ERAD (Travers et al., 2000). This important component of the UPR stimulates the degradation and clearance of unfolded proteins in the ER lumen.

Prolonged UPR activation leads to apoptotic cell death, in which IRE1 serves a proapoptotic function (Zhang et al., 2001). Activated IRE1 recruits Jun N-terminal inhibitory kinase (JIK) and TRAF2 to activate apoptosis-signaling kinase 1 (ASK1), which in turn activates JNK and mitochondria/Apaf1-dependent caspases (Leppa and Bohmann, 1999; Nishitoh et al., 2002; Yoneda et al., 2001). Procaspase-12 (pCSP-12) is an ER-associated proximal effector of apoptosis (Nakagawa et al., 2000). TRAF2 release from pCSP-12 permits the clustering and

activation of CSP-12. Activated CSP-12 activates CSP-9, which in turn activates CSP-3, leading to apoptosis. In addition, UPR activation induces CHOP/GADD153 expression through the PERK and ATF4 pathways. CHOP is a proapoptotic transcription factor that potentiates apoptosis (Ron, 2002).

Finally, attenuation of cyclin D1 translation in response to prolonged ER stress through PERK leads to cell cycle arrest during G1 phase. This provides an ER checkpoint to prevent cells from progressing through the cell cycle.

1.5 The Scope of Current Study

The goal of this study is initially aimed at understanding how PI3K/Akt signaling pathway confers the anti-apoptotic effect on the mechanistic level.

In chapter 2, I describe the discovery of an elevated ATP hydrolysis activity in PTEN-null MEF cell S100. Following this activity, Dr. Min Fang purified ENTPD5 and CMPK1, the two components contributing to ATP hydrolysis enzymatic cycle. With a hint from my mentor, I confirmed the third component to be Adenylate Kinase 1 (AK1). I then generated recombinant proteins for all three enzymes and reconstituted this coupled ATP hydrolysis reaction in vitro. I also showed that recombinant ENTPD5 have substrate selectivity against UDP and GDP. Using GFP-tagged expression construct, I confirmed that ENTPD5 is an ER enzyme. These data pointed us to explore the involvement of ENTPD5 in protein folding quality control process in the ER.

Finally I made Tet-inducible shRNA constructs for knocking down ENTPD5, which enabled the elucidation of its critical function in PI3K/PTEN/Akt signaling pathway both in vitro and in vivo.

In Chapter 3, I designed and carried out a HTS for ENTPD5 inhibitors, using synthetic chemical library of 350,000 compounds. In collaboration with Dr. MacMillan, I also identified a class of marine natural compounds as ENTPD5 inhibitors. Both synthetic and natural inhibitors can inhibit ENTPD5 activity in cultured cells, recapitulating the effects of ENTPD5 knockdown. More importantly, I demonstrated that PTEN^{-/-} MEF cell are more susceptible to compound inhibitor induced ER stress and cell death. This suggests that ENTPD5 inhibitors may cause synthetic lethality with PI3K/Akt active cancers, rendering these inhibitors promising candidates for cancer therapeutic agents.

Figure from Chapter 1

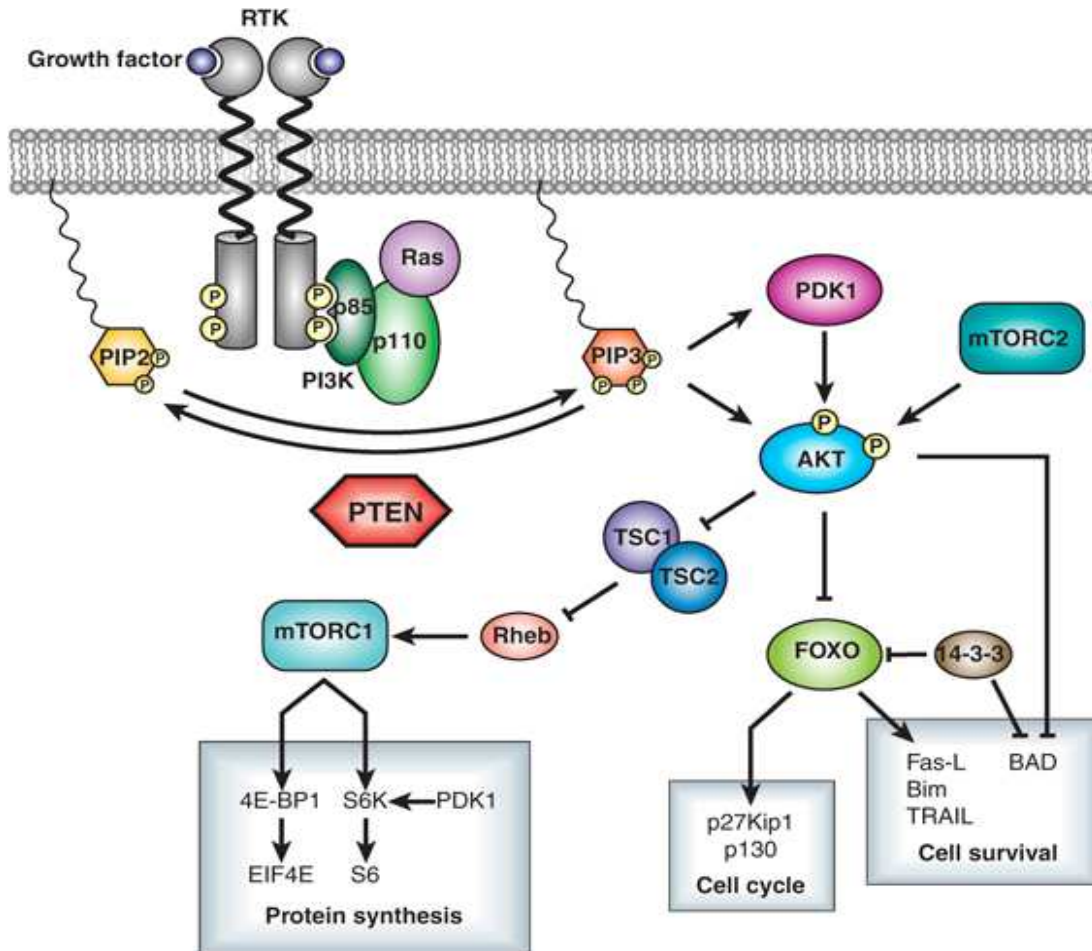


Figure 1-1 Overview of PI3K/PTEN/AKT Signaling Pathway.

Upon binding of extracellular ligand, such as a growth factor, receptor protein tyrosine kinases (RTK) dimerize and autophosphorylate each other on tyrosine residues. Phosphatidylinositol-3 kinase (PI3K) consisting of an adaptor subunit p85 and a catalytic subunit p110 is translocated to the cell membrane and binds to phosphotyrosine consensus residues of the RPTK through its adaptor

subunit. This results in allosteric activation of the catalytic subunit leading to the production of phosphatidyl inositol-3,4,5-triphosphate (PIP3). PIP3 recruits signaling proteins with pleckstrin homology (PH) domains to the cell membrane including AKT. PTEN (phosphatase and tensin homologue deleted from chromosome 10) is a PIP3 phosphatase and negatively regulates the PI3K-AKT pathway. The interaction of PIP3 with the PH domain of AKT likely induces conformational changes in AKT, thereby exposing the two main phosphorylation sites at T308 and S473. T308 and S473 phosphorylation by protein serine/threonine kinase 3'-phosphoinositide-dependent kinases 1 and 2 (PDK1 and PDK2) is required for maximal AKT activation. Activated AKT translocates to the nucleus and mediates the activation and inhibition of various targets resulting in cellular survival and cell growth and proliferation.

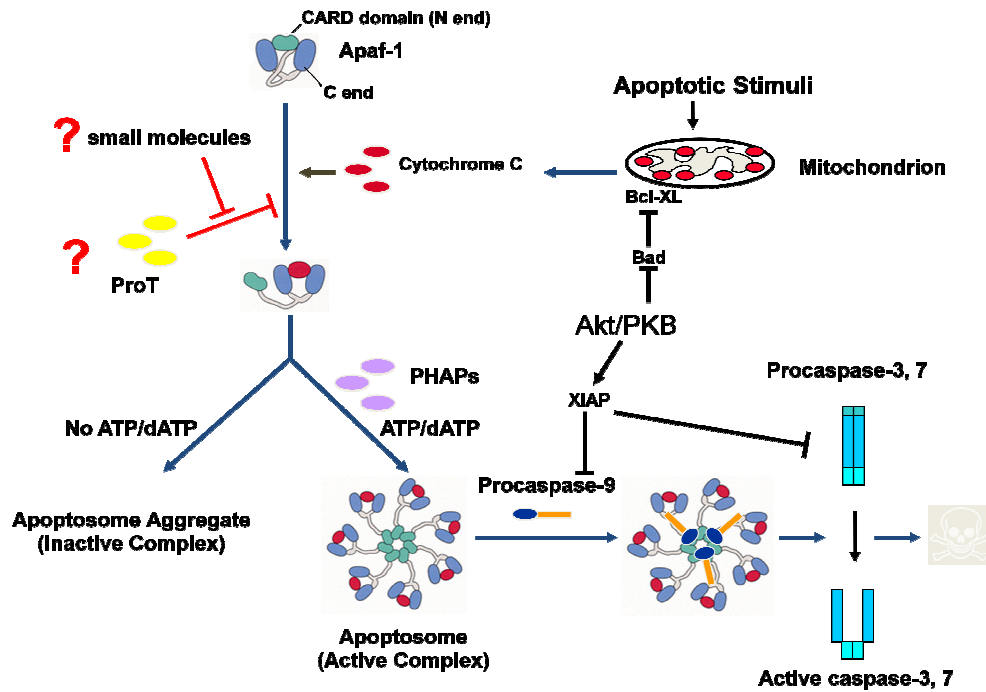


Figure 1-2 Reported Anti-apoptotic Mechanisms of Akt.

Apoptotic stimuli trigger the release of cytochrome c from the mitochondrial intermembrane space to the cytosol, such as which induces the formation of the apoptosome and the activation of procaspase-9. By the action of cytochrome c (Cyto C) and ATP/dATP the Apaf-1 protein adopts a conformation that allows the formation of a heptameric, wheel-like structure, the apoptosome (Zou et al., 1999b). Procaspase-9 molecules can bind to the inner “hub” region of the apoptosome and are activated by dimer formation. Active caspase-9 dimers further cleave and activate executioner Casp3 and Casp7. Akt negatively regulates apoptosis at multiple steps, including sequestering BAD from mitochondria, up-regulating IAP expression and direct phosphorylation of Caspase 9.

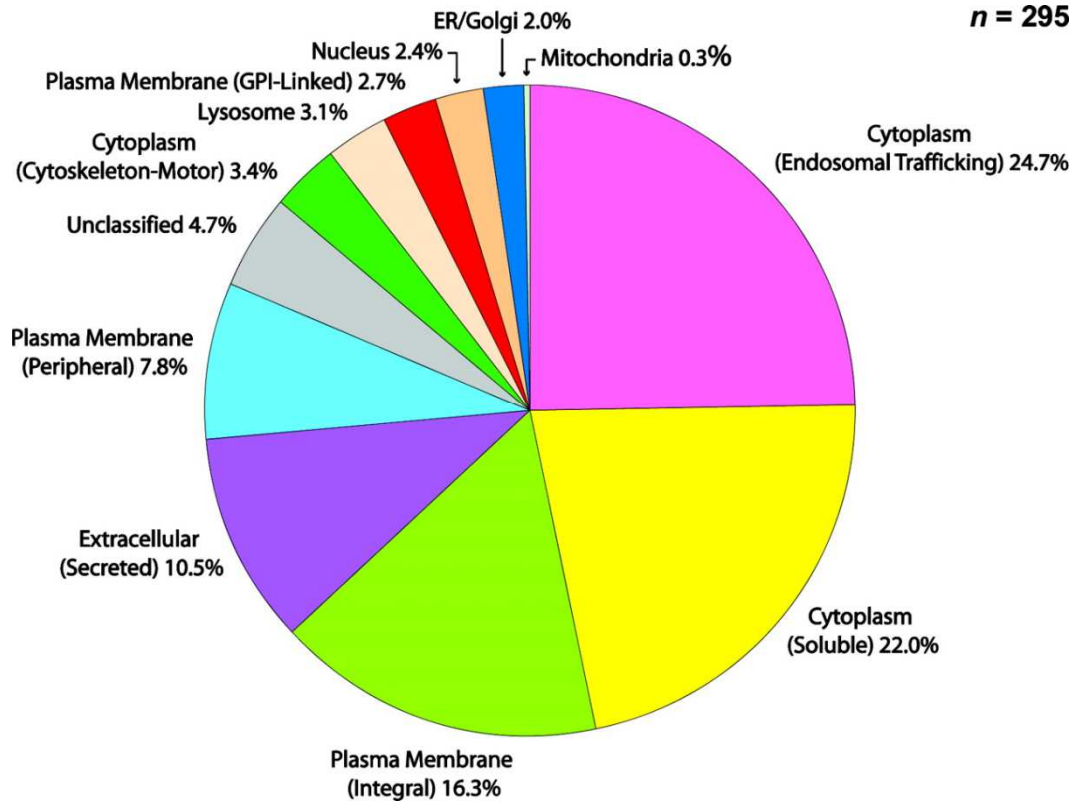


Figure 1-3 Distribution of mammalian proteins by subcellular origin

Adapted from PNAS September 7, 2004 vol. 101 no. 36 13368-13373

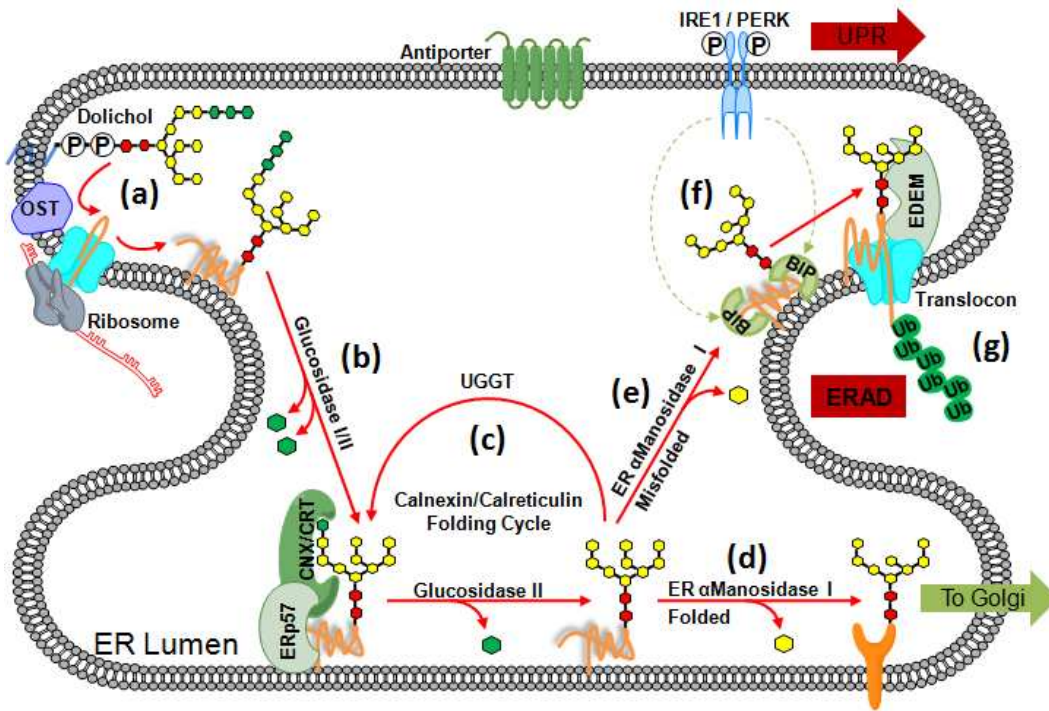


Figure 1-4 N-Glycosylation and Protein Folding in ER

(a) Tetradecasaccharides, $\text{Glc}_3\text{Man}_9\text{GlcNAc}_2$ synthesized on the dolichol pyrophosphate, are transferred en bloc onto the nascent proteins by oligosaccharyltransferase (OST) in the ER lumen. (b) Right after transfer, glucoses at the non-reducing ends are removed by glucosidase I/II. (c) The calnexin (CNX) cycle is mediated by the interplay between UGGT and glucosidase II, which are both inhibited by the action of ER-mannosidase I. If the unfolded proteins are glucosylated by UGGT, CNX or calreticulin (CRT) binds to the glucose residue at the terminal of N-linked glycans and the process is often followed by the correct disulfide formation aided by ERp57. (d) The correctly folded proteins escape from the recognition by UGGT and therefore from the

calnexin cycle. (e) On the other hand, glycoproteins bearing Man 8 (and in some cases shorter ones in which more Man are trimmed) also exit the cycle and are recognized by EDEM, which allows these proteins to be targeted for degradation. (f) Accumulation of improperly folded proteins in the ER lumen evokes Unfolded Protein Response. (g) Once in the cytosol after the retrotranslocation, the proteins are polyubiquitinated and degraded by 26S proteasome.

Chapter 2 : Identification and Characterization of ENTPD5

2.1 High ATP Hydrolysis Activity in PTEN-null Lysate

Our laboratory has been studying mammalian cell apoptotic pathways using biochemical approaches. In an attempt to study why PTEN knockout MEFs, in comparison to MEFs prepared from their heterozygote littermate, were resistant to several apoptotic stimuli, we prepared cytosolic extracts from these cells and studied their caspase-3 activation in vitro. As reported previously, the PTEN-null MEFs showed elevated levels of phosphorylated AKT and p70S6 kinase while the total protein level of these two kinases remained the same as in PTEN heterozygous MEFs (Stambolic et al., 1998). We quickly noticed that S-100 cell extracts (prepared after collecting the supernatants of 100,000 g spin of broken cells) from PTEN-null MEFs had a reduced ability to activate caspase-3 in vitro compared to that from the heterozygous MEFs (Figure 2-1). Surprisingly, there was no detectable difference in the level of protein components of core intrinsic apoptotic pathway including cytochrome c, Apaf-1, procaspase-9, and procaspase-3 (Li et al., 1997). The lower activity was caused by the decreased ATP level in S-100 from PTEN-null MEFs. Adding exogenous ATP or dATP, two energy sources for caspase-9/3 activation by Apaf-1/cytochrome c, leveled the difference in caspase-3 activation between these extracts (Figure 2-2). Given that cellular ATP levels are usually relatively stable, we reasoned that the

difference in ATP in S-100 was a result of S-100 preparation, which took about 1 hour. Indeed, as shown in Figure 2-3, the ATP levels in PTEN-null MEFs was only slightly lower than those in the heterozygous MEFs if the measurement was carried out right after cells were harvested. When the broken cell suspension, or supernatants after 10,000 g spin (S-10), or S-100 were incubated on ice for 2 hour before the ATP levels were measured, ATP concentrations in the extracts from PTEN knockout MEFs were much lower than those from heterozygous MEFs. The higher amount of ATP in S-10, we reasoned, might be due to ATP released from the organelle during preparation. Such an observation indicated that there was a higher ATP hydrolysis activity (or activities) in the PTEN knockout cell extracts. To measure this activity directly, we incubated α -P³²-ATP with the S-100 extracts and analyzed the radioactivity using thin layer chromatography. As shown in Figure 2-4, more radio-labeled ATP was hydrolyzed in the S-100 from PTEN knockout MEFs. Interestingly, the nucleotide was mostly hydrolyzed into AMP.

2.2 ENTPD5 Is Underlying the Elevated ATPase Activity

Dr. Min Fang purified this activity, starting with 800 milligrams of S-100 from PTEN-null MEFs followed by 5 column chromatographic steps. The identity of the enzyme turned out to be ectonucleoside triphosphate diphosphohydrolyase 5, ENTPD5, a member of the ENTPD enzyme family that hydrolyze tri- and/or

diphospho-nucleotide to mono-phosphonucleotide (Reviewed by Robson et al., 2006).

To verify that ENTPD5 is indeed the enzyme that caused higher rate of ATP hydrolysis to AMP in PTEN-null MEFs, we knocked down ENTPD5 in PTEN-null MEFs with siRNA oligos, and the ATP to AMP hydrolysis activity was diminished while a control siRNA oligo had no effect (Figure 2-6B). Knockdown of ENTPD5 also enhances UV induced apoptosis in PTEN-null cells (Figure 2-6A).

To demonstrate directly the nucleotide hydrolysis activity of ENTPD5, we generated recombinant human ENTPD5 protein in insect cells using a baculovirus vector and purified the enzyme to homogeneity. The purified enzyme was then incubated with ATP, ADP, CTP, CDP, GTP, GDP, UTP, and UDP and the released phosphate was measured. The purified recombinant ENTPD5 can only hydrolyze UDP and GDP directly with UDP being the best substrate (Figure 2-7).

The inability of purified, recombinant ENTPD5 to hydrolyze ATP to AMP was quite puzzling to us initially. However, recombinant ENTPD5 can replace PTEN-null S-100 to produce ATP to AMP conversion activity in the presence of PTEN^{+/-} S100. This puzzle was solved by the identification of small molecule co-factor and additional protein factors required for such a reaction.

2.3 ENTPD5, CMPK1, and AK1 Constitute an ATP to AMP

Hydrolysis Cycle

Based on the fact that purified ENTPD5 is unable to hydrolyze ATP directly, we realized that since the assay also included S-100 from PTEN heterozygous MEFs, there must be more factors in S100 that are also required to hydrolyze ATP to AMP. These factors seem to be also presented in other cell types as well. For example, when we added purified, recombinant ENTPD5 and UMP to the dialyzed S-100 from PTEN heterozygous MEFs, or large-scale cultured HeLa cells, the ATP to AMP hydrolysis was reconstituted. This observation made purification of these factors much easier since HeLa cell can be grown in large quantity in suspension. To identify these factors, we fractionated HeLa cell S-100, using a Q-Sepharose column, and collected both the flow through (Q-FL) and column-bound fraction eluted with 300 mM NaCl (Q-30). Neither fraction alone was able to hydrolyze ATP to AMP, although the Q-30 fraction, when ENTPD5 and UMP were present, hydrolyzed ATP to ADP. When both the Q-FL and Q-30 fractions were included, the ATP to AMP activity was fully reconstituted.

Dr. Min Fang purified the activity present in the Q-30 fraction. The activity present in the Q-30 fraction was purified by subjecting HeLa S-100 onto four sequential column chromatographic steps and finally onto a Mini Q column. The activity was eluted from this column with a linear salt gradient from 40 mM to 120

mM NaCl and fractions eluted from the column were assayed in the presence of recombinant ENTPD5, UMP, and the Q-FT fraction (Figure 2-8, right lower panel). A peak of activity was observed at the fractions 8-10. The same fractions were subjected to SDS-PAGE followed by silver staining and two protein bands close to 37 and 20-kDa markers correlated perfectly with activity (Figure 2-8). Both bands were identified by mass spectrometry as human UMP/CMP kinase-1 (CMPK1).

The identification of UMP/CMP kinase in the Q-30 fraction shed light on why UMP is a required co-factor for the ATPase activity and how ENTPD5 plus this enzyme generates ADP from ATP. For this reaction, co-factor UMP is phosphorylated into UDP by CMPK1 and ATP, generating ADP. UDP is subsequently hydrolyzed by ENTPD5 to UMP, completing the cycle with net conversion of ATP to ADP.

With this knowledge, we then made an educated guess that the third protein factor present in the Q flow through fraction is Adenylate kinase; which converts two ADP into one ATP and AMP, correlating to the observed ATP to AMP conversion seen in PTEN-null cell extracts. To confirm this, we took the Q flow through fraction and subjected it to a gel-filtration column and collected the fractions eluted from the column to assay for ATP to AMP hydrolysis in the presence of UMP, purified recombinant ENTPD5, and the Q-30 fraction that contains CMPK1. An activity peak centered at fractions 17-18 was observed (Figure 2-9 upper panel).

When these fractions were subjected to western blotting analysis using an antibody against Adenylate kinase-1 (AK1), the detected western blotting band correlated perfectly with the activity peak (Figure 2-9, lower panel). The correlation was maintained with additional chromatographic steps (not shown).

We subsequently generated recombinant CMPK1 and AK1 in bacteria and purified them to homogeneity (Figure 2-10, lanes 9, 12). Purified recombinant ENTPD5 expressed in insect cells runs as a triplet on SDS-PAGE gel that could be shifted down to a doublet after treatment by PNGase F, indicating that ENTPD-5 is glycosylated.

These purified recombinant proteins allowed us to reconstitute the ATP to AMP hydrolysis cycle. Only when all three enzymes and UMP co-factor were present, efficient ATP to AMP conversion was observed (Figure 2-10, lanes 1-8).

2.4 ENTPD5 Is an ER Enzyme

After purification and identification of ENTPD5 from PTEN-null cells, we realized that ENTPD5 is identical to a previously purified ER UDPase (Thometta and Helenious, 1999). Although we identified and purified ENTPD5 from the S-100, the enzyme most likely fractionated there as a result of broken ER from physical shearing during the cell-breaking process. The majority of the enzyme was indeed in

the pellet fraction that could only be solubilized by detergent. When we expressed an ENTPD5-GFP fusion protein in cells, the GFP signal was co-localized with the co-expressed ER-DsRed marker (Figure 2-11). The ER location of ENTPD5 and its preferred specificity for UDP suggested that ENTPD5 functions in the process of reglucosylation catalyzed by UGGT for calnexin/calreticulin-mediated protein folding (Thometta and Parodi, 2003). In this reaction, UDP is generated after the conjugated glucose gets transferred to the glycosidase I/II trimmed core glycan on N-glycosylated proteins. UDP-glucose is made in the cytosol and transported into ER through the UDP-sugar transporter, which is an antiporter that must exchange out one molecule of UMP for each UDP sugar conjugate (Hirschberg et al., 1998). UDP therefore needs to be hydrolyzed to UMP to prevent end-product feedback inhibition of UGGT, as well as to serve as substrate for the antiporter (Thometta and Helenious, 1999). UMP will then be phosphorylated back to UDP by CMPK1 in cytosol and the generated ADP will be converted to ATP and AMP by AK1 (diagramed in Figure 2-12).

2.5 Knockdown of ENTPD5 Causes ER Stress and Growth Inhibition

Since cells with activated PI3K/AKT pathway increase their cellular protein translation level, cells need to evolve a corresponding system in ER to accommodate the high demand for protein folding process. It is possible that cells may do so by

up-regulating ENTPD5 levels to increasing the conversion of UDP to UMP in ER. Thus, reducing the level of ENTPD5 in cells with active AKT and high level of protein translation should induce ER stress. In addition, since many growth-promoting cell membrane receptors are highly N-glycosylated, loss of function of ENTPD5 could affect their folding process, resulting in their reduction and subsequently cell growth arrest. To test this hypothesis, we engineered cell lines based on the PTEN-null MEFs in which the expression of ENTPD5 could be knocked down with the addition of Doxycycline (Dox), which turned on a Tet-suppressor-controlled shRNA targeting ENTPD5. As shown in Figure 2-13, comparing to PTEN-null MEFs expressing GFP shRNA, Dox addition to the culture media resulted in successfully knockdown of ENTPD5 expression in these cells. As a result, an ER stress marker, Bip, was induced. Cellular N-glycosylation level, as measured by PHA blotting, was down after Dox treatment (lanes 5-8). Interestingly, the levels of EGFR, Her-2/Erb-2, and type I insulin-like growth factor receptor (IGF-IR) β were significantly decreased after ENTPD5 knockdown.

To confirm the above-mentioned cellular effects after ENTPD5-targeting shRNA expression was specific, we introduced into these cells a cDNA encoding ENTPD5 with silent mutation in the shRNA target sequence. In these cells, although the endogenous ENTPD5 was still knocked down after addition of Dox (Figure 2-14, lanes 2, 4, 6), the expression of an shRNA resistant wild type transgene (three flag

tags were fused to ENTPD5 coding sequence so it migrated higher) led to complete reversal of Bip induction, lowered glycosylation, and down-regulation of growth factor receptors (lane 4). In contrast, introducing an E171A mutant that abolishes UDP hydrolysis activity of ENTPD5 was not able to rescue these phenotypes (lanes 6). These growth-promoting receptors are expressing at higher level in PTEN-null cells (Figure 2-15).

Consistent with the loss of highly N-glycosylated growth factor receptors after ENTPD5 knockdown, cell growth was also dramatically attenuated. As shown in Figure 5F, when ENTPD5 in PTEN-null MEFs was knocked down after addition of Dox, very few colonies grew on the culture dish after 10 days although same number of cells were plated initially and they were cultured under the same condition (left row). The growth inhibition was rescued when the shRNA resistant ENTPD5 cDNA was expressed (middle row) while the inhibition was exacerbated if an enzymatic dead mutant of ENTPD5 was expressed instead (right row).

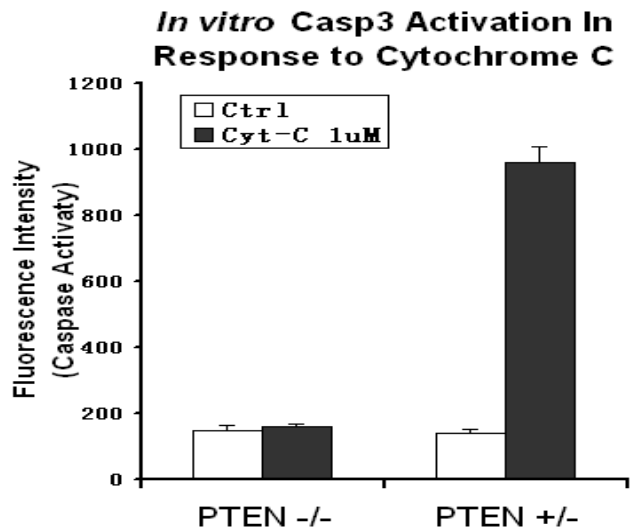
Figures from Chapter 2

Figure 2-1 In Vitro Casp3 Activation Defect in PTEN-null Lysate

S100 were prepared from *PTEN*^{+/-} and *PTEN*^{-/-} cells as described in Experimental procedure. Recombinant cytochrome c was added into S100 at 1uM final concentration, followed by 1hr incubation at 30°C. Caspase 3 activation was then assessed using fluorogenic substrate as described in Experimental procedure. Error bar represents standard deviation of two independent experiments. (by Dr. Min Fang)

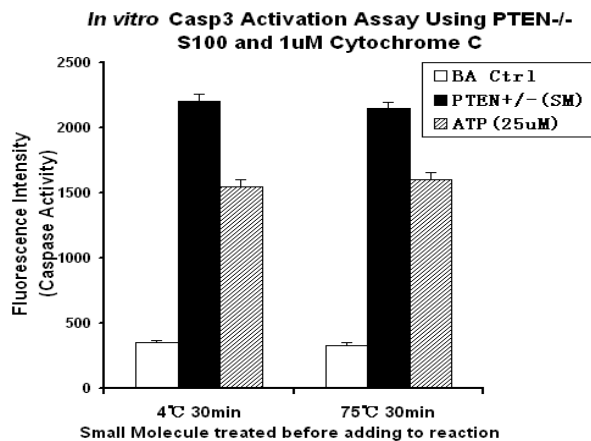


Figure 2-2 Casp3 Activation Defect is Due to Lack of ATP

S100 were prepared from *PTEN*^{+/-} and *PTEN*^{-/-} cells as described in Experimental procedure. Small molecule fraction from *PTEN*^{+/-} S100 is prepared with centrifugal filter with M.W. cutoff of 1000 Da. This small molecule fraction and ATP was heated at indicated temperature and mixed in to *PTEN*^{-/-} S100 at 1:1 ratio, followed by titration of cytochrome c at 1 μ M final concentration. After 1hr incubation at 30°C, Caspase 3 activation was assessed using fluorogenic substrate as described in Experimental procedure. Error bar represents standard deviation of two independent experiments. (by Dr. Min Fang)

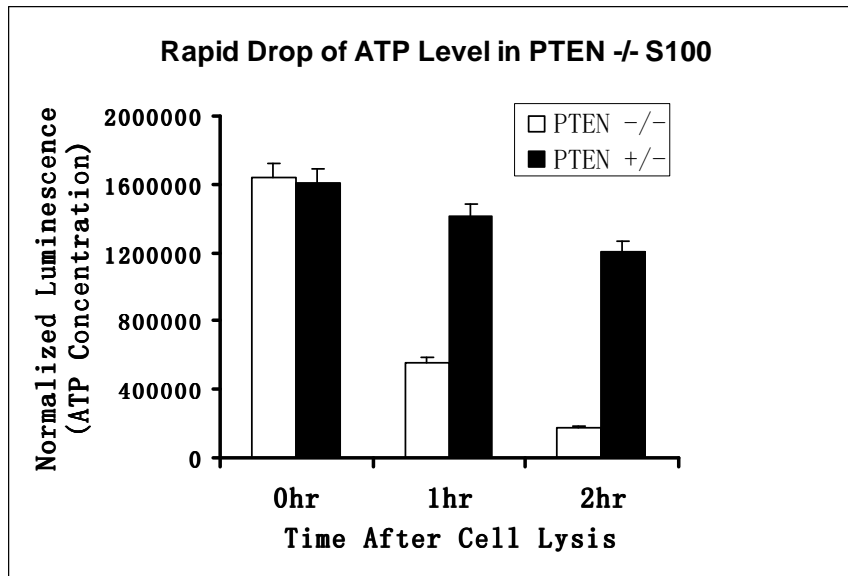


Figure 2-3 Rapid Depletion of ATP in PTEN-null Lysate

Cell extracts were prepared from *PTEN*^{+/-} and *PTEN*^{-/-} cells, aliquots of 20 μ l samples were incubated on ice for indicated time after cell breakage followed by immediate measurement of ATP using a Cell Titer-Glo kit. Error bar represents standard deviation of two independent experiments.

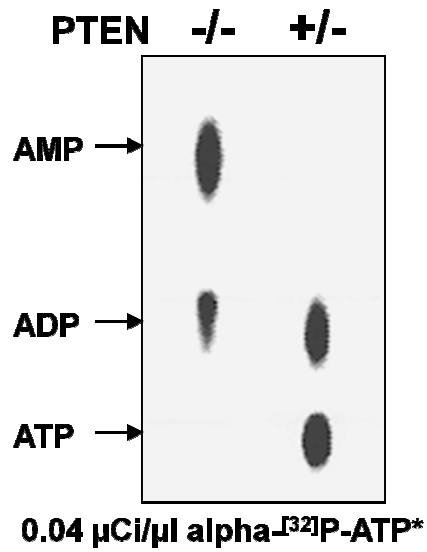


Figure 2-4 Tracing ATP Hydrolysis Products by TLC

Aliquots of 30 µg of S-100 fractions from *PTEN*^{+/-} or *PTEN*^{-/-} cells were incubated with α-P³²-labeled ATP and analyzed by TLC as described in the Experimental Procedure. Positions for ATP, ADP, or AMP were indicated.

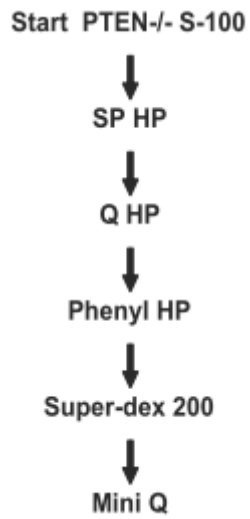


Figure 2-5 ENTPD5 Purification Scheme

Diagram of the purification scheme for ATP hydrolysis activity from S-100 of *PTEN*^{-/-} MEF cells.

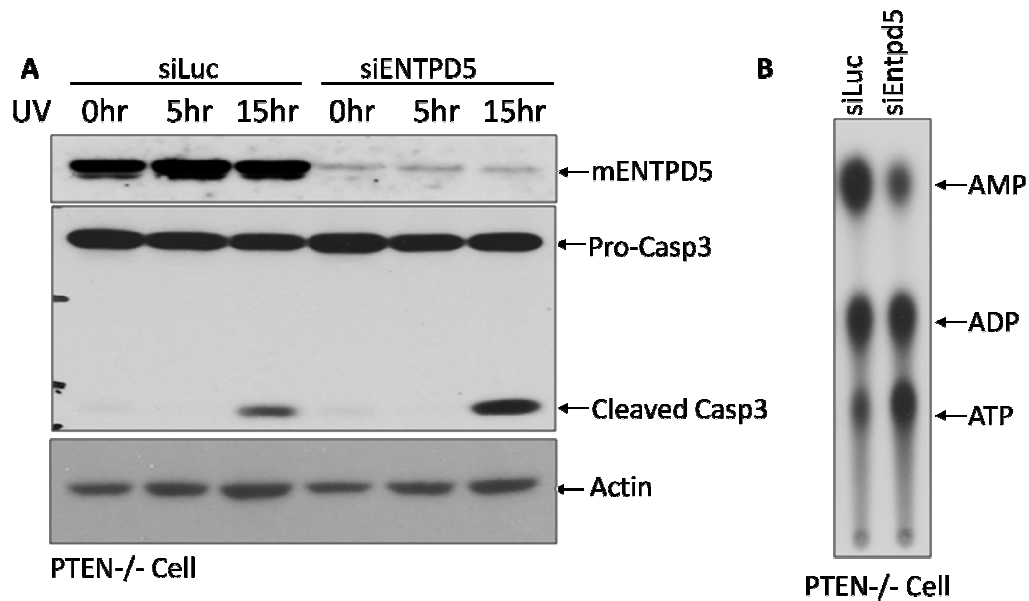


Figure 2-6 Confirmation of ENTPD5

(A) PTEN^{-/-} MEF Cell were transfected with control siRNA and mouse ENTPD5 siRNA. 48h after tranfection, cells were treated with UV irradiation. Cell lysates (S-100) were prepared at indicated time point after UV treatment. Aliquots of 30 μ g protein of indicated samples were subjected to 10% SDS-PAGE followed by western analysis of ENTPD5 and Casp3. (B) PTEN^{-/-} MEF Cell were transfected with control siRNA and mouse ENTPD5 siRNA. 48h after tranfection, cells were harvested, and S-100 were prepared and normalized. aliquots of 30 μ g were used for ATP hydrolysis assay. Positions of ATP, ADP, and AMP are indicated.

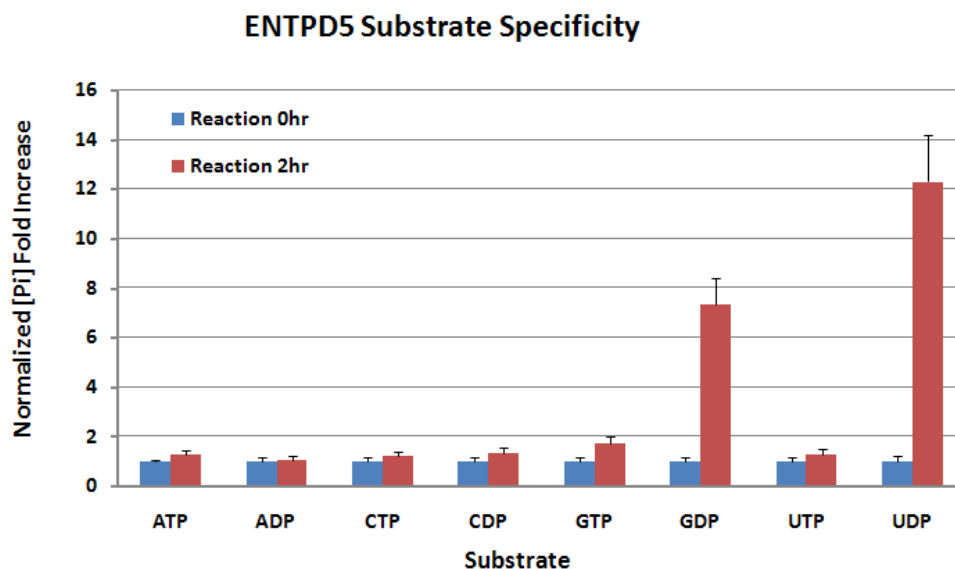


Figure 2-7 ENTPD5 Substrate Specificity

The recombinant human ENTPD5 was generated and purified as described in the Experimental Procedures. The nucleotide hydrolysis reactions were carried out in triplicate by mixing 0.1 mg/ml ENTPD5 with 50 μ M indicated nucleotides. After 2 hr incubation at 30°C, released free phosphate was measured by malachite green assay as described in the Experimental Procedures. Data shown are representative of three independent experiments. Error bars indicate SEM.

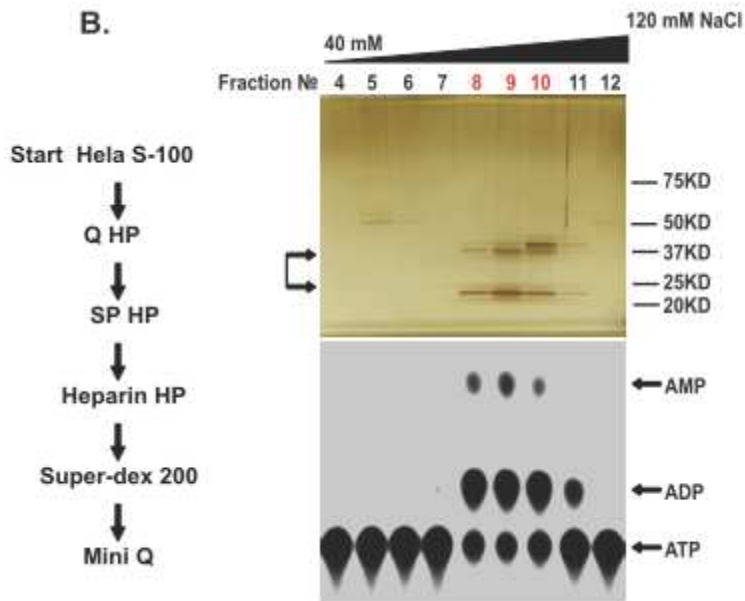


Figure 2-8 Purification of CMPK1

(Left) Diagram of the purification scheme for the required factor in Q-30. (Right) Final step of purification of CMPK1. (Top) Aliquots of 60 μ l indicated Mini Q fractions that were subjected to 4%–10% gradient SDS-PAGE followed by silver staining. Arrow indicates the protein band correlated with ATP hydrolysis activity. (Bottom) Aliquots of 5 μ l indicated fractions that were mixed with 15 μ l of dialyzed Q-FL fraction in the presence of 100 μ M UMP and 18 ng recombinant ENTPD5 and were assayed for ATP hydrolysis activity. (by Dr. Min Fang)

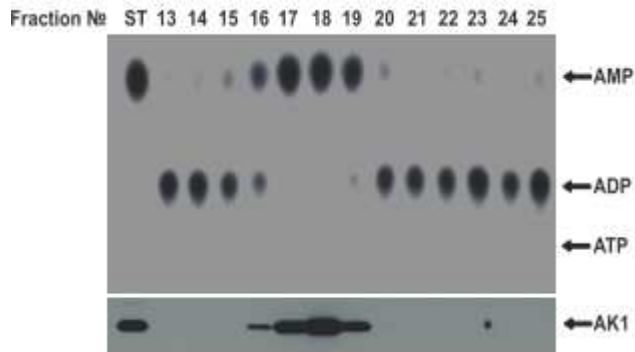


Figure 2-9 Confirmation of AK1 as the third factor

3 ml of the Q-FL fraction was concentrated to 600 μ l with a spin column and analyzed on a Supdex-200 column (10/30). Fractions of 1 ml were collected, and aliquots of 7.5 μ l of indicated fractions were combined with 7.5 μ l dialyzed Q-30 fraction, 100 μ M UMP, and 18 ng recombinant ENTPD5 and were assayed for ATP hydrolysis activity. Positions of radioactive ATP, ADP, and AMP are indicated. (Bottom) Aliquots of 10 μ l of indicated fractions were subjected to 10% SDS-PAGE followed by western blotting analysis using an antibody against human adenylate kinase 1 (AK1).

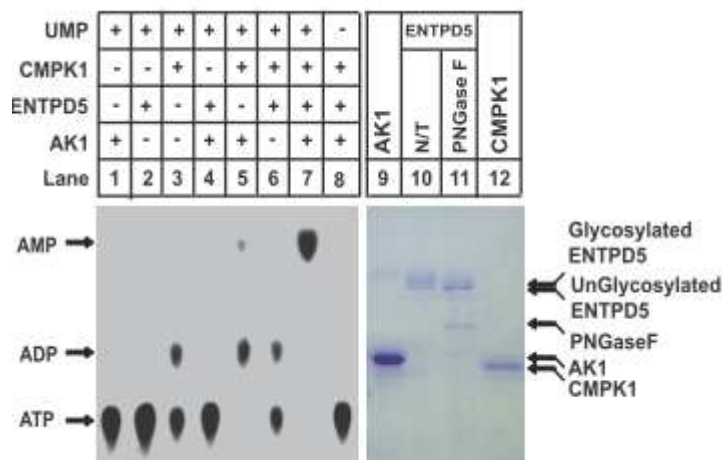


Figure 2-10 In Vitro Reconstitution of ATP Hydrolysis Cycle

(Left) Aliquots of recombinant AK1 (lane 1), ENTPD5 (lane 2), and CMPK1 (lane 3) (final concentration, 1 $\mu\text{g/ml}$) were incubated alone or were sequentially combined as indicated (lane 4 to 8) in the presence (lane 1 to 7) or absence (lane 8) of UMP (100 μM) for ATP hydrolysis activity. Position of ATP, ADP, or AMP was indicated. (Right) Aliquots of 10 μg recombinant AK1 (lane 9), ENTPD5 (lane 10) or ENTPD5 pretreat with PNGase F (NEB) (50 units/ μg ENTPD5) (lane 11), and CMPK1 (lane 12) were subjected to 10% SDS-PAGE followed by Coomassie brilliant blue staining.

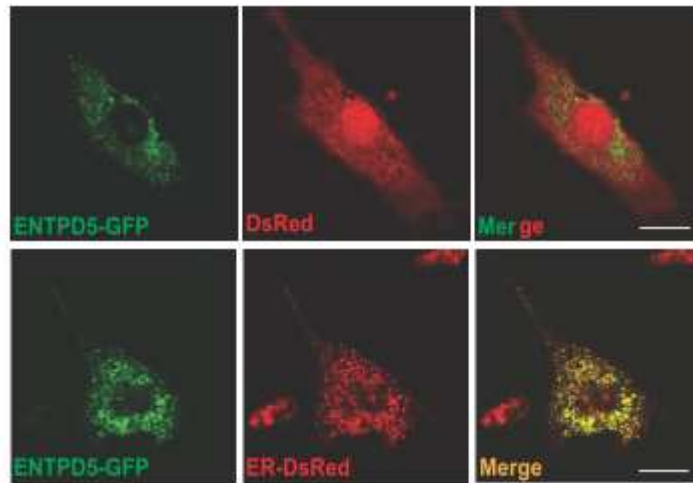


Figure 2-11 ENTPD5 is an ER Localized Enzyme

PTEN^{-/-} MEF cells were cotransfected with mouse ENTPD5-GFP and free DsRed or with ENTPD5-GFP and ER-localized DsRed (ER-DsRed). ENTPD5-GFP colocalized with ER-DsRed (bottom row), but no obvious codistribution with free DsRed was observed (top row). Scale bars, 10 μ m.

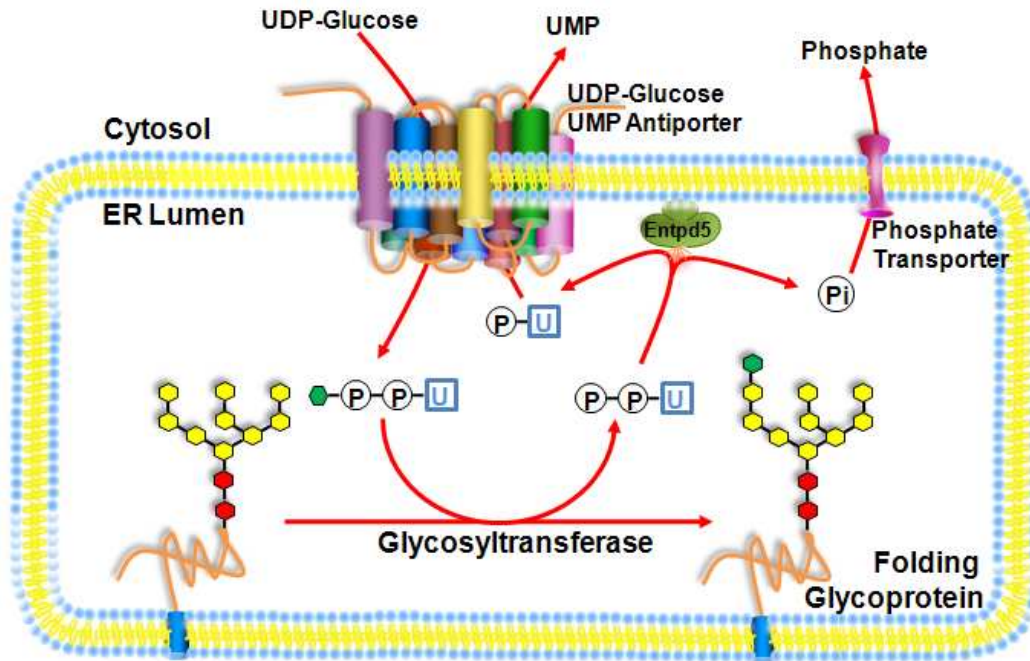


Figure 2-12 Working Model for ENTPD5

UDP-glucose is made in the cytosol and transported into ER through the UDP-sugar transporter, which is an antiporter that must exchange out one molecule of UMP for each UDP sugar conjugate (Hirschberg et al., 1998). UDP therefore needs to be hydrolyzed to UMP to prevent end-product feedback inhibition of UGGT, as well as to serve as substrate for the antiporter (Thometta and Helenious, 1999). UMP will then be phosphorylated back to UDP by CMPK1 in cytosol and the generated ADP will be converted to ATP and AMP by AK1 .

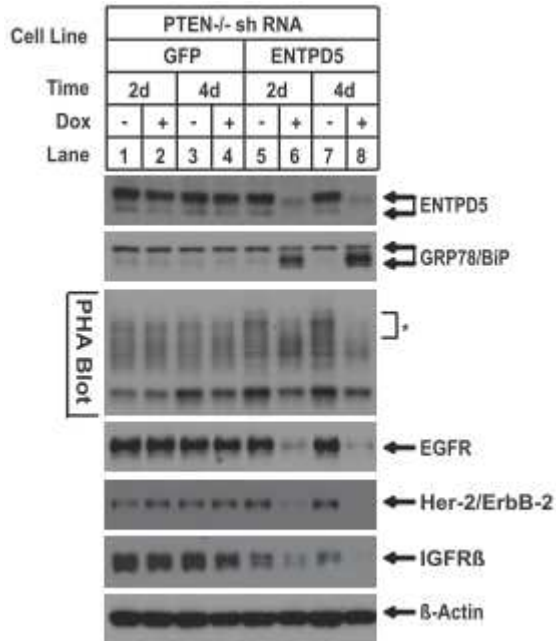


Figure 2-13 ENTPD5 Knockdown Induces ER Stress

PTEN^{-/-} MEF cells with doxycycline (Dox)-inducible expression of shRNA-targeting ENTPD5 was generated as described in the Experimental Procedures. After 2 or 4 days induction with Dox (0.125 μg/ml), cells were harvested and total cell lysates were prepared as described in the Extended Experimental Procedures. Aliquots of 10 μg protein were subjected to SDS-PAGE followed by western blotting analysis using the indicated antibodies. Glycosylation was visualized by PHA blot as indicated. Asterisk denotes decreased glycosylated proteins.

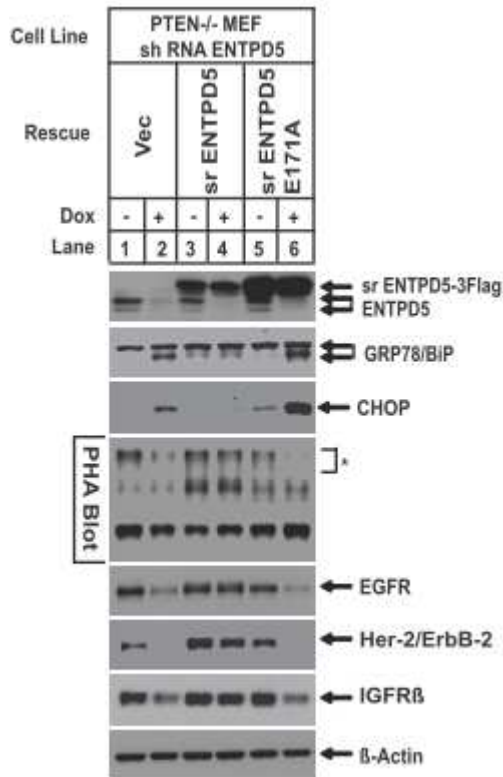


Figure 2-14 Rescue Experiment for ENTPD5 Knockdown

Rescue cell lines with expression of shRNA-resistant wild-type or catalytic dead mutant (E171A) ENTPD-5 were established as described in the Extended Experiments Procedures. Same as in (C), after 2 days culture, cells were harvested, and total cell lysates (10 μ g/lane) were subjected to SDS-PAGE followed by western analysis as indicated. Glycosylation was visualized by PHA blot analysis.

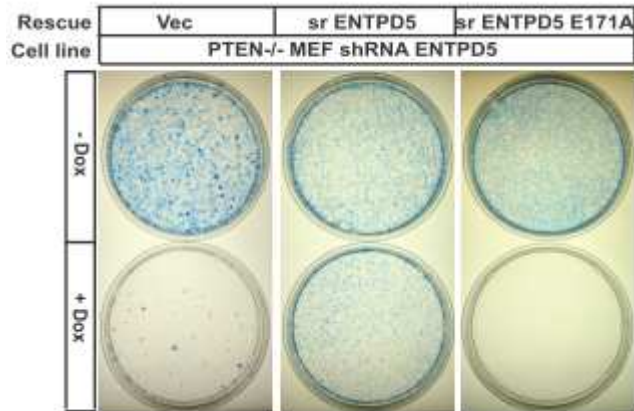


Figure 2-15 Knockdown of ENTPD5 Causes Growth Arrest

Rescue cell line was plated at density of 5×10^4 /100 mm dish and treated with Dox as in (C). Cell medium was changed each 3 days. After 10 days culture, the plates were stained by methylene blue.

Chapter 3 : Screen for ENTPD5 Inhibitors

3.1 Introduction

The phosphatidylinositol 3-kinase (PI3K) signaling axis impacts on cancer cell growth, survival, motility, and metabolism. This pathway is activated by several different mechanisms in cancers, including the prevalent somatic genetic alterations leading to the inactivation of the tumor suppressor gene PTEN and gain-of-function mutations targeting PIK3CA--the gene encoding the catalytic phosphoinositide-3 kinase subunit p110 alpha (Tokunaga et al., 2008).

These alterations trigger a cascade of biological events, from cell growth and proliferation to survival and migration, which contribute to tumor progression. Therefore, the PI3K/AKT/mTOR pathway has been considered an attractive target for the development of novel anti-cancer molecules. Indeed, several tyrosine kinase inhibitors and signal transduction inhibitors specifically targeting the kinases involved in this pathway have been developed.

Given the important role of ENTPD5 in PI3K/PTEN/Akt signaling cascade, we decided to employ high volume biochemical screening method to identify inhibitors for ENTPD5.

3.2 HTS Assay Development and Optimization

We have previously shown that insect cell expressed recombinant ENTPD5 specifically hydrolyze UDP and GDP in vitro. The initial design of primary screen assay is to directly measure inorganic phosphate (Pi) released from UDP hydrolysis by ENTPD5 (Figure 3-1A), using an colorimetric malachite green procedure (Baykov et al., 1988). This procedure is based on the reaction of inorganic phosphate with molybdate and malachite green dye, in the presence of 6N sulfuric acid, to generate a highly colored dye-phosphomolybdate complex with peak absorbance at between 610 nm and 635 nm. We adapted this assay into 384-well plate format, and screened an 8,000 compound test library in singlet. To our dismay, however, none of the cherry picked 64 primary hits can be verified when we repeat the assay in triplicate (data not shown). We later figured out that the highly viscous malachite green reagent sometimes caused random clogging (roughly 1% chance) of P30 screen robot pipette tips, which arise to false positive hits. Another concern is that a large portion of the HTS library consists of colored compounds, which may interfere with malachite green readout at OD620, and thus leads to false negative results. Besides, the acidity of malachite green reagent also poses a serious threat toward the stainless steel pipette modules of the screen robot. Therefore the malachite green assay is not ideal for large scale primary screen.

So we designed a new assay by coupling the ENTPD5 catalyzed UDP hydrolysis to the UMP Kinase catalyzed UMP phosphorylation (Figure 3-1B). These two reactions form a futile cycle of UMP/UDP interconversion, and the net result is one molecule of ATP being consumed in each hydrolysis/phosphorylation cycle. Inhibition of either enzyme will result in an increase of residual ATP at the end of the reaction, which can be readily detected by well-established HTS compatible luciferase assay. The luminescence readout should not only improve sensitivity and signal/noise ratio of the assay, but is also insusceptible to the influence of compound color. The remaining caveats are: 1) in order to enrich ENTPD5 inhibitors, we have to make sure that ENTPD5 is the rate limiting enzyme in the coupled reaction; and 2) properly designed counter screens are needed to filter out UMP Kinase inhibitors and non-specific inhibitors from primary hit list.

To implement this idea, we first cloned the UMP kinase gene *pyrH*, from enterobacteria *Escherichia coli* genome, which encodes a peptide of 239 amino acids, into pET28a expression vector with N-terminal polyhistidine (6xHis) tag. The *E. coli* UMP Kinases (UMPKeco) are hexamers regulated by GTP (allosteric activator) and UTP (inhibitor), and have no homologs in eukaryotes (Serina et al., 1995). We introduced a D159N mutation by site directed mutagenesis on UMKeco to increase its solubility at neutral pH (Serina et al., 1996). The pET28a-UMPKecoD159N construct was transformed into competence *E. coli*

BL21 (DE3). After induction by IPTG for 4hr at 37°C, the recombinant UMPKeco D159N protein was extracted from the bacteria and purified using Nickel beads (Figure 3-2A).

To test whether the coupled reaction could indeed happen in vitro, we titrated the recombinant human ENTPD5 protein, expressed and purified from insect cell, into a mixture of 18ng of UMPKeco recombinant protein, 50µM of UMP and 25µM of GTP in a total 40µl volume to produce the Enzyme Mixture. The reaction was started by adding in 10µl Substrate Solution containing 500µM ATP. After incubation at 37°C for one hour, reaction was stopped by adding 10µl of luciferase based Cell Titer Glo reagent into each well to quantify the residual ATP (Figure 3-2B). The data indicate that 3ng of recombinant ENTPD5 protein is enough to consume about 90% ATP in the reaction, creating a robust 10-fold readout window to assess inhibition. Further increasing recombinant ENTPD5 would compromise the sensitivity of the coupled reaction.

The second critical variable is UMP concentration. In the coupled reaction, UMP is converted by UMPKeco into UDP, the direct substrate of ENTPD5. To determine the optimal concentration range of UMP, we then titrated UMP into the Enzyme Mixture containing 3ng ENTPD5, 18ng UMPKeco and 25µM GTP. Reaction is started by adding 10µl Substrate Solution and residual ATP was measured after incubation at 37°C for indicated time (Figure 3-3). After 90 min

incubation at 37°C, 33μM UMP could already provide satisfactory reaction speed. Since the final concentration of library compound will be 5μM, higher UMP concentration is not advisable, because competitive inhibitors may be missed out if excessive substrate molecules are available to ultimately displace them. The UMP concentration in Enzyme Mixture was fixed at 25μM.

We then went on to test whether ENTPD5 is the rate limiting enzyme in the coupled reaction. Due to lack of published ENTPD5 inhibitors, we have to use enzyme dilutions to mimic inhibition. We diluted both ENTPD5 and UMPKeco by 3 fold to mimic 66% inhibition of the enzymes (Figure 3-4), and the luminescence reading readily reflected this inhibition. And then we dilute ENTPD5 or UMPKeco respectively by 3 fold, to see which one is rate-limiting. The data shows that ENTPD5 dilution accounts for the luminescence reading increase of the double enzyme dilution (Figure 3-5). This means that UMPKeco is in excess and the assay is biased to preferentially pick up ENTPD5 inhibitors.

To accommodate as many plates as possible in each four-hour screen session assigned by HTS laboratory, and to simplify the incubation condition, we finally optimized the screen assay to perform at room temperature for 3 hours (Figure 3-6).

3.3 Counter Screen Design

In order to filter out potential false positive hits from primary screen result, we split the coupled reaction apart, as secondary (counter screen) UMPKeco assay and tertiary (confirmatory) malachite green assay (Figure 3-7). The secondary assay is based on UMPKeco catalyzed UMP phosphorylation yielding UDP, during which ATP will be consumed. Secondary Enzyme Mixture consists of 18ng UMPKeco protein, 25 μ M GTP (allosteric activator), and 500 μ M of UMP in a total 40 μ l volume. Assay was started by adding 10 μ l of 250 μ M ATP into the Enzyme Mixture. After one hour incubation at room temperature, reaction was stopped by 10 μ l Cell Titer Glo reagent, and residual ATP was quantified 5 minutes later by luminometer.

For the tertiary assay, the Enzyme Mixture contains 3ng ENTPD5 protein in 40 μ l buffer, and the reaction was started by addition of 10 μ l of 500 μ M UDP. After one hour incubation at room temperature, the released inorganic phosphate was quantified by malachite green reagent.

We rehearsed the optimized primary screen assay on a chemical library at National Institute of Biological Sciences (NIBS, Beijing, CHINA), and got a handful of hits. Our top hit, cmpd4, did not inhibit UMPKeco in secondary assay (Figure 3-8A), but completely inhibited ENTPD5 as indicated by tertiary malachite green assay (Figure 3-8B). Such results of secondary and tertiary assays

combined form a profile for each primary hits, based on which one can tell whether a particular primary hits is a specific inhibitor, a false positive inhibitor, or non-specific inhibitor (Figure 3-9). Cmpd4 clearly exemplified a true inhibitor of ENTPD5 and later served as positive compound control in our UT Southwestern HTS library screen.

The robustness and reproducibility of all three assays was examined quantitatively using a simple statistic parameter, Z' factor, formulated by Zhang *et al* (Zhang *et al.*, 1999). Plate Z' factor reflects the signal/noise ratio of given assay and the consistency of data quality among plates, and is defined as:

$$Z' = 1 - 3*[Stdev(PosCtrl) + Stdev(NegCtrl)]/|mean(PosCtrl) - mean(NegCtrl)| \quad \text{Eq.1}$$

In order to assess the data quality within the sample region of the plate, we also calculated Z'_{sample} ,

$$Z'_{\text{sample}} = 1 - 3*[Stdev(PosCtrl) + Stdev(Sample)]/|mean(PosCtrl) - mean(Sample)| \quad \text{Eq.2}$$

where sample wells data are used instead of negative control data to calculate the Z' factor. According to these equations, a perfect noise-free assay yields a Z' of 1.0; assays having values > 0.5 are generally considered robust and suitable for single replicate high-throughput screening. We determined Z' and Z'_{sample} of all three assays to be around 0.8 in mock plate tests (data not shown), as being in the “excellent assay” range. During the large scale screen, the raw plate

data was batch processed on a daily basis by HTS personnel using home-made PERL (Practical Extraction and Reporting Language) scripts. Those plates with a Z' factor below 0.7 will be discarded and redone on the next day, as a quality control procedure.

3.4 Identification of Confirmation of ENTPD5 Inhibitors

With the optimized primary assay we screened the 200,000 compounds from UT Southwestern HTS library, consisting of commercially available drug-like small molecule compounds and a marine natural products collection provided by Dr. John MacMillan's laboratory. Each compound was tested at a 5 μ M final concentration in singlet along with DMSO control wells in each screening plate.

The activity of each screening compound was calculated as normalized fold increase over negative control average:

$$\text{NormData} = \text{SampleData} / \text{mean}(\text{NegCtrl}) \quad \text{Eq.3}$$

Criteria for selecting hits are that sample reading be at least three times standard deviation of the daily sample collection above the daily sample reading average (zScore ≥ 3), where zScore for each compound was calculated as:

$$\text{zScore} = [(\text{SampleData} - \text{mean}(\text{DailySample})) / \text{Stdev}(\text{DailySample})] \quad \text{Eq.4}$$

We identified about 1,500 potential hits in the primary screen according to the above criteria. We ranked the hit list by inhibition potency, reflected by

NormData, and cherry-picked the top 640 compounds for counter screen confirmation.

The selected 640 compounds were first serial diluted into 1 μM , 2.5 μM , 5 μM and 10 μM final concentrations and then tested by primary screen assay, and secondary/tertiary counter screen assays in triplicate respectively. The data collected for each compound was used to construct a dose response profile of this compound in all three screen assays. By analysis these profiles, one can distinguish verified positive hits from false positive and non-specific inhibitors. With real ENTPD5 inhibitors, one expects to see a dose dependent increase of inhibition in primary assay (increase of residual ATP readings) and in tertiary malachite green assay (decrease of free Pi production), while the activity of coupling enzyme was not affected as indicated in secondary UMPKeco assay (Figure 3-11). In contrast, false positive inhibitors will give a similar positive primary assay readout, which was due to inhibition of UMPKeco activity (increase of residual ATP readings in secondary assay), but rather than ENTPD5 inhibition, as evidenced by no decrease of free phosphate formation in tertiary assay (Figure 3-11). At last, the non-specific or promiscuous inhibitors kill both UMPKeco and ENTPD5 activity to generate positive primary assay readout (Figure 3-12). We eventually verified 160 compounds out of the 640 cherry-picked according to this scheme as true *in vitro* ENTPD5 inhibitors. We ranked

the 160 compounds according to their primary assay readout at 10 μ M, and assigned them PID# as future identifier.

3.5 Structural Classification of Verified Compounds

The 160 verified inhibitors were clustered based on Tanimoto similarity into eight structural classes (Figure 3-13). Each class of compounds shares some distinctive common core structural features.

It is worth mention that class II compounds represented about one third of all verified hits. They clearly share a common core structure of uracil-like ring, including barbiturate and 2-thiobarbiturate rings, with 5-Z-olefin bond (Figure 3-14).

This Z-configuration of the olefin bond seems to be stereo specific for ENTPD5, because E-configuration isomers do exist in the library, but were not picked up by our screen assay. Since the preferred substrate of ENTPD5 is UDP, the highly enriched uracil-like core structure implies that this class of compounds may occupy the catalytic site of ENTPD5 and function as competitive inhibitors. Class IV compounds share urea or thiourea substructure, which may also compete for uracil ring interacting residuals within the catalytic pocket of ENTPD5.

3.6 Bioactivity Directed Purification of Natural Compounds

Among the 160 verified inhibitors, three were from MacMillan natural product collection. Initial screening results of inhibitors of the enzyme target Entpd5 revealed that the hexane and dichloromethane (BA07-092-DCM) soluble extracts from the sponge *Smenospongia aurea* exhibited a 6 fold increase in luminescence at a concentration of 10 mg/mL (Figure 3-16), an indication of Entpd5 inhibition. Following the process of bioassay guided fractionation we began pursuing the active components from these active fractions.

Fraction BA07-092-hex was further purified using flash SiO₂ chromatography using a gradient from 100:0 hexane: EtOAc to 50:50 hexane:EtOAc over 2.5 L of solvent to give a total of 17 fractions that were tested for their ability to inhibit Entpd5 in an enzyme based assay. A number of these fractions, A8-A10 and A12-15 showed strong inhibitory effects at a concentration of ~20 µg/mL in DMSO (Figure 3-17). Based on NMR and MS profiles it was determined that these fractions were enriched in small diterpene compounds – as indicated by in the NMR spectra by a series of methyl singlets from 1.2-1.7 ppm. Further analysis by MS indicated molecular weights in the range of m/z 310 -360, indicative of a terpene with 2 – 4 oxygen atoms. Based on the complexity of the NMR spectra, we initially pursued fraction A10, as it appeared to be predominately composed of a single compound. Normal phase HPLC purification

using isocratic conditions of 95:5 *n*-hexane:IPA gave a single pure compound that was subsequently analyzed with ENTPD5 enzyme assay to obtain dose-response data, revealing an IC₅₀ of 20 μM for fraction A10 (Figure 3-18).

Using NMR and MS data we were able to determine the structure of this compound as aureol (**1**) (Figure 3-20), a previously reported diterpene in the literature (Djura et al., 1980), that is characterized by the fusion of the diterpene core to an aromatic ring through a furan ring. The NMR data for aureol and match identically the literature reports for this compound.

After establishing the active component of fraction A10, we took a more in depth analysis of fraction A9, a more complex mixture of compounds. Normal phase HPLC purification using isocratic conditions of 95:5 *n*-hexane:*i*-PrOH gave three additional pure compounds, in addition to aureol. The three additional compounds are all sesquiterpene hydroquinone metabolites related to aureol. BA07-092-A9-8 (**2**) (IC₅₀ = 30 μM) lacks the C ring furan, BA07-092-A9-11 (**3**) (IC₅₀ = 30 μM) has a rearranged terpene skeleton giving an exocyclic double bond in the A ring, and BA07-092-A9-10 (**4**) (IC₅₀ = 10 μM) has an alternate cyclization forming the C ring furan. Analysis of the NMR data for **4** revealed the known compound 8-epichromazonarol, previously reported by the Faulkner lab (Djura et al., 1980). The IC₅₀ curves for these three compounds can be seen in (Figure 3-19). In addition to sesquiterpene hydroquinone analogs **1** – **4**, we have

isolated an additional four analogs that are undergoing further biological evaluation.

Aureol (**1**) has received considerable attention for broad biological activity, including anti-viral (Amy E. Wright et al., 1993), anti-tumor and neurological (Hamann et al., 2009). However, there have been no reports of a specific target for aureol or analogs. We are aware of no reports on the biological activity of molecules with the carbon backbone of **4**. Additionally, the hydrocarbon nature of **1 – 4**, makes significant functionalization and SAR projects challenging. The few analogs of aureol are simple derivatives on the phenol group or naturally occurring halogenated analogs on the aromatic ring. We have designed a semi-synthetic route that provides access to more functionalized analogs, derivatized at the unfunctionalized aromatic positions. This involves the formation of nitro substitution, which provides a further handle for chemistry. Additional compounds of the sesquiterpenoid hydroquinone and quinone structural family have been isolated with variations in the stereochemistry of the angular methyl groups as well as the ring architecture (Minale et al., 1974; Ravi et al., 1979) (Figure 3-18).

3.7 Cellular Effects of in vitro Confirmed Compound Inhibitors

Our previous study has shown that ENTPD5 is essential for maintaining ER homeostasis in AKT hyperactive cancer cells. Knockdown of ENTPD5 by

siRNA leads to ER stress, GRP78/BiP upregulation and degradation of EGF receptor (Figure 3-21). With our newly identified chemical inhibitors targeting ENTPD5, we expect to see similar phenotype, if the compounds are cell permeable.

We tested representative members from each structural class of synthetic compounds on PTEN knockout MEF cells at 30 μ M for 24 hours, and monitored GRP78/BiP expression level by Western Blotting as an indicator of ER stress. Six tested compounds induced strong GRP78/BiP upregulation. Five out of the six belongs to the Class II structural group featuring Uracil-like ring, and the other one falls into the Class IV containing a urea/thiourea substructure (Figure 3-22). The reason that most confirmed synthetic inhibitors have no cellular effect is probably due to their poor cell permeability, rather than their inhibitory potency against ENTPD5.

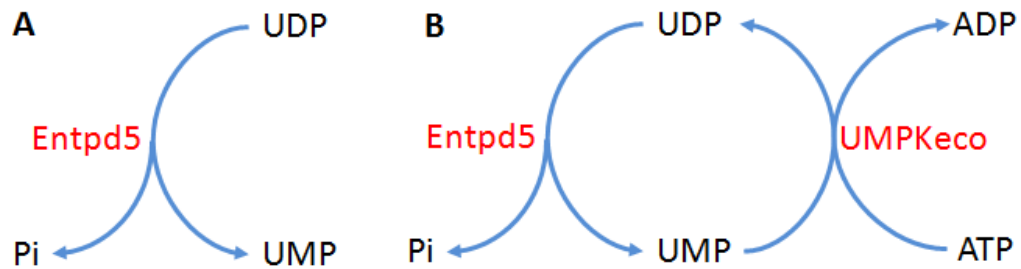
The two most potent synthetic inhibitors, PID#38 and PID#51 were then tested for cellular dose response on PTEN knockout MEF cells. As shown in Figure 3-23, both compounds could induce ER stress evidenced by GRP78/BiP increase and EGF receptor decrease in a dose dependent manner, recapitulating ENTPD5 siRNA knockdown. PTEN heterozygous cells also show ER stress in response to inhibitor treatment, but to a much lesser extent.

The purified natural compounds from sea sponge are highly lipophilic, therefore are readily cell permeable. They could also induce ER stress in PTEN knockout MEF cells in a dose dependent manner. More interestingly, the strength of ER stress induction correlates with their *in vitro* potency, reflected by IC₅₀ (Figure 3-24). Aureol at 30 μ M starts to show cytotoxicity.

It has been shown that even subtle variations in PTEN dose would affect cancer susceptibility (Alimonti et al., 2010). We then ask whether ENTPD5 inhibitors would distinguish between cells with different level of PTEN loss and Akt activation. When treated with the same dosage, would PTEN-null cells be more sensitive to these inhibitors than PTEN heterozygous. As shown in Figure 3-25, PTEN knockout MEF cells are indeed more sensitive to synthetic inhibitor induced ER stress. Similar results were observed with purified natural compound inhibitors (Figure 3-26).

Prostate cancer is the second leading cause of cancer death for men in the United States. PTEN is frequently mutated or deleted in both prostate cancer cell lines and primary prostate cancers. Acquired mutations in the PTEN gene have been reported in up to 30–60% of prostate cancer tumors, and are associated with advanced stage, and poor prognosis (McMenamin et al., 1999; Teng et al., 1997). LNCaP/C4-2 was a highly tumorigenic PTEN-null, androgen-independent bone metastatic subline derived from androgen-dependent non-metastatic LNCaP

human prostate cancer cells. We tested both synthetic and natural compounds on C4-2 cells to see how malignant PTEN-null human prostate cancer cells respond to these inhibitors. The results show dose dependent induction of BiP expression and EGFR degradation, consistent with our PTEN-null MEF cell model (Figure 3-27).

Figures from Chapter 3**Figure 3-1 Primary Screen Assay Design**

The coupling of UDP hydrolysis by ENTPD5 and UMP phosphorylation by *E. coli* UMP kinase forms a futile cycle that consumes ATP. Inhibition of either ENTPD5 or UMPKeco will result in increase of residual ATP at the end of assay.

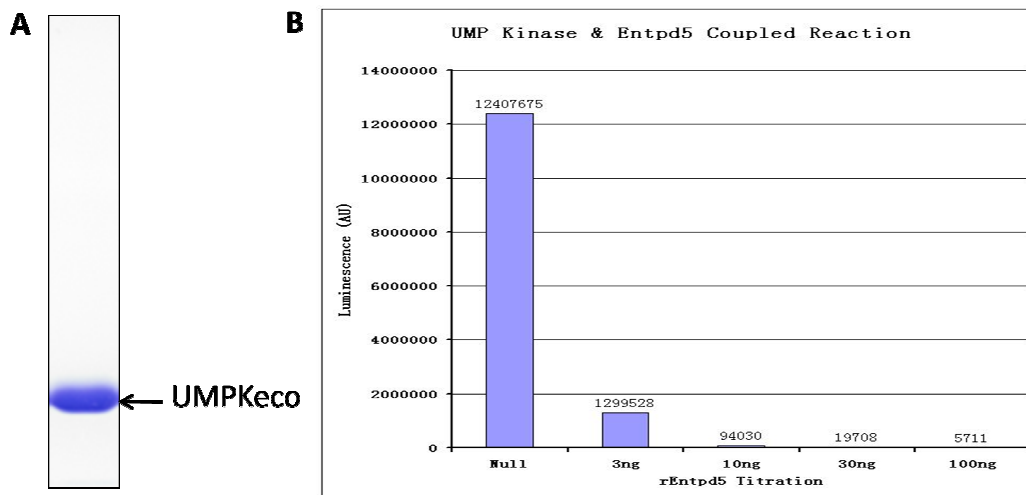


Figure 3-2 Coupled Reaction of Recombinant ENTPD5 and UMPKeco

(On the left) Bacterial expressed His-tagged *E. coli* UMP Kinase (UMPKeco D159N) recombinant protein resolved on 10% PAGE gel and stained with blue coomassie. (On the right) Titration of indicated amount of ENTPD5 recombinant protein into a mixture of 18ng of UMPKeco recombinant protein, 50 μ M of UMP and 25 μ M of GTP in a total 40 μ l volume to produce the Enzyme Mixture. The reaction was started by adding in 10 μ l Substrate Solution containing 500 μ M ATP. After incubation at 37 $^{\circ}$ C for one hour, reaction was stopped by adding 10 μ l of luciferase based Cell Titer Glo reagent into each well to quantify the residual ATP.

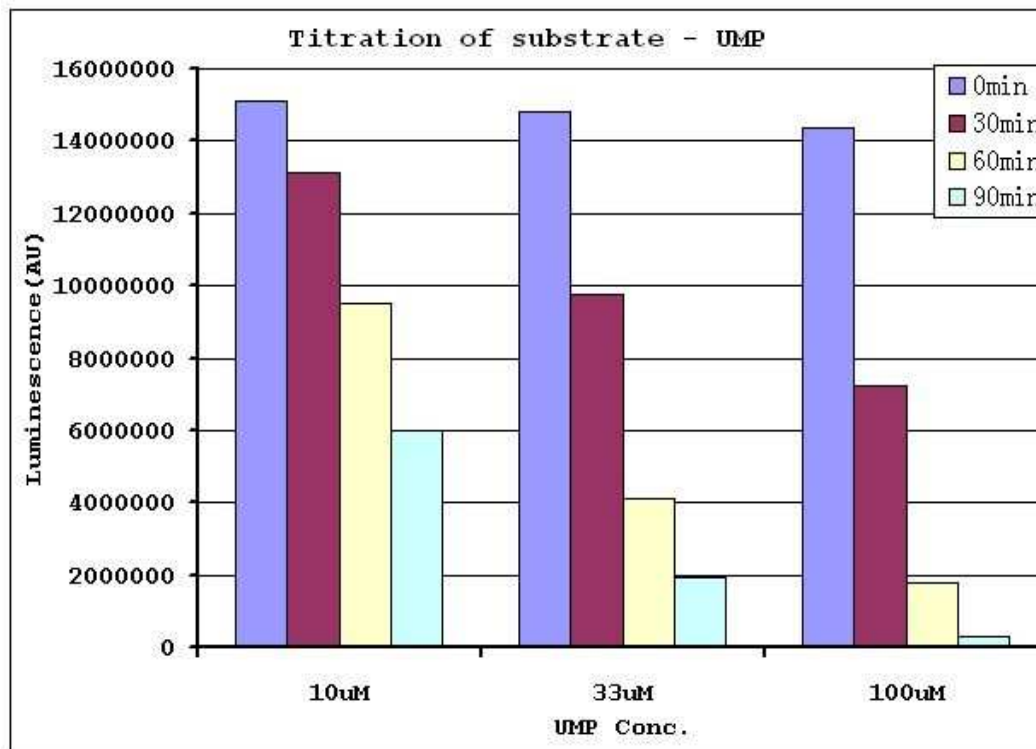


Figure 3-3 Titration of Substrate UMP

Titration with indicated amount of substrate UMP into a mixture of 3ng ENTPD5 recombinant protein, 18ng UMPKeco recombinant protein, and 25 μ M of GTP in a total 40 μ l volume to produce the Enzyme Mixture. The reaction was started by adding in 10 μ l Substrate Solution containing 500 μ M ATP. After indicated time of incubation at 37°C, reactions were stopped by adding 10 μ l of luciferase based Cell Titer Glo reagent into each well to quantify the residual ATP.

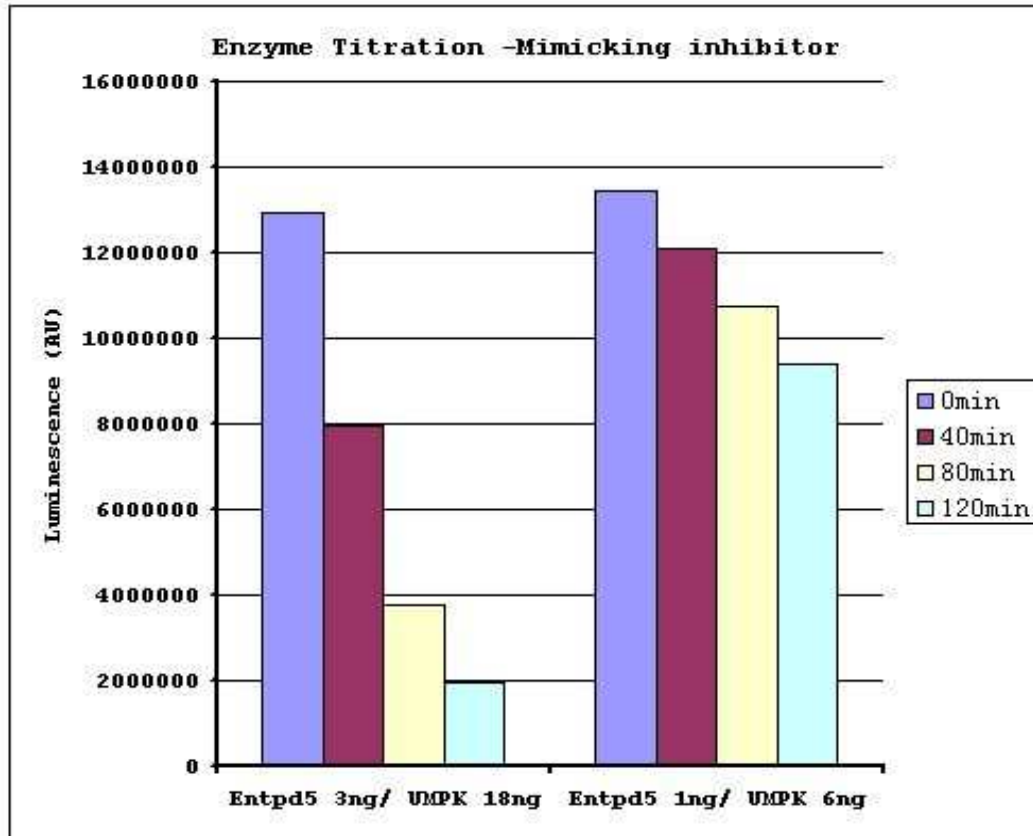


Figure 3-4 Test of Assay Sensitivity and Linearity

Due to lack of known inhibitor of ENTPD5 as positive control, we test the sensitivity of screen assay by a three-fold dilution of the proteins to mimic 66% inhibition of both enzymes. Assay setup is similar as previously described, with indicated amount of protein and incubated at 37°C for indicated time period before measuring residual ATP.

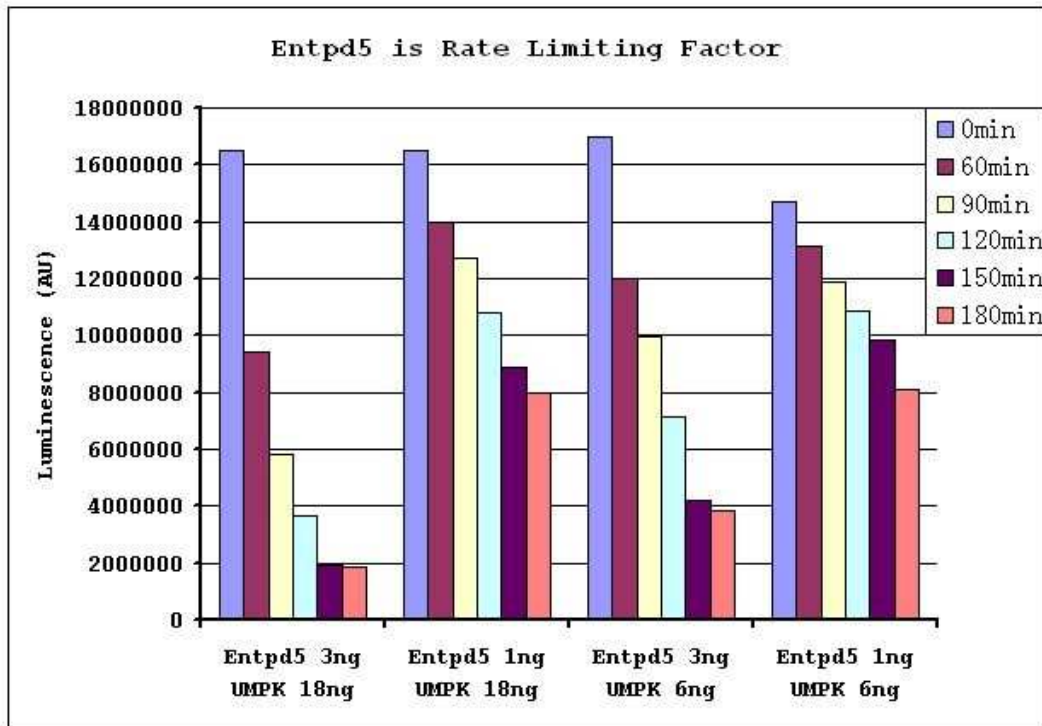


Figure 3-5 ENTPD5 is the Rate-Limiting Enzyme

To test if ENTPD5 is the rate-limiting step of the coupled reaction, assays were setup similarly as previously described, with indicated amount of protein and incubated at 37°C for indicated time period before measuring residual ATP.

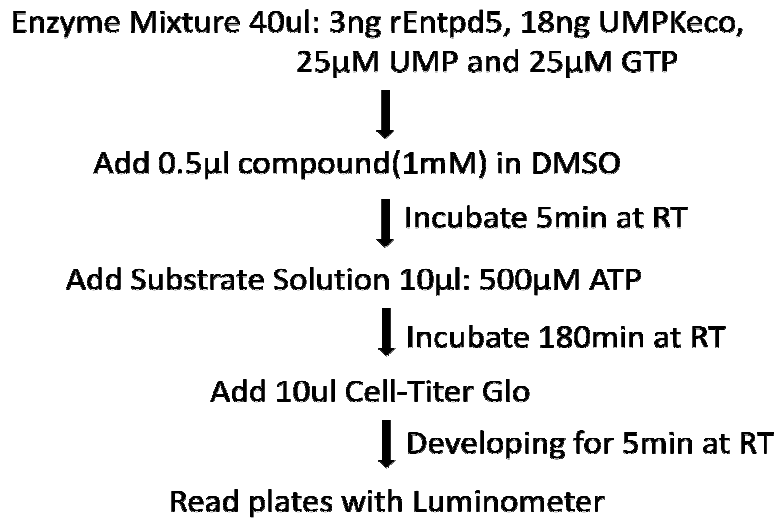


Figure 3-6 Primary Screen Assay Protocol

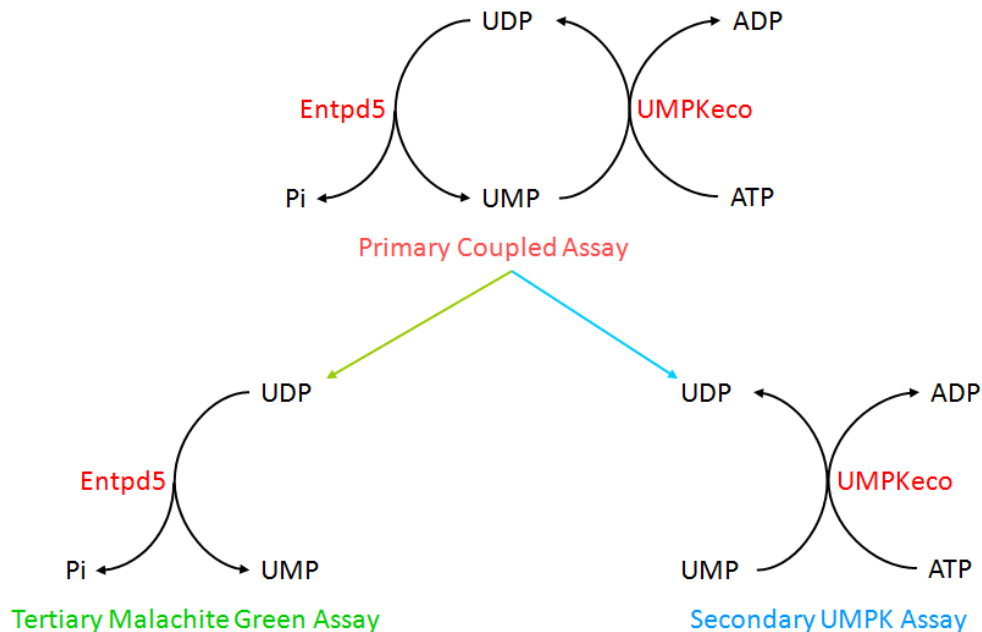


Figure 3-7 Counter Screen Design

Each arm of the primary coupled reaction was used as a counter screen assay. Secondary assay test whether the compound inhibits UMPKeco, which will generate false positive readout in primary coupled assay. Tertiary assay confirms if a compound could directly inhibit ENTPD5, using malachite green assay to assess free phosphate release from ENTPD5 substrate UDP.

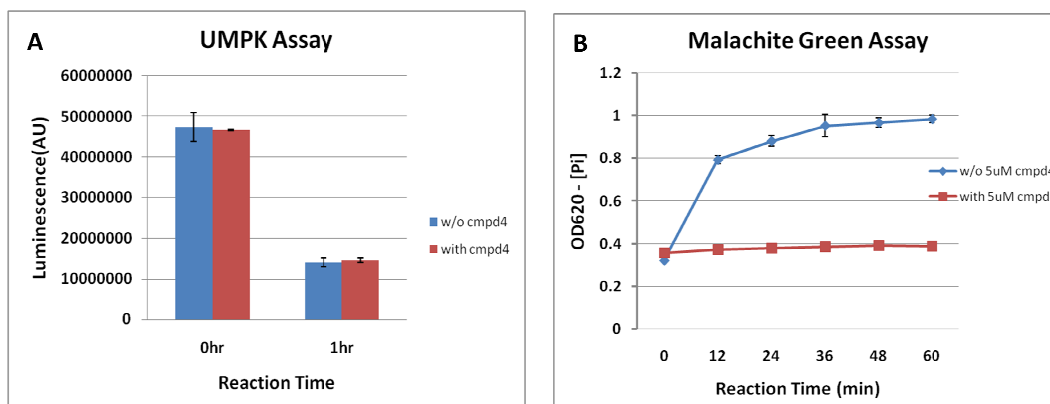


Figure 3-8 Secondary & Tertiary Assays

Representative readout of secondary and tertiary counter screen assay. An ideal inhibitor should not inhibit UMPKeco in secondary assay (A), while give positive readings in tertiary malachite green assay (B).

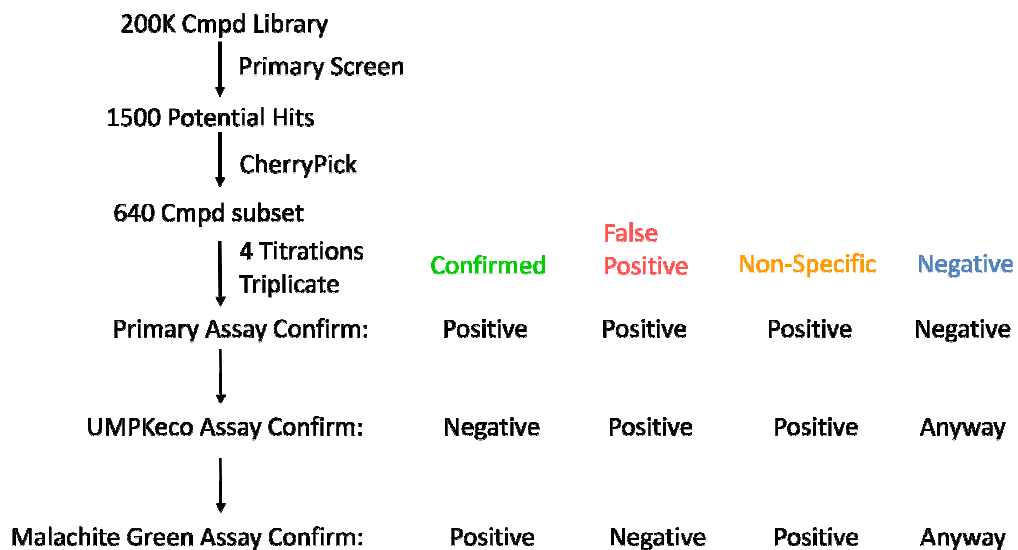


Figure 3-9 HTS Screen Flow Chart

(On the left) Summary flowchart of UTSW compound library screen. (On the right) Criteria for classifying screen hits by combining results from all three rounds of assays.

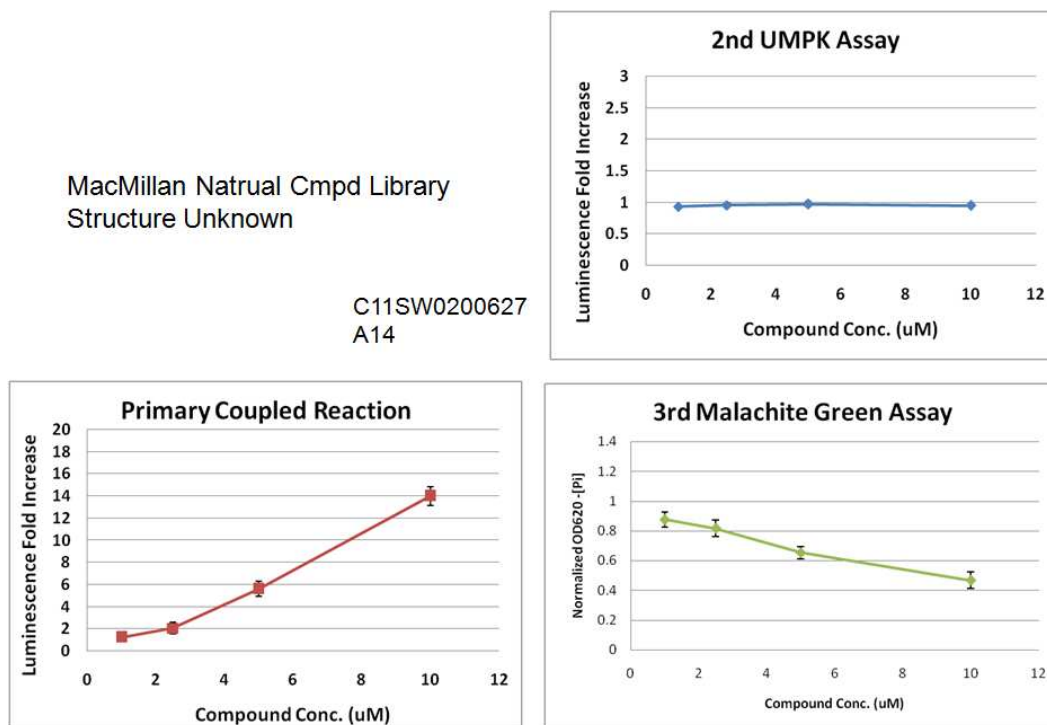


Figure 3-10 Representative True ENTPD5 Inhibitor Profile

Primary assay positive, secondary assay negative and tertiary assay positive indicates that compound truly inhibits ENTPD5 but not UMPKeco.

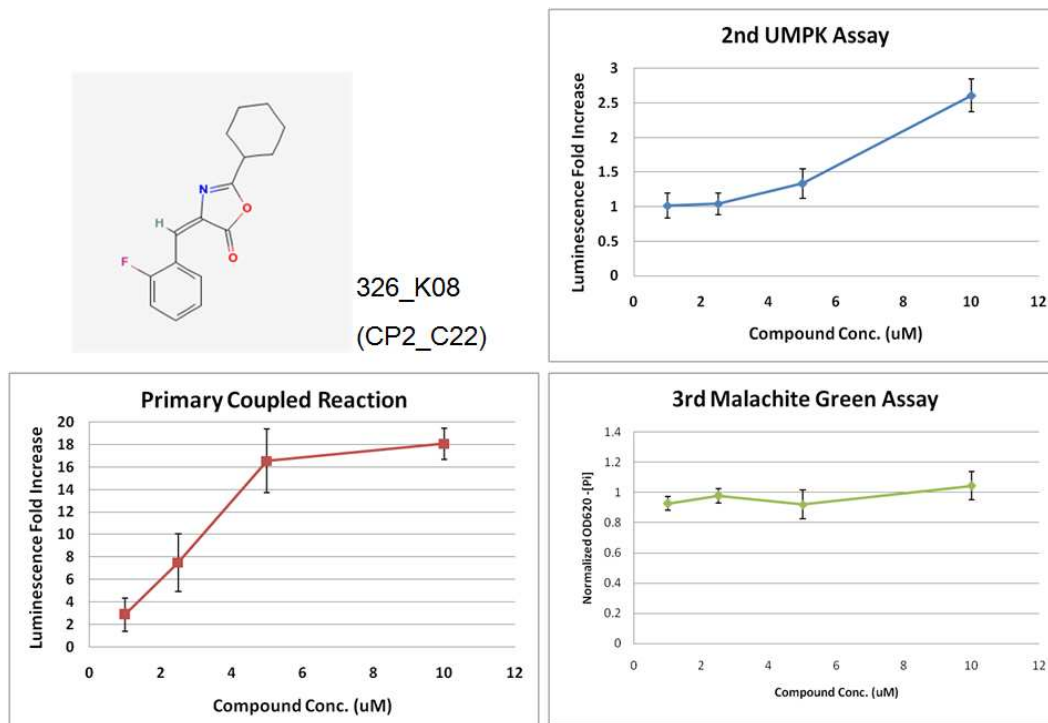


Figure 3-11 Representative False Positive ENTPD5 Inhibitor Profile

Primary and secondary assay positive, but tertiary negative, indicates that the compound is an inhibitor of UMPKeco, give rise to false positive readout in primary screen.

McMillan's Collection
Marine Bacteria Compound mixture

627_O04
(CP3_C22)

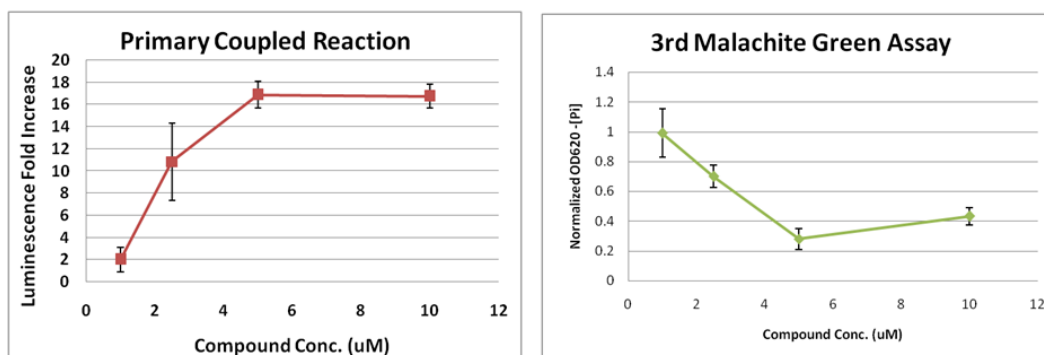


Figure 3-12 Representative Non-specific ENTPD5 Inhibitor Profile

All three assays are positive, meaning this compound is non-specific inhibitor of both ENTPD5 and UMPKeco.

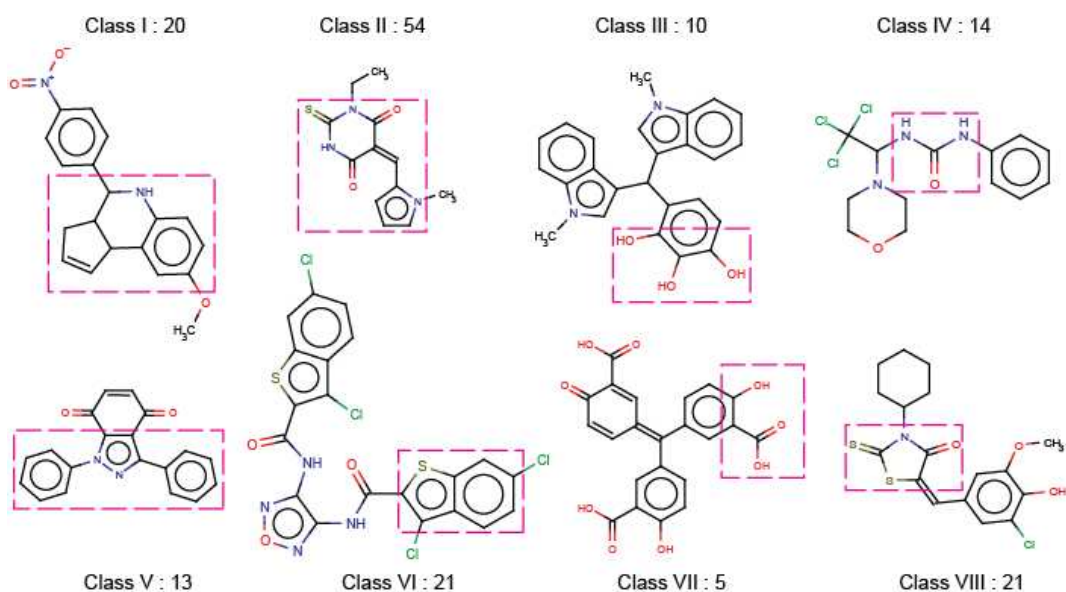


Figure 3-13 Structural clustering of Confirmed Synthetic Inhibitors

Compound structure classification based on similarity. Dashed rectangular indicates the common core structure of each class. Number after class name indicates the common core structure of each class. Number after class name indicates how many compounds belongs to it.

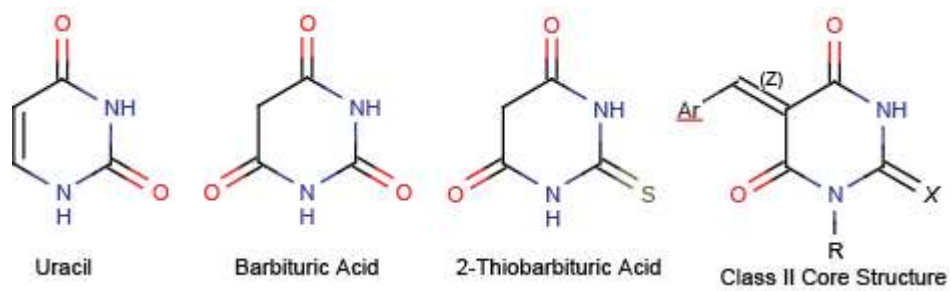


Figure 3-14 Class II Core Structure Resembles ENTPD5 Substrate

Comparison of ENTPD5 native substrate uracil ring with common core structure of class II inhibitors. X = O, S.

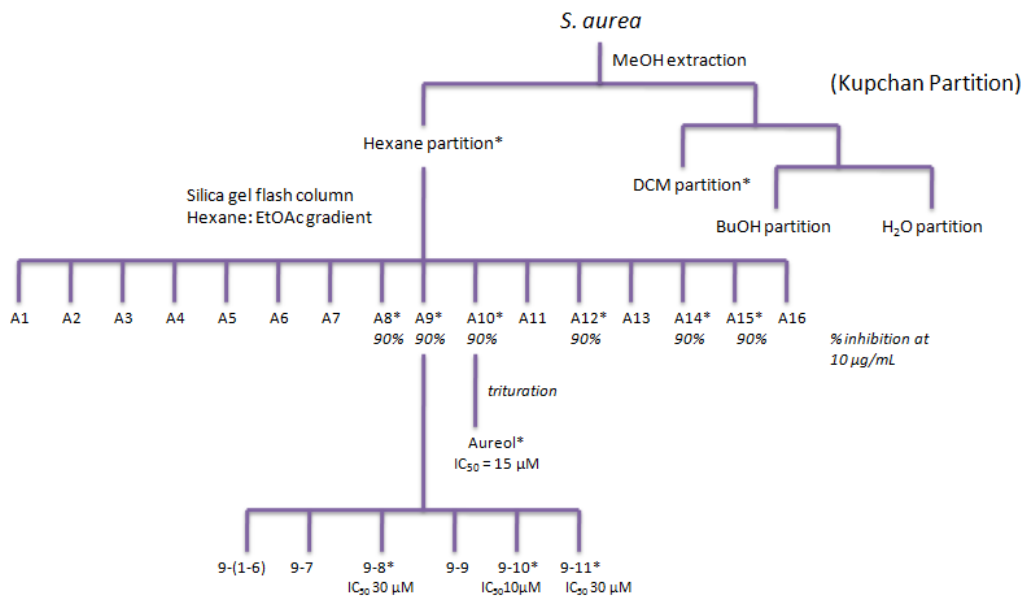


Figure 3-15 Natural Compounds Purification Scheme

Bioactivity directed purification of ENTPD5 inhibitor from sea sponge *S. aurea* crude extracts. Star indicates fractions with inhibition activity.

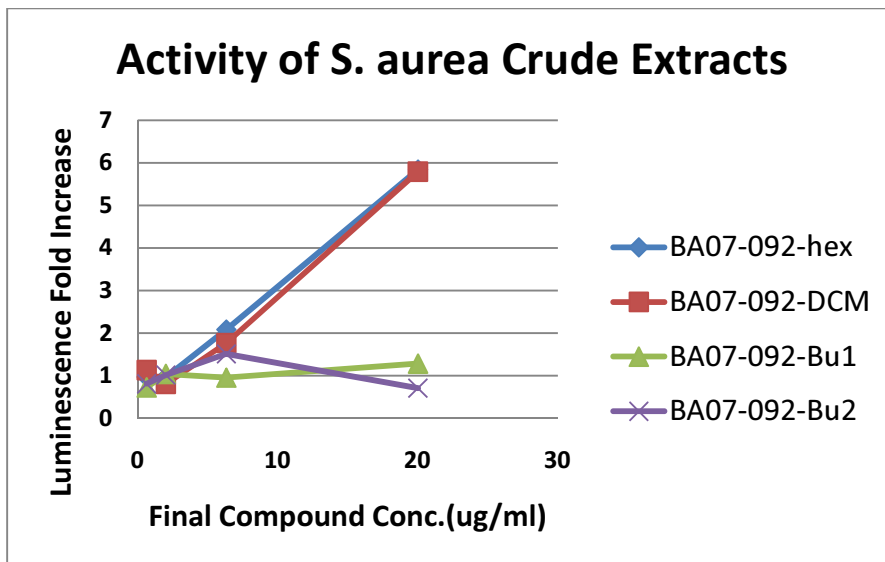


Figure 3-16 Activity of Crude Extracts from *S. aurea*

Indicated concentration of crude fractions from *S. aurea* were titrated into a mixture of 3ng ENTPD5 recombinant protein, 18ng UMPKeco recombinant protein, and 25 μ M of UMP and 25 μ M of GTP in a total 40 μ l volume to produce the Enzyme Mixture. The reaction were started by adding 10 μ l Substrate Solution containing 500 μ M ATP. After incubation at 37 $^{\circ}$ C for three hours, reactions were stopped by adding 10 μ l of luciferase based Cell Titer Glo reagent into each well to quantify the residual ATP.

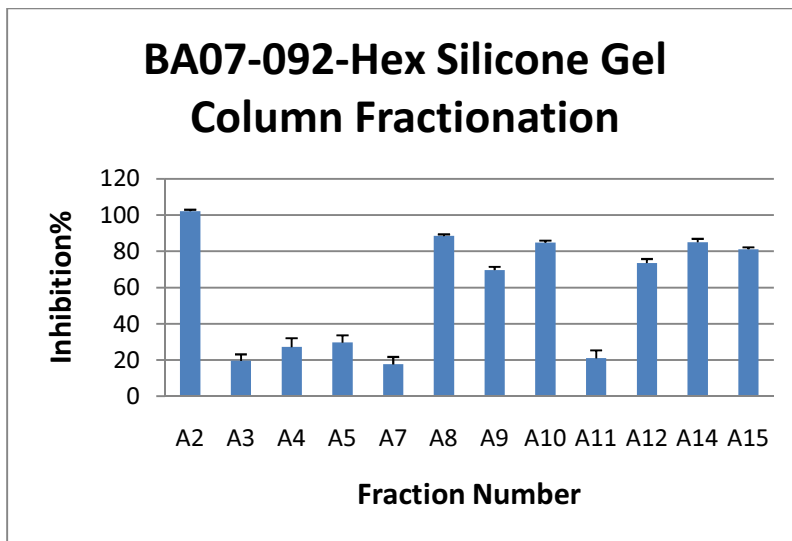


Figure 3-17 Response of BA07-092-Hex Silicone Gel Column Fractions

Fractions of BA07-092-Hex on silicone gel column were titrated into a mixture of 3ng ENTPD5 recombinant protein, 18ng UMPKeco recombinant protein, and 25 μ M of UMP and 25 μ M of GTP in a total 40 μ l volume to produce the Enzyme Mixture. The reaction were started by adding in 10 μ l Substrate Solution containing 500 μ M ATP. After incubation at 37°C for three hours, reaction were stopped by adding 10 μ l of luciferase based Cell Titer Glo reagent into each well to quantify the residual ATP. Readings were normalized to null control to generate percentage inhibition.

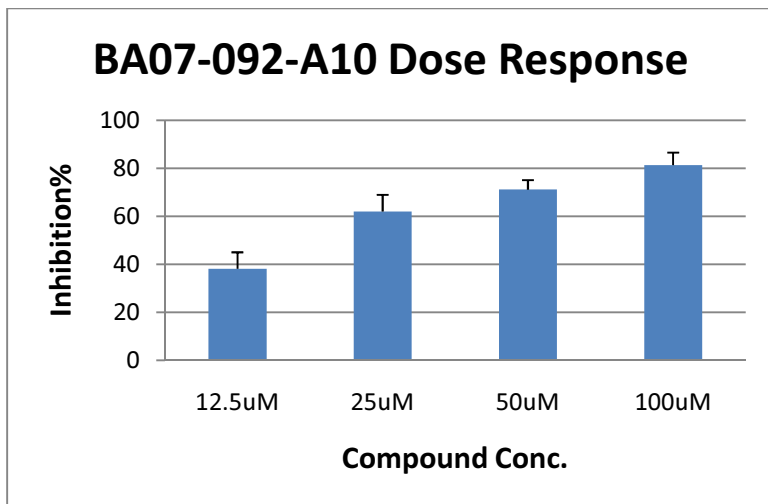


Figure 3-18 Aureol (BA07-092-A10) Dose Response

Purified compound Aureol was tested. Assay setup is similar as above.

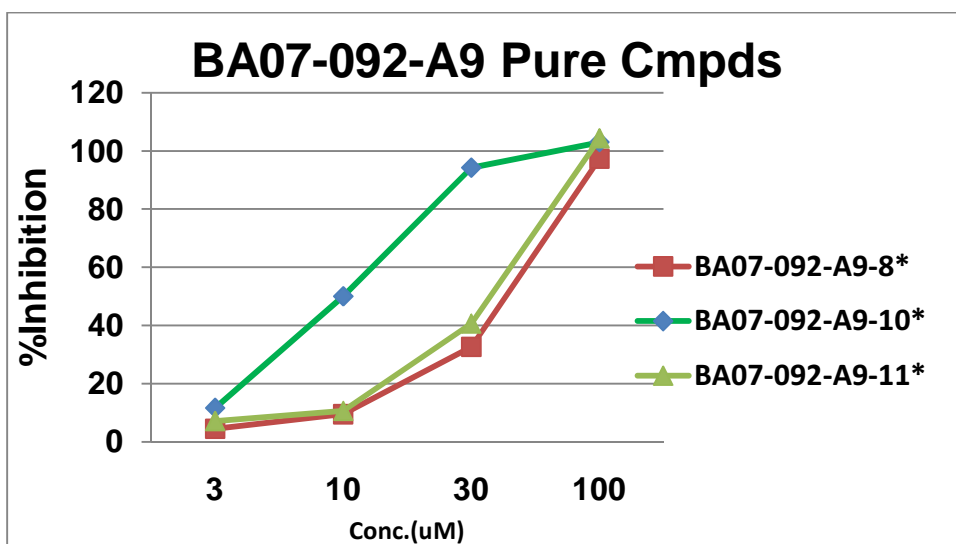


Figure 3-19 Dose Response of BA07-092-A9 HPLC Fractions

Indicated concentrations of individual purified fractions are tested. Assay setup is similar as above.

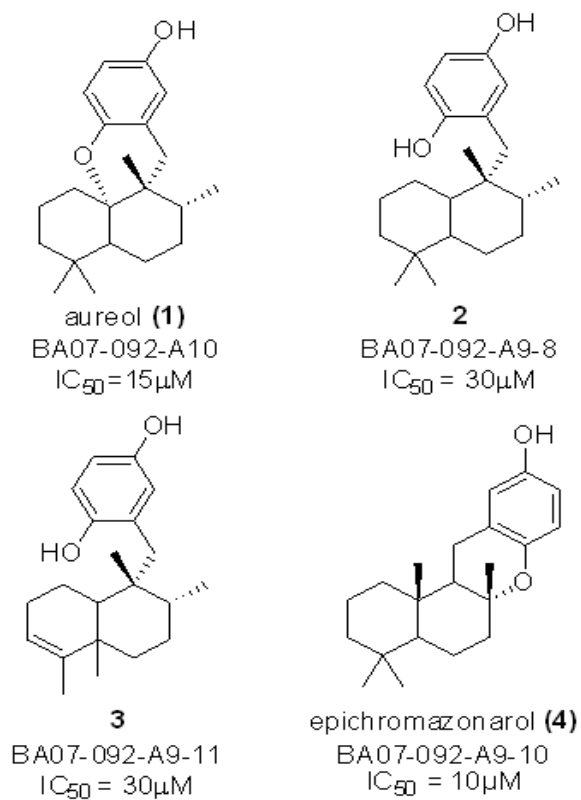


Figure 3-20 Sesquiterpene Hydroquinones Natural Compound Inhibitors

Structure and IC_{50} of four natural compound inhibitor of ENTPD5 isolated from sea sponge *S. aurea*.

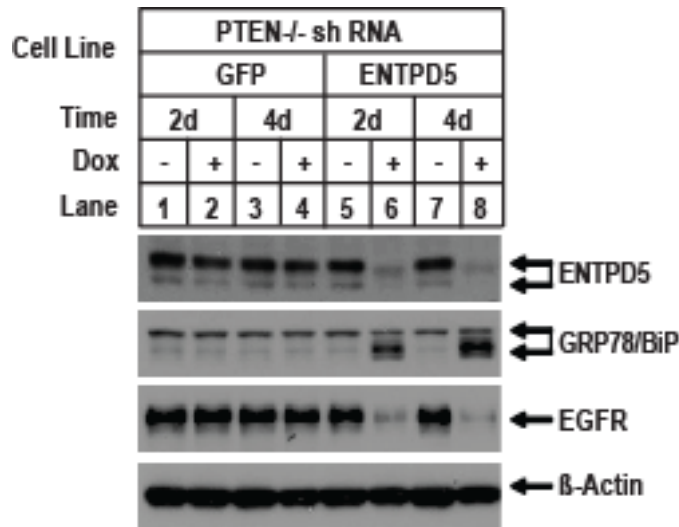


Figure 3-21 Knockdown ENTPD5 Induces BiP Increase and EGFR Decrease

PTEN^{-/-} MEF cells with doxycycline (Dox)-inducible expression of shRNA-targeting ENTPD5 was generated as described in the Experimental Procedures. After 2 or 4 days induction with Dox (0.125 μ g/ml), cells were harvested and total cell lysates were prepared as described in the Extended Experimental Procedures. Aliquots of 10 μ g protein were subjected to SDS-PAGE followed by western blotting analysis using the indicated antibodies.

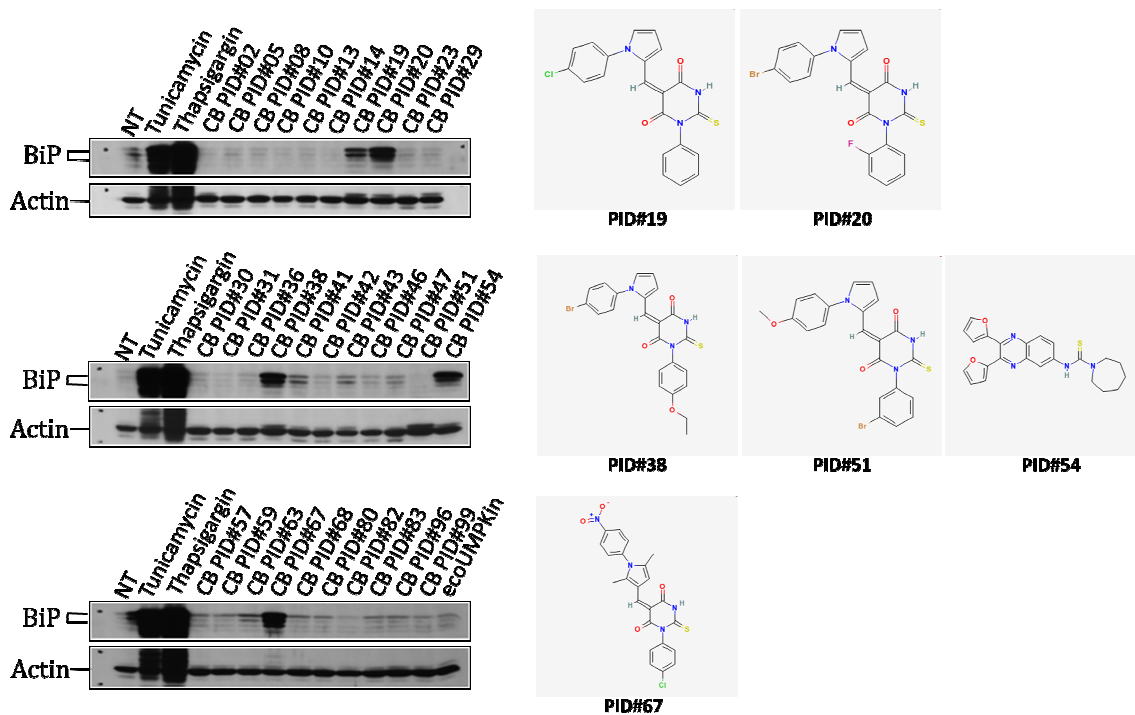


Figure 3-22 Synthetic ENTPD5 Inhibitors Induce ER Stress in PTEN-null Cells

(On the left) PTEN^{-/-} MEF cells was treated with 30 μ M of each indicated compounds. After 24h, cell lysate were prepared and normalized. Aliquots of 30 μ g protein were subjected to SDS-PAGE followed by Western blotting analysis using the indicated antibodies. (On the right) Structures of inhibitors that induce strong BiP upregulation.

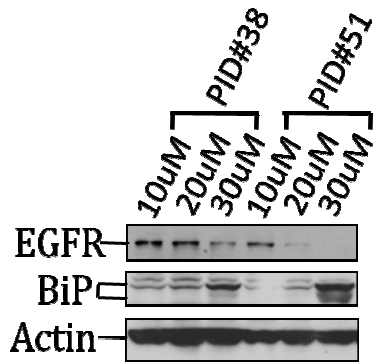


Figure 3-23 Dose Response of Synthetic Inhibitors

PTEN^{-/-} MEF cells were treated with increasing dose of each indicated compounds. After 24h, cell lysate were prepared and normalized. Aliquots of 30 μ g protein were subjected to SDS-PAGE followed by Western blotting analysis using the indicated antibodies.

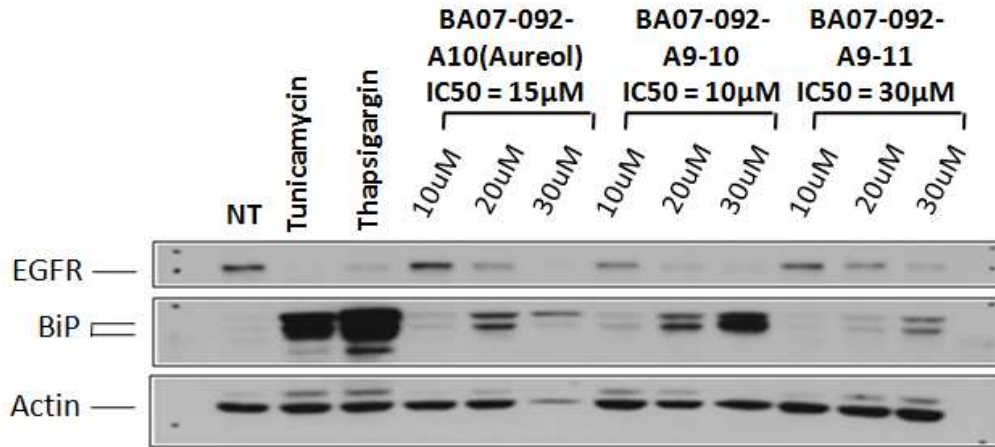


Figure 3-24 ER Stress Intensity Correlates with *in vitro* Potency of Natural Inhibitors

PTEN^{-/-} MEF cells were treated with increasing doses of each indicated compound. After 24h, cell lysates were prepared and normalized. Aliquots of 30 μg protein were subjected to SDS-PAGE followed by Western blotting analysis using the indicated antibodies.

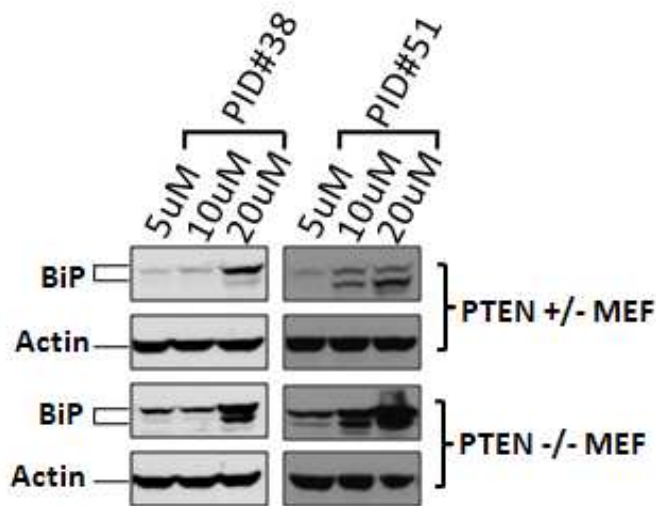


Figure 3-25 PTEN^{-/-} MEF is More Susceptible to Synthetic Compound Inhibitor than PTEN^{+/-} MEF

PTEN^{-/-} and PTEN^{+/-} MEF cells were treated with increasing doses of each indicated compound. After 24h, cell lysates were prepared and normalized. Aliquots of 30 μg protein were subjected to SDS-PAGE followed by western blotting analysis using the indicated antibodies.

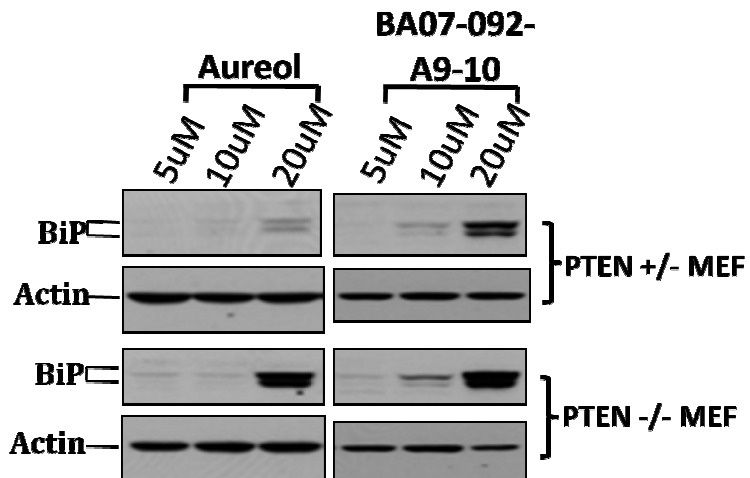


Figure 3-26 Natural Compound Inhibitors Induces Stronger ER Stress in PTEN^{-/-} MEF

PTEN^{-/-} and PTEN^{+/-} MEF cells was treated with increasing dose of each indicated compounds. After 24h, cell lysate were prepared and normalized. Aliquots of 30 μg protein were subjected to SDS-PAGE followed by western blotting analysis using the indicated antibodies.

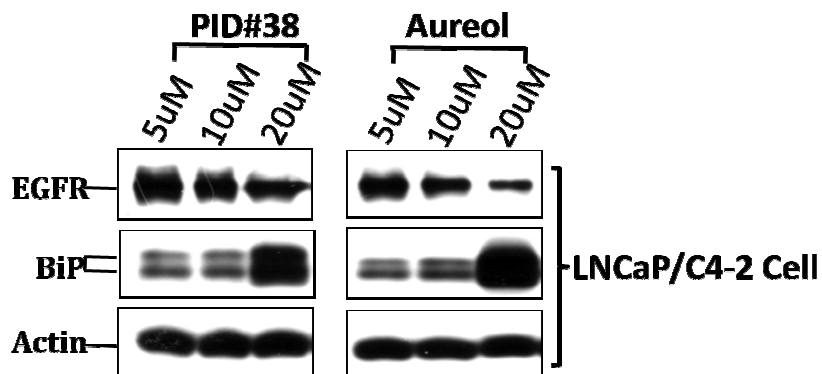


Figure 3-27 Effects of Inhibitors on Human Prostate Cancer Cell Line

Human prostate cancer LNCaP/C4-2 cells were treated with increasing dose of each indicated compounds. After 24h, cell lysate were prepared and normalized. Aliquots of 30 μg protein were subjected to SDS-PAGE followed by western blotting analysis using the indicated antibodies.

Chapter 4 : Conclusions and Discussions

4.1 ENTPDase Family

The ecto-nucleoside triphosphate diphosphohydrolases (ENTPD) family, previously called apyrase protein family, comprises enzymes capable of cleaving nucleotide tri- and diphosphates in a calcium- or magnesium dependent manner, not being affected by P-type, F-type, or V-type NTPase inhibitors. The “ecto-” denotes that their catalytic domain are facing either extracellular space or luminal spaces of ER, GA, secretory vacuoles and lysosomes, which are topologically equivalent to extracellular space. The eight members, ENTPD1-8 can be further divided into three groups based on cellular localization and substrate specificity.

Group I includes typical cell surface ENTPDase1,2,3, and 8, that are anchored by both N-terminal and C-terminal transmembrane helixes on the plasma membrane. In the extracellular space, ATP serves as a signalling substance. It acts on P2X receptors, which are ligand-gated ion channels, or on the P2Y receptors, which are G-protein coupled receptors. These signalling pathways via ATP and other nucleotides are termed purinergic signalling. By hydrolyzing extracellular nucleoside tri- and diphosphates, especially ATP and ADP, ENTPDases modulate extracellular nucleotide levels, thereby regulating purinergically controlled physiological processes, such as platelet aggregation and synaptic transmission (Dunwiddie et al., 1997; Enjyoji et al., 1999).

Group II is known as luminal ENTPDases, consisting of ENTPD5 and 6. They are anchored by single N-terminal transmembrane helix, with the catalytic domain facing the lumen of secretory pathway of eukaryotes. ENTPD5 resides in ER, while ENTPD6 is localized to Golgi Apparatus. They both possess UDPase/GDPase activity. ENTPD5 prefers UDP as substrate over GDP, but ENTPD6 has a higher activity towards GDP.

Table 4-1 Activated Sugar Donors in Mammalian Cell

Sugar Donor	Conjugate
UDP-glucose	UDP
UDP-galactose	
UDP-GlcNAc	
UDP-GalNAc	
UDP-xylose	
UDP-glucuronic acid	
GDP-mannose	GDP
GDP-fructose	
CMP-sialic acid	CMP

It is known that mammalian cells use 9 sugar-nucleotides as substrates for glycosylation (Table 4-1). All of them are conjugated to UDP/GDP, except sialic acids, which are the only monosaccharides in animals activated as a mononucleotide, CMP-Sia. Judged by the substrate specificity and subcellular

localization of ENTPD5 and 6, they may function in the protein glycosylation and folding pathway. They hydrolyze nucleoside diphosphates resulting from glycosyltransferase-mediated reactions, yielding nucleoside monophosphates. The latter are weaker inhibitors of glycosyltransferases than the former and are also antiporters for the transport of nucleotide sugars from the cytosol to the endoplasmic reticulum (ER) and Golgi apparatus (GA) lumen.

The last group consists of ENTPD4 and ENTPD7. ENTPD4, also called LALP70, is a lysosomal membrane protein containing an apyrase domain in its N-terminal. The two splice variants of ENTPD4 show distinct substrate preference and divalent cation dependency (Biederbick et al., 2000; Wang et al., 1998). ENTPD7 has an intracellular vesicular distribution (Braun et al., 2000). The function of these lysosome/vacuole-associated ENTPDases are still largely unexplored.

4.2 ENTPD5 is an Indispensible Component of PI3K/Akt Pathway

PI3K/Akt pathway is frequently constitutively activated in human cancer through loss or inactivating mutations of the tumor suppressor gene PTEN, the gain-of-function mutations in the PIK3CA gene itself encoding the p110 α catalytic subunit of PI3K and the constitutively active mutant forms of receptor tyrosine kinases or the Ras oncogene (Keniry and Parsons, 2008). One of the

downstream effects of PI3K/Akt pathway is to stimulate protein synthesis through activation of mTOR, to support the rapid cell growth and proliferation. The increased influx of newly synthesized peptides proposed a challenge for the ER protein glycosylation and folding machinery. In order to meet this challenge, ENTPD5, an ER UDPase is transcriptionally upregulated by Akt. Since proteins entering the secretory pathway, including membrane proteins and secreted proteins, are often N-glycosylated, a process critical for the proper folding and functions of these proteins, elevated ENTPD5 will concurrently increase the protein reglucosylation activity for proper protein folding mediated by the calnexin/calreticulin system. ENTPD5 hydrolyzes UDP, a product of UGGT, to UMP. This reaction not only relieves the end-product feedback inhibition by UDP, but also provides UMP for exchange of UDP-glucose, the substrate for UGGT. By accelerating glycosylation process, ENTPD5 help increase the ER folding capacity to accommodate the increased protein translation speed. Knockdown of ENTPD5 in PTEN-null cells result in ER stress and growth arrest. Therefore ENTPD5 seems to be the key ENTPDase family member responsive to higher protein translation activity promoted by active AKT, and is an essential link within PI3K/Akt signaling pathway.

One interesting note is that PTEN loss is most prevalent in endometrial, glioblastoma, prostate, breast and liver cancers (Keniry and Parsons, 2008), all of which have high secretory activity. ENTPD5 is also highly expressed in adult

liver, kidney and prostate. It is possible that these tumors would face particularly high demand for glycoprotein processing and therefore high pressure to activate AKT and ENTPD5. It will be interesting in future studies to see whether such a correlation holds true in a larger panel of cancer cells. If so, it might serve as a biomarker for potential treatment with ENTPD5 inhibitors.

4.3 ENTPD5 Contributes to Warburg Effect

One of the surprising findings reported here is how quickly ATP can be consumed as a result of ENTPD5 up-regulation. Through the aid of UMP/CMP kinase-1 and Adenylate kinase in the cytosol, which are present in similar amounts in cells regardless of PTEN status, ENTPD5 drives this futile ATP cycle to convert ATP to ADP/AMP. One naturally raised question is where the extra-consumed ATP comes from since the intracellular ATP level is relatively stable. After measuring both oxygen consumption and lactate generation, it was obvious that it was the lactate production that was elevated in these PTEN-null cells, consistent with previous reports (Vander Heiden et al., 2009). What was surprising was that when ENTPD5 was knocked down, higher lactate production returned to normal, indicating that ENTPD5 is actually a critical player in causing the Warburg effect, i.e. elevated lactate production under aerobic condition, in these PTEN-null cells.

The possible mechanism for ENTPD5 to increase glycolysis is its ability to generate ADP/AMP discovered here. Elevated AMP level (to a lesser extent, ADP), activates phosphofuctokinase and inhibits fructose diphosphatase to drive glycolysis and prevent gluconeogenesis, resulting in higher lactate production (Gevers and Krebs, 1966).

The elevated glycolysis may also point the outlet of generated ADP/AMP from ENTPD5/CMPK1/AK activities. Since AK reversibly catalyzes the conversion between ADP to ATP and AMP, AMP can be converted to ADP at the expense of ATP. ADP is then used for regenerating ATP through glycolysis. This may explain why we did not observe the activation of AMPK in PTEN-null cells.

Glucose not only provides the metabolic energy needed by cells but also participates directly in glycoprotein folding as a component of oligosaccharide structures. In addition to compensating more ATP consumption, the elevated ENTPD5 should accelerate import of UDP conjugated glucose into ER and their conjugation to proteins. This activity should shunt more glucose-6-phosphate to glycosylation pathway. This finding is consistent with the observation that in all cancer cells examined, a catalytically less efficient pyruvate kinase isoform M2 was expressed to slow down the rate of glycolysis so that the intermediates can be used for synthesizing macromolecules (Christofk et al., 2008).

4.4 ENTPD5 is a Potential Anti-cancer Target

The current study highlighted ENTPD5 as a critical link in PI3K/PTEN pathway that promotes cell growth and survival, a pathway that is often activated in cancer cells. Prostate cancer is one of the most common malignancies in males throughout the world. Activation of PI3K-AKT (AKT) signaling pathway in prostate cancer occurs through loss of PTEN. Current estimates suggest that PI3K/Akt/mTOR signaling is upregulated in 30-50% of prostate cancers, often through loss of PTEN.

ENTPD5 seems to mediate a critical part of many of the observed features in fast growing cells. By being a critical enzyme to help accommodating higher level of protein translation promoted by activated AKT, inhibition of this enzyme, similar to knockdown, can potentially generate multi-factual benefits for anti-cancer activity. It will induce more severe ER stress in cells with active AKT so that ENTPD5 inhibition may cause synthetic lethal in these cells, which otherwise enjoy survival advantage and resistance to common anti-cancer drugs. Prolonged ER stress may stop cell growth and cause cell death. It will also lower many growth factor receptors on the cell surface due to their high N-glycosylation nature, a phenomenon that may reflect the evolutionary connection between fast growth and nutrient availability in mammalian cells (Lau et al., 2007). Among such receptors, EGFR, Her2/ErB2, and IGFR levels are down after ENTPD5 knockdown. Antagonistic

antibodies and small molecule inhibitors for EGFR and Her2/ErB2 are already huge successes in clinics for treating cancer (Ciardiello and Tortora, 2008; Paik et al., 2008). The inhibition of ENTPD5 may be particularly effective in cancer cells that secrete lots of glycoproteins.

Using biochemical HTS approach, we identified several structural classes of synthetic compound inhibitors of ENTPD5. The best represented class II inhibitors contains a core structure of barbiturate or thiobarbiturate ring linked to an aryl group through a double bond in (*Z*) configuration. Treatment of these inhibitors to cultured PTEN-null MEF cells induces ER stress in a dose dependent manner, recapitulating ENTPD5 knockdown phenotype. Compared to PTEN heterozygous MEF cells, PTEN-null cells are more susceptible to ENTPD5 inhibitor induced ER stress, supporting the synthetic lethal model of ENTPD5 inhibitors with Akt hyperactive tumor. PTEN-null human prostate cancer cell line LNCaP/C4-2 also show dose dependent response to these synthetic compounds.

We also identified a family of sesquiterpene hydroquinones natural compounds from sea sponge as ENTPD5 inhibitors through bioactivity directed purification. These sesquiterpene hydroquinones have been shown to possess anti-tumor and anti-angiogenesis activity (Amy E. Wright et al., 1993; Djura et al., 1980; Ravi et al., 1979), but no specific cellular target has been reported. We demonstrate that ER stress signal induced by these natural compound inhibitors in PTEN-null

MEF cells correlates with their in vitro IC_{50} against ENTPD5. Considering that ENTPD5 shows about 90% protein sequence homology with ENTPD1/CD39, which is involved in purinergic signaling and angiogenesis, it will not be surprising if the anti-angiogenesis effects of these sesquiterpene hydroquinones turns are due to cross reaction with ENTPD1.

Chronic Inhibition of ENTPD5 may cause liver and male fertility defects since mice with ENTPD5 deficiency show hepatopathy and aspermia (Read, et al., 2009). These defects in mice, however, only become obvious after 1 year of age. Given the gloomy nature of PTEN mutation in human cancers and potential synthetic lethal effect of AKT activation and ENTPD5 inhibition, there is reason to be optimistic for a therapeutic window for cancer with ENTPD5 inhibitors.

Materials and Methods

General Reagents and Methods

General chemicals are from Sigma unless otherwise described.

We obtained α -P³² labeled ATP from GE Healthcare. All of other nucleotides are from Sigma. Non-hydrolyzable Uracil and Guanine nucleotides analogs are from Gena Bioscience (Germany).

Antibodies used for western blot analysis are listed below: ENTPD5 (Sigma, Ca# HPA002927); PTEN, AKT, phosphorylated AKT, EGF receptor, Her-2/ErbB-2, IGF recetper β subunit, human integrin β 3, Bip and β -actin (Cell Signaling, Ca#9559, 9272, 9271, 2646, 2165, 3027, 4702, 3177 and 4970 respectively). Antibody for Tet repressor is from Gene Tex Inc (Ca#GTX70489).

HRP-conjugated E-type PHA is from USBioLogical (Ca#P3371-25). Puromycin, Blasticidin and Hygromycin, which are used for establishment and maintenance of stable cell lines, are purchased from Invivogen (Ca#ant-pr-1, ant-bl-1 and ant-hg-1 respectively). G418 is from Calbiochem (Ca#345810).

Protein concentration was determined by Bradford assay. Molecular weight marker for SDS-PAGE and Gel-filtration are from Bio-Rad. General molecular biology methods were used as described in Sambrook et al., 1989.

Cell Culture

PTEN^{+/-} and PTEN^{-/-} MEF cells are established previously (Stambolic et al., 1998). Human prostate cancer cell line LNCaP, human colon cancer cell line HT-29, human breast cancer cell line MCF-7, MBA231, SKBR-3 and T47D and HeLa cell are from ATCC. Other human prostate cancer line PC-3, DU145, LAPC4, and C42 were kindly provided by Dr. Jer-Tsong Hsieh at UT Southwestern. All the cell lines except LNCaP, T47D and LAPC4 are grown in DMEM medium supplemented with 10% fetal bovine serum (FBS) (Invitrogen) plus 200 unit/ml penicillin/streptomycin (Hyclone). LNCaP and T47D are cultured in RPMI 1640 medium containing 10% FBS plus 200 unit/ml penicillin/streptomycin and 20 mM Glutamine (Hyclone) while LAPC4 is cultured in Iscove's medium supplemented with 10% FBS and 200 unit/ml penicillin/streptomycin. The culture flasks were kept in humidified 37°C incubator in the presence of 5% CO₂.

Total Cell Extracts Preparation

Cultured cells after various treatments were scraped and collected with centrifugation at 800 g force at 4 °C for 6 minutes, washed once with cold PBS (Invitrogen). The cell pellets were resuspended in approximately 5 volumes of buffer A (20 mM Hepes, 10 mM KCl, 1.5 mM MgCl₂, 1mM EDTA, 1 mM EGTA,

1mM DTT, 0.1 mM PMSF, complete protease inhibitor from Roche, 1% Triton X-100 and Phosphatase Inhibitor I and II) and then vortexed for 30 seconds, set on ice for 20 minutes followed by centrifugation at 14000 rpm at 4 °C for 15 minutes in a microcentrifuge. The supernatants were collected for Western-blot analysis.

Preparation of S-100 Fractions

PTEN^{+/-} and PTEN^{-/-} MEF cells were cultured in monolayer at 37 °C in an atmosphere of 5% CO₂ in DMEM medium as described above. Two days after plating, cells were scraped and harvested. After washing once with cold PBS, cell pellets were re-suspended in 5 volumes of ice-cold buffer A. After sitting on ice for 20 minutes, the cells were broken by passing 22 times through a G22 needle attached onto a 1 ml syringe. The resulting broken cell mixtures were centrifuged at 14000 rpm for 10 minutes. The supernatants were further centrifuged at 10⁵×g force for 1 hour in a tabletop ultracentrifuge (Beckman). The resulting supernatant (S-100) was stored at -80 °C and used for ATP hydrolysis assay as well as purification of ENTPD5.

Suspension cultured HeLa S3 cells were obtained from Cell Culture Center in Minneapolis, MN. S-100 was prepared as in Li et al., 1997 was used as a source for the purification of UMP/CMP kinase-1 and Adenylate kinase as well as identification of the small molecule co-factor.

In Vitro ATP Hydrolysis Assay and Thin-layer Chromatography (TLC) Analysis

Aliquots of 30 μg of S-100 in 20 μl of volume either from PTEN^{+/+} or PTEN^{-/-} MEF cells were incubated with 3 μl of 1 mM ATP, 3 μl of 0.4 $\mu\text{Ci}/\mu\text{l}$ α - P^{32} -ATP and 3 μl of 100 mM MgCl_2 in total volume of 30 μl adjusted with buffer A at 30 °C for 1 hour. The reactions were stopped by adding 3.5 μl 100% (W/V) trichloroacetic acid (TCA). After vortex, the reaction mixtures were centrifuged for 10 minutes at 14000 rpm at 4°C. Aliquots of 1 μl resulting supernatant were spotted on a TLC plate (Analtech, Ca#105016) and air-dried. After being developed overnight in solvent (132 ml isobutyric acid plus 36 ml ddH₂O and 6 ml of 30% ammonia hydroxide), the plate was air-dried and imaged either by exposing to an X-ray film at room temperature for 2 hours, or to a phosphor-imaging plate for 30 minutes.

Purification of ENTPD5

All purification steps were carried out at 4 °C. All chromatography steps were carried out using an automatic fast protein liquid chromatography (FPLC) station (Pharmacia).

Eighty milliliters (0.32 g of protein) of S-100 from PTEN^{-/-} cells were prepared as described above and applied to a 10 ml SP-Sepharose HP column (Pharmacia) that was freshly equilibrated with buffer A. Flow through fraction was collected and loaded onto a 5 ml Q-Sepharose HP column (Pharmacia). The column was eluted with a linear gradient of 100 ml buffer A to buffer A containing 300 mM NaCl, followed by washing with another 50 ml buffer A containing 1 M NaCl. Fractions of 5 ml were collected, dialyzed overnight, and assayed for ATP hydrolysis activity. The active fractions (10 ml) were pooled, and ammonium sulfate was added directly to these fractions to a final concentration of 1 M. The mixture was equilibrated by rotating for 3 hr at 4 °C followed by centrifugation at 35000×g for 1 hr. The resulting supernatant was loaded onto a 1 ml Phenyl-Superose column (Pharmacia) equilibrated with buffer A containing 1 M ammonium sulfate. After washing with 10 ml buffer A containing 0.5 M ammonium sulfate, the column was eluted with a 10 ml linear gradient of buffer A containing 0.5 M ammonium sulfate to buffer A. Fractions of 1 ml were collected, dialyzed overnight, and assayed for ATP hydrolysis activity. 3 ml of active fractions were pooled, concentrated by a spin column (Amicon® Ultra) to 1 ml and loaded in two separate runs on a Superdex 200 (10/30) gel filtration column equilibrated with buffer A containing 50 mM NaCl. The column was eluted with the same buffer. Fractions of 1 ml were collected and assayed for ATP hydrolysis activity. A total of 4 ml active fractions were

pooled and loaded on a Mini Q (Pharmacia) column. The column was washed with 1 ml buffer A plus 1ml buffer A containing 100 mM NaCl. The column was eluted with a 2 ml linear gradient of 100 mM NaCl to 150 mM NaCl, both in buffer A. Fractions of 100 μ l were collected and assayed for ATP hydrolysis activity. Active fractions were aliquoted with addition of 10% (v/v) final concentration of glycerol and stored at -80°C .

Purification of UMP/CMP Kinase-1

160 ml S-100 (0.8 g of protein) from HeLa S3 cells were prepared as described above and applied to a 10 ml Q-Sepharose HP column (Pharmacia) equilibrated with buffer A. The column was eluted with a 200 ml linear gradient of buffer A to buffer A containing 200 mM NaCl. Fractions of 10 ml were collected and dialyzed against buffer A overnight at 4°C , assayed for ATP hydrolysis activity. Active fractions (20 ml) were pooled, dialyzed, and passed through 1 ml SP-Sepharose HP column (Pharmacia). The flow through fraction was collected and directly loaded on a 1 ml Heparin HP column (Pharmacia). After washing with five column volumes of buffer A, the column was eluted with 20 ml linear gradient of buffer A to buffer A containing 600 mM NaCl. Fractions of 1 ml were collected, dialyzed against buffer A overnight at 4°C , and assayed for ATP hydrolysis activity. Active fractions were pooled and loaded in 8

separate runs on a Superdex 200 (10/30) column (Pharmacia) equilibrated with buffer A containing 50 mM NaCl. The column was eluted with same buffer. Fractions of 1 ml were collected and assayed for ATP hydrolysis activity. A total of 16 ml of active fractions were pooled and loaded on Mini Q column. The column was eluted with 2 ml linear gradient of buffer A to buffer A containing 200 mM NaCl. Fractions of 100 μ l were collected and aliquots of 1 μ l was assayed for ATP hydrolysis activity assay and another aliquots of 15 μ l for SDS-PAGE followed by silver staining.

Small Molecular Recovery from S-100 Fraction

S-100 fractions from PTEN^{+/-}, PTEN^{-/-} MEFs c and HeLa S3 cells were obtained as described above. 2 ml of S-100 were applied to a 2 ml spin column (10K Cut off Centrifugal Filter Devices) (Centricon, Cat# 4205). The columns were centrifuged at 10000 rpm in JA-21 Centrifuge (Beckman) according to manufacturer's protocol. 1.8 ml of solution was centrifuged through the filter and used as source for small molecule identification.

Plasmid and siRNA Oligo

ENTPD5 Expression Constructs:

Human ENTPD5 (hENTPD5) was cloned into modified pCI-Neo vector with C-terminal 3xFlag tag. Mouse ENTPD5 (mENTPD5) was cloned into modified pcDNA3.1(+)-hygro with C-terminal 3xFlag tag.

ENTPD5 shRNA constructs:

Six tandem hENTPD5 shRNA (5'-CAT ATT AGC TTG GGT TAC T-3') expression cassettes driven by H1 promoter were cloned into pSuperior.puro vector following the protocol as previously described (Zhong et al., 2005). Similarly, mENTPD5 shRNA (5'-GGA AAA GCC TGG CCC GAA A-3') and control GFP shRNA (5'- CTG GAG TTG TCC CAA TTC C-3') constructs were made with four copies of tandem cassettes.

Rescue experiment constructs:

The shRNA resistant hENTPD5 (sr-hENTPD5) expression construct was generated by introducing four silent point mutations within the shRNA targeted region (5'-CAT CTT AGC CTG GGT CAC C-3') of pCI-Neo-hEntpd5-3xFlag. Since the mouse shRNA is targeting 3'-UTR of endogenous ENTPD5 mRNA, this region was deleted in the cDNA to generate shRNA resistant mENTPD5 (sr-mENTPD5).

For the catalytic-dead form of human ENTPD5 (sr-hENTPD5CD), hENTPD5 E172A mutation was introduced by site directed mutagenesis in the above shRNA resistant expression construct. Similarly, mouse catalytic-dead

ENTPD5 construct (sr-mENTPD5CD) was made by introducing E171A mutation into mouse rescuing construct.

Human and mouse siRNA against ENTPD5 were from Dharmacon ON-TARGET plus siRNA pools of four oligoes. ihENTPD5D3 (5'-CAU AUU AGC UUG GGU UAC UUU-3'), ihENTPD5D4 (5'-CGA GAU GGU UGG AAG CAG AUU-3'), imENTPD5D1 (5'-GGA CAU ACG UUU CGA AGU GUU-3'), imENTPD5D2 (5'-GGA AAA GCC UGG CCC GAA AUU-3') and control siRNA iGFP (5'- CUG GAG UUG UCC CAA UUC CUU-3') were synthesized by Dharmacon.

Preparation of Recombinant ENTPD5, CMPK1, and Adenylate Kinase

Human ENTPD5 recombinant protein was generated using Bac-to-Bac Baculovirus Expression Systems (Invitrogen Cat# 10359-016). Full-length human ENTPD5 cDNA was cloned into pFastBac1 with C-terminal-fused 6xHis and FLAG double tags. Baculovirus was produced and amplified to 2×10^9 pfu/ml following manufacturer's instructions. SF9 cells were grown to 2×10^6 cells/ml in SFM 900 II media (Invitrogen Cat# 10902096), and then infected with ENTPD5 expressing baculovirus at multiplicity of Infection (MOI) of 4. After 72 hr of infection, cells were harvested and homogenized in buffer A by douncing as described previously (Zou et al., 1999a). The recombinant protein was purified

using Ni-NTA agarose beads (Qiagen Cat#30230) following manufacturer's protocol.

Human CMPK1 and human AK1 cDNA were cloned into pET21a (Novagen Cat#69740-3), with C-terminal 6His tag. BL21DE3 bacteria was transformed and grown at 37°C to an OD600 of about 0.6. Then the bacteria culture was switched to 20°C, and recombinant protein expression was induced by 0.2 mM IPTG for overnight. Bacteria were harvested by centrifugation and lysed by sonication. The recombinant proteins were purified following standard Ni-NTA purification protocols.

Generation of Stable Cell Lines

To generate ENTPD5 ectopic expression cells, 4 µg of expression plasmids containing mouse ENTPD5 were transfected into PTEN^{+/-} MEF cells using Lipofectamin 2000 (Invitrogen) according manufacturer's instruction. Twenty-four hours post transfection, cells were split at 1 to 30 dilution and selected by adding 0.6 mg/ml Hygromycin in complete DMEM medium for 3 weeks. Clones were lifted and tested for expression of transgene by western blot analysis.

To establish tetracycline repressor expression cells, an expression plasmid containing tetracycline repressor (TetR) was transfected into either PTEN^{-/-} MEF

cells or LNCaP cells as described above and selected by 15 or 10 $\mu\text{g/ml}$ blasticidine respectively. Inducible mouse or human ENTPD5 shRNA construct was then stably introduced into PTEN^{-/-} TetR or LNCaP TetR cells, selected with 2 or 0.25 $\mu\text{g/ml}$ puromycin respectively. Finally, wild type or catalytic dead version of ENTPD5 rescue cells were generated by transfecting either PTEN^{-/-} MEF ENTPD5 shRNA cells or LNCaP EENTPD5 shRNA cells with mouse or human shRNA resistant ENTPD5 expression constructs and selected with 0.8 mg/ml Hygromycin or 0.5 mg/ml G418 respectively. To maintain transgene expression, all the stable cell lines were cultured in complete medium supplemented with various antibiotics as indicated.

Measurement of Cell Respiration Rates

O₂ consumption was determined by measuring O₂ concentration dynamics with the Oroboros-2k oxygraph (Oroboros, Austria). Each polarographic oxygen sensor (POS) was calibrated prior to use following manufacturer's instructions. Cultured cells were trypsinized, counted, and resuspended into 10⁶ cells/ml suspension, which will be loaded into the two 2cm³ air-tight chambers. Respiration measurements were carried out at 37°C, the same temperature as the cultures. The decreasing O₂ concentration was recorded at a two second interval using Datalab 4.3 software (Oroboros, Austria), and O₂ consumption rate was

calculated in real time by applying a linear regression on the O₂ concentrations, where the slope corresponds to respiration rate. To minimize the fluctuation of signal, 5 min of steady state respiration rate data was averaged and then normalized to cell density as final readout.

Measurement of Lactate Production in Cell Culture Medium

We purchased Lactate Assay kit from Biovision (Cat#K627-100). Measurement of Lactate concentration in cell culture medium was performed according the manufacturer's instruction..

Malachite Green Assay

Free phosphate released from the hydrolyzed nucleotides was measured by PiColorlock Gold Kit (Novus Cat#303-0030), following manufacturer's instructions.

Quantitative PCR Analysis

Total RNA from PTEN^{+/-} and PTEN^{-/-} MEF cells was extracted by the Trizol reagent (Invitrogen). One microgram of total RNA was used for first strand cDNA synthesis with superscript reverse transcriptase (RT) (Invitrogen). Real-time quantitative PCR was performed by the fluorescent dye SYBR Green

methodology using Power SYBR Green PCR kit (Applied Biosystems) and the 7900 HT Fast Real-Time PCR System (Applied Biosystems). Primer pairs for target genes were chosen with the Primers Express software (Applied Biosystem): ENTPD5, sense 5'-ATGACCCTGCCTCCACAGGAGTGTGAGC AG-3', antisense 5'-GCCTGGGCTTTCTGCTCAGGCAGCAAACG-3' 18S, sense 5'-GCC TGAGAAACGGCTACCA-3', antisense 5'-GTCGGGAGTGGGTAATTTGC-3'. Briefly, cDNA was mixed with 25 µl Master Mix containing 10× reaction buffer, 25 mM MgCl₂, 2.5 mM dNTP, 300 nM of each primer, 0.025 U/µl AmpliTaq Gold® DNA Polymerase and 0.75 µl of 1/2000 diluted SYBR green stock in a final volume of 50 µl. A first step of 10 min at 95 °C was followed by 40 cycles of amplification (95 °C for 15 s and 60 °C for 60 s). Using the comparative Ct method, the amount of ENTPD5 mRNA was normalized to the 18S amount.

Cell Survival Assay

Cell survival analysis was performed using the Cell Titer-Glo Luminescent Cell Viability Assay kit (Promega) following manufactory instruction with minor modification. In brief, 25 µl of Cell Titer-glo reagent was added to the cell culture medium. Cells were place on a shaker for 10 min and

were then incubated at room temperature for an additional 10 min. Luminescent reading was carried on Tecan SPECTRAFluor Plus reader (Tecan).

HTS Assay Reaction Buffer

All enzymes/substrates dilutions and subsequent reactions mentioned in this study was performed with this buffer, which contains 100mM Hepes at pH 7.5, 50mM NaCl, 10mM MgCl₂, 0.1 mg/ml BSA, 10% Glycerol.

HTS Equipments

The primary and counter screen assays were performed by using MicroFlo™ liquid dispenser to handle enzyme mixtures and substrate solutions and a Biomek® FX robotic pipetter with Biomek AP 384 P30 pipette tips (Beckman Coulter, Fullerton, CA) to add compounds. An EnVision™ 2102 plate reader (Perkin Elmer) was used to read the absorbance and luminescence.

HTS Chemical Library

HTS compound library of 200,000 compounds, dissolved in dimethyl sulfoxide (DMSO), was provided by the University of Texas Southwestern Medical Center, Department of Biochemistry HTS Laboratory. This library contains drug-like small molecules purchased from ChemiDiv Inc. (San Diego,

CA), Chembridge Corp. (San Diego, CA) and TimTec (Newark, DE), covering a reasonably large chemical space. Also included is a collection of natural compound crude extracts from marine organisms, provided by Dr. John MacMillan.

The 8,000 compounds in the test library are randomly selected out of the HTS library. All other chemicals used in this study, including the nucleotides, are from Sigma (St. Louis, MO), if not indicated otherwise.

HTS Assay Plate Setup and Results Analysis

The setup of 384-well plate for the primary screen is as following: 1) The first column of 16 wells (A1-P1) were set as positive control (PosCtrl), containing reaction buffer and Substrate Solution in the presence of 1% DMSO but no Enzyme Mixture, corresponding to theoretical 100% inhibition. 2) The second and 23rd column (A2-P2, A23-P23) were used as negative control (NegCtrl), which contain both Enzyme Mixture and Substrate Solution plus 1% DMSO, reflecting null inhibition. And 3) the 24th column (A24-P24) was the positive compound control (CmpdCtrl), where 0.5 μ l of 0.5mM Cmpd4 in DMSO was added into the complete enzymatic reaction. 4) The rest of the plate, 320 wells (C1-P22), was designated for the library compounds (Sample) to be assayed in

complete enzymatic reaction. The secondary and tertiary assay plate setups were similar, with their respective Enzyme Mixture and Substrate Solution used.

The structure clustering of cherry picked compounds was performed by pipeline pilot software from Accelrys (San Diego).

Bibliography

Alessi, D.R., James, S.R., Downes, C.P., Holmes, A.B., Gaffney, P.R., Reese, C.B., and Cohen, P. (1997). Characterization of a 3-phosphoinositide-dependent protein kinase which phosphorylates and activates protein kinase B α . *Curr Biol* 7, 261-269.

Alimonti, A., Carracedo, A., Clohessy, J.G., Trotman, L.C., Nardella, C., Egia, A., Salmena, L., Sampieri, K., Haveman, W.J., Brogi, E., *et al.* (2010). Subtle variations in Pten dose determine cancer susceptibility. *Nat Genet* 42, 454-458.

Altiok, S., Batt, D., Altiok, N., Papautsky, A., Downward, J., Roberts, T.M., and Avraham, H. (1999). Heregulin induces phosphorylation of BRCA1 through phosphatidylinositol 3-Kinase/AKT in breast cancer cells. *J Biol Chem* 274, 32274-32278.

Amy E. Wright, F.P.F.L., Sue S. Cross, F.P.F.L., Neal S. Burres, H.P.F.L., and Frank Koehn, F.P.F.L. (1993). Novel antiviral and anti-leukemia terpene hydroquinones and methods of use (US).

Baykov, A.A., Evtushenko, O.A., and Avaeva, S.M. (1988). A malachite green procedure for orthophosphate determination and its use in alkaline phosphatase-based enzyme immunoassay. *Anal Biochem* 171, 266-270.

Bi, L., Okabe, I., Bernard, D.J., Wynshaw-Boris, A., and Nussbaum, R.L. (1999). Proliferative defect and embryonic lethality in mice homozygous for a deletion in the p110 α subunit of phosphoinositide 3-kinase. *J Biol Chem* 274, 10963-10968.

Biederbick, A., Kosan, C., Kunz, J., and Elsasser, H.P. (2000). First apyrase splice variants have different enzymatic properties. *J Biol Chem* 275, 19018-19024.

Braun, N., Fengler, S., Ebeling, C., Servos, J., and Zimmermann, H. (2000). Sequencing, functional expression and characterization of rat NTPDase6, a nucleoside diphosphatase and novel member of the ecto-

nucleoside triphosphate diphosphohydrolase family. *Biochem J* 351 Pt 3, 639-647.

Brunet, A., Bonni, A., Zigmond, M.J., Lin, M.Z., Juo, P., Hu, L.S., Anderson, M.J., Arden, K.C., Blenis, J., and Greenberg, M.E. (1999). Akt promotes cell survival by phosphorylating and inhibiting a Forkhead transcription factor. *Cell* 96, 857-868.

Brunet, A., Kanai, F., Stehn, J., Xu, J., Sarbassova, D., Frangioni, J.V., Dalal, S.N., DeCaprio, J.A., Greenberg, M.E., and Yaffe, M.B. (2002). 14-3-3 transits to the nucleus and participates in dynamic nucleocytoplasmic transport. *J Cell Biol* 156, 817-828.

Cantley, L.C., and Neel, B.G. (1999). New insights into tumor suppression: PTEN suppresses tumor formation by restraining the phosphoinositide 3-kinase/AKT pathway. *Proc Natl Acad Sci U S A* 96, 4240-4245.

Cardone, M.H., Roy, N., Stennicke, H.R., Salvesen, G.S., Franke, T.F., Stanbridge, E., Frisch, S., and Reed, J.C. (1998). Regulation of cell death protease caspase-9 by phosphorylation. *Science* 282, 1318-1321.

Chang, H.J., Jesch, S.A., Gaspar, M.L., and Henry, S.A. (2004). Role of the unfolded protein response pathway in secretory stress and regulation of INO1 expression in *Saccharomyces cerevisiae*. *Genetics* 168, 1899-1913.

Cho, H., Mu, J., Kim, J.K., Thorvaldsen, J.L., Chu, Q., Crenshaw, E.B., Kaestner, K.H., Bartolomei, M.S., Shulman, G.I., and Birnbaum, M.J. (2001a). Insulin resistance and a diabetes mellitus-like syndrome in mice lacking the protein kinase Akt2 (PKB beta). *Science* 292, 1728-1731.

Cho, H., Thorvaldsen, J.L., Chu, Q., Feng, F., and Birnbaum, M.J. (2001b). Akt1/PKBalpha is required for normal growth but dispensable for maintenance of glucose homeostasis in mice. *J Biol Chem* 276, 38349-38352.

Christofk, H.R., Vander Heiden, M.G., Harris, M.H., Ramanathan, A., Gerszten, R.E., Wei, R., Fleming, M.D., Schreiber, S.L., and Cantley,

- L.C. (2008). The M2 splice isoform of pyruvate kinase is important for cancer metabolism and tumour growth. *Nature* 452, 230-233.
- Ciardiello, F., and Tortora, G. (2008). EGFR antagonists in cancer treatment. *N Engl J Med* 358, 1160-1174.
- Datta, S.R., Brunet, A., and Greenberg, M.E. (1999). Cellular survival: a play in three Akts. *Genes Dev* 13, 2905-2927.
- Di Cristofano, A., Pesce, B., Cordon-Cardo, C., and Pandolfi, P.P. (1998). Pten is essential for embryonic development and tumour suppression. *Nat Genet* 19, 348-355.
- Dijkers, P.F., Medema, R.H., Lammers, J.W., Koenderman, L., and Coffey, P.J. (2000). Expression of the pro-apoptotic Bcl-2 family member Bim is regulated by the forkhead transcription factor FKHR-L1. *Curr Biol* 10, 1201-1204.
- Djura, P., Stierle, D.B., Sullivan, B., Faulkner, D.J., Arnold, E.V., and Clardy, J. (1980). Some metabolites of the marine sponges *Smenospongia aurea* and *Smenospongia* (.ident.Polyfibrospongia) *echina*. *The Journal of Organic Chemistry* 45, 1435-1441.
- Dorner, A.J., Wasley, L.C., and Kaufman, R.J. (1989). Increased synthesis of secreted proteins induces expression of glucose-regulated proteins in butyrate-treated Chinese hamster ovary cells. *Journal of Biological Chemistry* 264, 20602-20607.
- Downward, J. (1998). Ras signalling and apoptosis. *Curr Opin Genet Dev* 8, 49-54.
- Dunwiddie, T.V., Diao, L., and Proctor, W.R. (1997). Adenine nucleotides undergo rapid, quantitative conversion to adenosine in the extracellular space in rat hippocampus. *J Neurosci* 17, 7673-7682.
- Easton, R.M., Cho, H., Roovers, K., Shineman, D.W., Mizrahi, M., Forman, M.S., Lee, V.M.-Y., Szabolcs, M., de Jong, R., Oltersdorf, T., *et al.* (2005). Role for Akt3/Protein Kinase B $\{\gamma\}$ in Attainment of Normal Brain Size. *Mol Cell Biol* 25, 1869-1878.

- Engelman, J.A., Luo, J., and Cantley, L.C. (2006). The evolution of phosphatidylinositol 3-kinases as regulators of growth and metabolism. *Nat Rev Genet* 7, 606-619.
- Enjyoji, K., Sevigny, J., Lin, Y., Frenette, P.S., Christie, P.D., Esch, J.S., Imai, M., Edelberg, J.M., Rayburn, H., Lech, M., *et al.* (1999). Targeted disruption of cd39/ATP diphosphohydrolase results in disordered hemostasis and thromboregulation. *Nat Med* 5, 1010-1017.
- Franke, T.F., Kaplan, D.R., Cantley, L.C., and Toker, A. (1997). Direct regulation of the Akt proto-oncogene product by phosphatidylinositol-3,4-bisphosphate. *Science* 275, 665-668.
- Frias, M.A., Thoreen, C.C., Jaffe, J.D., Schroder, W., Sculley, T., Carr, S.A., and Sabatini, D.M. (2006). mSin1 is necessary for Akt/PKB phosphorylation, and its isoforms define three distinct mTORC2s. In *Curr Biol* (England), pp. 1865-1870.
- Fruman, D.A., Meyers, R.E., and Cantley, L.C. (1998). Phosphoinositide kinases. *Annu Rev Biochem* 67, 481-507.
- Furnari, F.B., Huang, H.J., and Cavenee, W.K. (1998). The phosphoinositidase activity of PTEN mediates a serum-sensitive G1 growth arrest in glioma cells. *Cancer Res* 58, 5002-5008.
- Galetic, I., Andjelkovic, M., Meier, R., Brodbeck, D., Park, J., and Hemmings, B.A. (1999). Mechanism of protein kinase B activation by insulin/insulin-like growth factor-1 revealed by specific inhibitors of phosphoinositide 3-kinase--significance for diabetes and cancer. *Pharmacol Ther* 82, 409-425.
- Gevers, W., and Krebs, H.A. (1966). The effects of adenine nucleotides on carbohydrate metabolism in pigeon-liver homogenates. *Biochem J* 98, 720-735.
- Gu, J., Tamura, M., Pankov, R., Danen, E.H., Takino, T., Matsumoto, K., and Yamada, K.M. (1999). Shc and FAK differentially regulate cell motility and directionality modulated by PTEN. *J Cell Biol* 146, 389-403.

Hamann, M.T.O.M.S., Kochanowska, A.J.O.M.S., El-Alfy, A.O.M.S., Matsumoto, R.R.M.W.V., and Boujos, A.P. (2009). Method to Use Compositions Having Antidepressant Anxiolytic and Other Neurological Activity and Compositions of Matter (US).

Hammond, C., Braakman, I., and Helenius, A. (1994). Role of N-linked oligosaccharide recognition, glucose trimming, and calnexin in glycoprotein folding and quality control. *101073/pnas0802535105 91*, 913-917.

Harding, H.P., Novoa, I., Zhang, Y., Zeng, H., Wek, R., Schapira, M., and Ron, D. (2000). Regulated translation initiation controls stress-induced gene expression in mammalian cells. *Mol Cell 6*, 1099-1108.

Harding, H.P., Zhang, Y., and Ron, D. (1999). Protein translation and folding are coupled by an endoplasmic-reticulum-resident kinase. *Nature 397*, 271-274.

Haze, K., Yoshida, H., Yanagi, H., Yura, T., and Mori, K. (1999). Mammalian transcription factor ATF6 is synthesized as a transmembrane protein and activated by proteolysis in response to endoplasmic reticulum stress. *Mol Biol Cell 10*, 3787-3799.

Hollien, J., and Weissman, J.S. (2006). Decay of endoplasmic reticulum-localized mRNAs during the unfolded protein response. *Science 313*, 104-107.

Horwich, A. (2002). Protein aggregation in disease: a role for folding intermediates forming specific multimeric interactions. *J Clin Invest 110*, 1221-1232.

Inoki, K., Li, Y., Zhu, T., Wu, J., and Guan, K.-L. (2002). TSC2 is phosphorylated and inhibited by Akt and suppresses mTOR signalling. *Nat Cell Biol 4*, 648-657.

Kane, L.P., Shapiro, V.S., Stokoe, D., and Weiss, A. (1999). Induction of NF-kappaB by the Akt/PKB kinase. *Curr Biol 9*, 601-604.

Keniry, M., and Parsons, R. (2008). The role of PTEN signaling perturbations in cancer and in targeted therapy. *Oncogene 27*, 5477-5485.

Khwaja, A. (1999). Akt is more than just a Bad kinase. *Nature* 401, 33-34.

Konishi, H., Kuroda, S., Tanaka, M., Matsuzaki, H., Ono, Y., Kameyama, K., Haga, T., and Kikkawa, U. (1995). Molecular cloning and characterization of a new member of the RAC protein kinase family: association of the pleckstrin homology domain of three types of RAC protein kinase with protein kinase C subspecies and beta gamma subunits of G proteins. *Biochem Biophys Res Commun* 216, 526-534.

Kops, G.J., and Burgering, B.M. (1999). Forkhead transcription factors: new insights into protein kinase B (c-akt) signaling. *J Mol Med* 77, 656-665.

Kozutsumi, Y., Segal, M., Normington, K., Gething, M.-J., and Sambrook, J. (1988). The presence of malfolded proteins in the endoplasmic reticulum signals the induction of glucose-regulated proteins. *Nature* 332, 462-464.

Lau, K.S., Partridge, E.A., Grigorian, A., Silvescu, C.I., Reinhold, V.N., Demetriou, M., and Dennis, J.W. (2007). Complex N-glycan number and degree of branching cooperate to regulate cell proliferation and differentiation. *Cell* 129, 123-134.

Leppa, S., and Bohmann, D. (1999). Diverse functions of JNK signaling and c-Jun in stress response and apoptosis. *Oncogene* 18, 6158-6162.

Li, D.M., and Sun, H. (1997). TEP1, encoded by a candidate tumor suppressor locus, is a novel protein tyrosine phosphatase regulated by transforming growth factor beta. *Cancer Res* 57, 2124-2129.

Li, J., Yen, C., Liaw, D., Podsypanina, K., Bose, S., Wang, S.I., Puc, J., Miliareis, C., Rodgers, L., McCombie, R., *et al.* (1997). PTEN, a putative protein tyrosine phosphatase gene mutated in human brain, breast, and prostate cancer. *Science* 275, 1943-1947.

- Maehama, T., Taylor, G.S., and Dixon, J.E. (2001). PTEN and myotubularin: novel phosphoinositide phosphatases. *Annu Rev Biochem* 70, 247-279.
- Manning, B.D., Tee, A.R., Logsdon, M.N., Blenis, J., and Cantley, L.C. (2002). Identification of the tuberous sclerosis complex-2 tumor suppressor gene product tuberlin as a target of the phosphoinositide 3-kinase/akt pathway. *Mol Cell* 10, 151-162.
- McMenamin, M.E., Soung, P., Perera, S., Kaplan, I., Loda, M., and Sellers, W.R. (1999). Loss of PTEN expression in paraffin-embedded primary prostate cancer correlates with high Gleason score and advanced stage. *Cancer Res* 59, 4291-4296.
- Minale, L., Riccio, R., and Sodano, G. (1974). Avarol a novel sesquiterpenoid hydroquinone with a rearranged drimane skeleton from the sponge. *Tetrahedron Letters* 15, 3401-3404.
- Montagnani, M., Chen, H., Barr, V.A., and Quon, M.J. (2001). Insulin-stimulated activation of eNOS is independent of Ca²⁺ but requires phosphorylation by Akt at Ser(1179). *J Biol Chem* 276, 30392-30398.
- Mori, K., Ogawa, N., Kawahara, T., Yanagi, H., and Yura, T. (2000). mRNA splicing-mediated C-terminal replacement of transcription factor Hac1p is required for efficient activation of the unfolded protein response. *Proc Natl Acad Sci U S A* 97, 4660-4665.
- Myers, M.P., Pass, I., Batty, I.H., Van der Kaay, J., Stolarov, J.P., Hemmings, B.A., Wigler, M.H., Downes, C.P., and Tonks, N.K. (1998). The lipid phosphatase activity of PTEN is critical for its tumor suppressor function. *Proc Natl Acad Sci U S A* 95, 13513-13518.
- Myers, M.P., and Tonks, N.K. (1997). PTEN: sometimes taking it off can be better than putting it on. *Am J Hum Genet* 61, 1234-1238.
- Nakagawa, T., Zhu, H., Morishima, N., Li, E., Xu, J., Yankner, B.A., and Yuan, J. (2000). Caspase-12 mediates endoplasmic-reticulum-specific apoptosis and cytotoxicity by amyloid-beta. *Nature* 403, 98-103.

Nelen, M.R., van Staveren, W.C.G., Peeters, E.A.J., Ben Hassel, M., Gorlin, R.J., Hamm, H., Lindboe, C.F., Fryns, J.-P., Sijmons, R.H., Woods, D.G., *et al.* (1997). Germline Mutations in the PTEN/MMAC1 Gene in Patients With Cowden Disease. *Human Molecular Genetics* 6, 1383-1387.

Nishitoh, H., Matsuzawa, A., Tobiume, K., Saegusa, K., Takeda, K., Inoue, K., Hori, S., Kakizuka, A., and Ichijo, H. (2002). ASK1 is essential for endoplasmic reticulum stress-induced neuronal cell death triggered by expanded polyglutamine repeats. *Genes Dev* 16, 1345-1355.

Okano, J., Gaslightwala, I., Birnbaum, M.J., Rustgi, A.K., and Nakagawa, H. (2000). Akt/protein kinase B isoforms are differentially regulated by epidermal growth factor stimulation. *J Biol Chem* 275, 30934-30942.

Ozes, O.N., Mayo, L.D., Gustin, J.A., Pfeffer, S.R., Pfeffer, L.M., and Donner, D.B. (1999). NF-kappaB activation by tumour necrosis factor requires the Akt serine-threonine kinase. *Nature* 401, 82-85.

Paik, S., Kim, C., and Wolmark, N. (2008). HER2 status and benefit from adjuvant trastuzumab in breast cancer. *N Engl J Med* 358, 1409-1411.

Patil, C., and Walter, P. (2001). Intracellular signaling from the endoplasmic reticulum to the nucleus: the unfolded protein response in yeast and mammals. *Curr Opin Cell Biol* 13, 349-355.

Podsypanina, K., Ellenson, L.H., Nemes, A., Gu, J., Tamura, M., Yamada, K.M., Cordon-Cardo, C., Cattoretti, G., Fisher, P.E., and Parsons, R. (1999). Mutation of Pten/Mmac1 in mice causes neoplasia in multiple organ systems. *Proc Natl Acad Sci U S A* 96, 1563-1568.

Potter, C.J., Pedraza, L.G., and Xu, T. (2002). Akt regulates growth by directly phosphorylating Tsc2. *Nat Cell Biol* 4, 658-665.

Ramaswamy, S., Nakamura, N., Vazquez, F., Batt, D.B., Perera, S., Roberts, T.M., and Sellers, W.R. (1999). Regulation of G1 progression by the PTEN tumor suppressor protein is linked to

inhibition of the phosphatidylinositol 3-kinase/Akt pathway. *Proc Natl Acad Sci U S A* *96*, 2110-2115.

Ravi, B.N., Perzanowski, H.P., Ross, R.A., Erdman, T.R., Scheuer, P.J., Finer, J., and Clardy, J. (1979). Recent research in marine natural products: the puupehenones. *Pure Appl Chem* *51*, 1893-1900.

Romashkova, J.A., and Makarov, S.S. (1999). NF-kappaB is a target of AKT in anti-apoptotic PDGF signalling. *Nature* *401*, 86-90.

Ron, D. (2002). Translational control in the endoplasmic reticulum stress response. *J Clin Invest* *110*, 1383-1388.

Sarbassov, D.D., Guertin, D.A., Ali, S.M., and Sabatini, D.M. (2005). Phosphorylation and regulation of Akt/PKB by the rictor-mTOR complex. *Science* *307*, 1098-1101.

Scheuner, D., Song, B., McEwen, E., Liu, C., Laybutt, R., Gillespie, P., Saunders, T., Bonner-Weir, S., and Kaufman, R.J. (2001). Translational control is required for the unfolded protein response and in vivo glucose homeostasis. *Mol Cell* *7*, 1165-1176.

Schlessinger, J. (2000). Cell signaling by receptor tyrosine kinases. *Cell* *103*, 211-225.

Serina, L., Blondin, C., Krin, E., Sismeiro, O., Danchin, A., Sakamoto, H., Gilles, A.M., and Barzu, O. (1995). Escherichia coli UMP-kinase, a member of the aspartokinase family, is a hexamer regulated by guanine nucleotides and UTP. *Biochemistry* *34*, 5066-5074.

Serina, L., Bucurenci, N., Gilles, A.M., Surewicz, W.K., Fabian, H., Mantsch, H.H., Takahashi, M., Petrescu, I., Batelier, G., and Barzu, O. (1996). Structural properties of UMP-kinase from Escherichia coli: modulation of protein solubility by pH and UTP. *Biochemistry* *35*, 7003-7011.

Sousa, M.C., Ferrero-Garcia, M.A., and Parodi, A.J. (1992). Recognition of the oligosaccharide and protein moieties of glycoproteins by the UDP-Glc:glycoprotein glucosyltransferase. *Biochemistry* *31*, 97-105.

Stambolic, V., Suzuki, A., de la Pompa, J.L., Brothers, G.M., Mirtsos, C., Sasaki, T., Ruland, J., Penninger, J.M., Siderovski, D.P., and Mak, T.W. (1998). Negative regulation of PKB/Akt-dependent cell survival by the tumor suppressor PTEN. *Cell* 95, 29-39.

Stambolic, V., Tsao, M.S., Macpherson, D., Suzuki, A., Chapman, W.B., and Mak, T.W. (2000). High incidence of breast and endometrial neoplasia resembling human Cowden syndrome in *pten*^{+/-} mice. *Cancer Res* 60, 3605-3611.

Steck, P.A., Pershouse, M.A., Jasser, S.A., Yung, W.K., Lin, H., Ligon, A.H., Langford, L.A., Baumgard, M.L., Hattier, T., Davis, T., *et al.* (1997). Identification of a candidate tumour suppressor gene, MMAC1, at chromosome 10q23.3 that is mutated in multiple advanced cancers. *Nat Genet* 15, 356-362.

Suzuki, A., de la Pompa, J.L., Stambolic, V., Elia, A.J., Sasaki, T., del Barco Barrantes, I., Ho, A., Wakeham, A., Itie, A., Khoo, W., *et al.* (1998). High cancer susceptibility and embryonic lethality associated with mutation of the PTEN tumor suppressor gene in mice. *Curr Biol* 8, 1169-1178.

Tamura, M., Gu, J., Danen, E.H., Takino, T., Miyamoto, S., and Yamada, K.M. (1999). PTEN interactions with focal adhesion kinase and suppression of the extracellular matrix-dependent phosphatidylinositol 3-kinase/Akt cell survival pathway. *J Biol Chem* 274, 20693-20703.

Tamura, M., Gu, J., Matsumoto, K., Aota, S., Parsons, R., and Yamada, K.M. (1998). Inhibition of cell migration, spreading, and focal adhesions by tumor suppressor PTEN. *Science* 280, 1614-1617.

Teng, D.H., Hu, R., Lin, H., Davis, T., Iliev, D., Frye, C., Swedlund, B., Hansen, K.L., Vinson, V.L., Gumpfer, K.L., *et al.* (1997). MMAC1/PTEN mutations in primary tumor specimens and tumor cell lines. *Cancer Res* 57, 5221-5225.

Tokunaga, E., Oki, E., Egashira, A., Sadanaga, N., Morita, M., Kakeji, Y., and Maehara, Y. (2008). Deregulation of the Akt pathway in human cancer. *Curr Cancer Drug Targets* 8, 27-36.

- Travers, K.J., Patil, C.K., Wodicka, L., Lockhart, D.J., Weissman, J.S., and Walter, P. (2000). Functional and Genomic Analyses Reveal an Essential Coordination between the Unfolded Protein Response and ER-Associated Degradation. *Cell* 101, 249-258.
- Trombetta, S.E., and Parodi, A.J. (1992). Purification to apparent homogeneity and partial characterization of rat liver UDP-glucose:glycoprotein glucosyltransferase. *Journal of Biological Chemistry* 267, 9236-9240.
- Vander Heiden, M.G., Cantley, L.C., and Thompson, C.B. (2009). Understanding the Warburg effect: the metabolic requirements of cell proliferation. *Science* 324, 1029-1033.
- Vanhaesebroeck, B., Ali, K., Bilancio, A., Geering, B., and Foukas, L.C. (2005). Signalling by PI3K isoforms: insights from gene-targeted mice. *Trends Biochem Sci* 30, 194-204.
- Vanhaesebroeck, B., and Waterfield, M.D. (1999). Signaling by distinct classes of phosphoinositide 3-kinases. *Exp Cell Res* 253, 239-254.
- Vazquez, F., and Sellers, W.R. (2000). The PTEN tumor suppressor protein: an antagonist of phosphoinositide 3-kinase signaling. *Biochim Biophys Acta* 1470, 21-35.
- Wang, T.F., Ou, Y., and Guidotti, G. (1998). The transmembrane domains of ectoapyrase (CD39) affect its enzymatic activity and quaternary structure. *J Biol Chem* 273, 24814-24821.
- Ware, F.E., Vassilakos, A., Peterson, P.A., Jackson, M.R., Lehrman, M.A., and Williams, D.B. (1995). The molecular chaperone calnexin binds Glc₁Man₉GlcNAc₂ oligosaccharide as an initial step in recognizing unfolded glycoproteins. *Journal of Biological Chemistry* 270, 4697-4704.
- Whitman, M., Downes, C.P., Keeler, M., Keller, T., and Cantley, L. (1988). Type I phosphatidylinositol kinase makes a novel inositol phospholipid, phosphatidylinositol-3-phosphate. *Nature* 332, 644-646.

Whitman, M., Kaplan, D.R., Schaffhausen, B., Cantley, L., and Roberts, T.M. (1985). Association of phosphatidylinositol kinase activity with polyoma middle-T competent for transformation. *Nature* 315, 239-242.

Wullschleger, S., Loewith, R., and Hall, M.N. (2006). TOR signaling in growth and metabolism. *Cell* 124, 471-484.

Yaffe, M.B., Rittinger, K., Volinia, S., Caron, P.R., Aitken, A., Leffers, H., Gambin, S.J., Smerdon, S.J., and Cantley, L.C. (1997). The structural basis for 14-3-3:phosphopeptide binding specificity. *Cell* 91, 961-971.

Yoneda, T., Imaizumi, K., Oono, K., Yui, D., Gomi, F., Katayama, T., and Tohyama, M. (2001). Activation of caspase-12, an endoplasmic reticulum (ER) resident caspase, through tumor necrosis factor receptor-associated factor 2-dependent mechanism in response to the ER stress. In *J Biol Chem* (United States), pp. 13935-13940.

Yoshida, H., Haze, K., Yanagi, H., Yura, T., and Mori, K. (1998). Identification of the cis-acting endoplasmic reticulum stress response element responsible for transcriptional induction of mammalian glucose-regulated proteins. Involvement of basic leucine zipper transcription factors. *J Biol Chem* 273, 33741-33749.

Zhang, C., Cai, Y., Adachi, M.T., Oshiro, S., Aso, T., Kaufman, R.J., and Kitajima, S. (2001). Homocysteine induces programmed cell death in human vascular endothelial cells through activation of the unfolded protein response. *J Biol Chem* 276, 35867-35874.

Zhang, J.H., Chung, T.D., and Oldenburg, K.R. (1999). A Simple Statistical Parameter for Use in Evaluation and Validation of High Throughput Screening Assays. *J Biomol Screen* 4, 67-73.

Zhong, Q., Gao, W., Du, F., and Wang, X. (2005). Mule/ARF-BP1, a BH3-only E3 ubiquitin ligase, catalyzes the polyubiquitination of Mcl-1 and regulates apoptosis. *Cell* 121, 1085-1095.

Zhou, B.P., Liao, Y., Xia, W., Spohn, B., Lee, M.H., and Hung, M.C. (2001). Cytoplasmic localization of p21Cip1/WAF1 by Akt-induced

phosphorylation in HER-2/neu-overexpressing cells. *Nat Cell Biol* 3, 245-252.

Zimmermann, S., and Moelling, K. (1999). Phosphorylation and regulation of Raf by Akt (protein kinase B). *Science* 286, 1741-1744.

Zou, H., Li, Y., Liu, X., and Wang, X. (1999a). An APAF-1·cytochrome c multimeric complex is a functional apoptosome that activates procaspase-9. *J Biol Chem* 274, 11549-11556.

Zou, H., Li, Y., Liu, X., and Wang, X. (1999b). An APAF-1·Cytochrome c Multimeric Complex Is a Functional Apoptosome That Activates Procaspase-9. *Journal of Biological Chemistry* 274, 11549-11556.